
Politecnico di Torino

Politecnico di Torino

Dipartimento di Scienze Matematiche
Laurea Magistrale in Ingegneria Matematica

# Spread and containment of infectious disease epidemics: a kinetic approach.

Supervisor:
Prof. Andrea Tosin
Co-supervisor:
Dr. Nadia Loy

Candidate:
Giacomo Masali

Academic Year 2020/2021

*A nonno Luciano,*

Abstract

In this thesis, we propose a Boltzmann-type kinetic approach in order to study the spread of an infectious disease. In particular, a mass-varying interacting multi-agent system is used to model a population and the confinement strategies that are adopted to stem the on-going epidemic in it, namely quarantine and vaccination. Every agent is characterized by a microscopic state, a *viral load*, and a label, that indicates the group the agent belongs to. The viral load changes as a consequence of interactions, while the label follows a Markov-type state dependent jump process. The quarantine strategy is firstly analyzed and the requirements for it to be effective outlined: a prompt isolation of the infected successfully stem the epidemic. A step further is taken by including a spatial network, e.g. of cities, in which the agents can move. This is accomplished by the means of the same label-based framework. We then focus on the vaccine strategy, numerically evaluating a threshold for the herd immunity condition. We then propose a version of the vaccination model enriched with an age-based distinction of the agents. Different interaction rates based on age are taken into account: the herd immunity threshold is shown to depend on these interaction rates. The four models are discussed analytically and numerically. General kinetic equations are derived in order to describe the statistical distribution of the agents. From those, we also derive macroscopic ODE systems for each model, both for constant and variable parameters. To do so, in the latter case we rely on the hydrodynamic limit. Finally, a Monte Carlo simulation via the Nanbu-Babovsky's scheme is carried out to confirm theoretical findings and to investigate complicated configurations of the parameters.

# *Ringraziamenti*

Per primi vorrei ringraziare il professor Andrea Tosin e la dottoressa Nadia Loy per la disponibilità e il prezioso aiuto che mi hanno fornito in questi mesi. Se questo campo di ricerca mi ha appassionato è anche merito loro.

Vorrei poi spendere alcune parole per dire grazie alle persone che mi hanno accompagnato più da vicino in questo percorso, una a testa.

Ai miei genitori Cristina e Luca, per la pazienza e il supporto.

A Giancarlo, per l'entusiasmo.

A tutti i Cavalieri, per la sicurezza.

A Ismaele, per la curiosità.

A Lara, per la direzione.

# Contents

# 1 Introduction

In this thesis, we study the spread of infectious diseases with a Boltzmann-type kinetic approach. Classical epidemiology is built on ODEs systems that describe the evolution of the epidemic through the relative size of different compartments of people. In the present agent-based description, the ODEs are not stated a priori, they emerge from the microscopic interactions between agents by relying on kinetic equations. Every member of the population is characterized by a microscopic state representing their *viral load*. When two agents interact, they exchange some *viral load* depending on a microscopic interaction rule. When a large population is considered, equations for macroscopic properties such as density or mean *viral load* can be derived.

In order to contextualize this dissertation, a brief description of the main mathematical epidemiology models is given in this introduction, as well as the thesis' structure and some bibliographical references of the state of the art in applications of kinetic theory.

## 1.1 Structure of the thesis

This thesis is organized as follows. In the following introductory chapters, a brief description of the classical epidemiological models known as SIR (sec. 1.2.1) and SIS (sec. 1.2.2) is given, followed by some bibliographical references on the application of kinetic theory of gasses in the most various fields of study (sec. 1.3). sec. 2 contains a detailed description of the mathematical and theoretical tools applied in the dissertation. In particular an informal derivation of the Boltzmann equation is provided in sec. 2.1, followed by the description of binary interaction processes in sec. 2.2, the introduction of a Markov type jump process in the kinetic framework in sec. 2.3 and the description of the hydrodynamic limit in sec. 2.4. Finally, the description of the numerical methods used in the dissertation to simulate the models is carried out in sec. 2.5. sec. 3 describes the models developed in the dissertation. After showing how the classical epidemiological models SIR and SIS can be obtained from a microscopic kinetic description (sec. 3.1), the four models object of the thesis are presented in sequence in sec. 3.2, sec. 3.3, sec. 3.4 and sec. 3.5. Finally, the outcomes of the numerical tests performed are presented in sec. 4, divided by model. Conclusive section sec. 5 outlines the findings of the thesis and contains final comments.

## 1.2 Classical mathematical epidemiology

Epidemiology is the science that studies diseases at a population level. The main issues are distribution, patterns and factors that can influence the appearance and diffusion of various illnesses. The origins of epidemiology are ancient, but a mathematical approach to the matter is fairly new. While statistics has been used since the second half of fifteenth century [1], the first rigorous epidemiological model was proposed by Daniel Bernoulli in 1776 [2, 3]. It aimed to evaluate the life expectancy gain produced by eliminating smallpox as cause of death through the inoculation of a mild form of the virus and the subsequent immunization. For this purpose, Bernoulli used in his model a compartmentalization of the population in two groups: susceptibles and immunes. Other important works for the development of mathematical epidemiology in the first half of the twentieth century are from W. Hamer, H.E. Soper and Sir R. Ross [4, 5, 6]. In 1927 W. O. Kermack and A. G. McKendrick published the first epidemiological model [7] that included the labels susceptible, infected and recovered to describe the state of a population member with respect to the disease. The SIR and SIS models described later in this section derive directly from this work and its later additions [8, 9]. In more recent years, the mathematical approach to epidemiology has gained more and more space and a manifold of models and theories have been proposed [10, 11, 12]. For an exhaustive description of the main models and findings of mathematical epidemiology see [13].

### 1.2.1 The SIR model

The SIR model is a simple ODE-based epidemiological model first introduced by Kermack and McKendrick. Here, is proposed an essential description of the model based on the second chapter of [13]. It describes the evolution of an epidemic by introducing three epidemic compartments - susceptible, infected and removed. Susceptible individuals are healthy and have not yet contracted the disease; they can become ill if exposed. Infected individuals are the ill individuals; in a first approximation, they are assumed to be also infectious. The removed individuals have been infected and are no longer susceptible to the disease because of immunization or death. Let us call the normalized number of people in the three classes, respectively, $S = \frac{\#susceptible}{N}$, $I = \frac{\#infectiuos}{N}$ and $R = \frac{\#removed}{N}$, where $N$ is the total population; hence the name of the model, SIR. The total number of people is assumed constant, this yields $S(t)+I(t)+R(t) = 1, \forall t$. The population in the classes changes during the evolution of the epidemic due to dynamics that derives from the nature of infectious diseases: if a susceptible person has a contact with an infectious one, they can contract the illness with a certain probability. they can then heal or die and leave

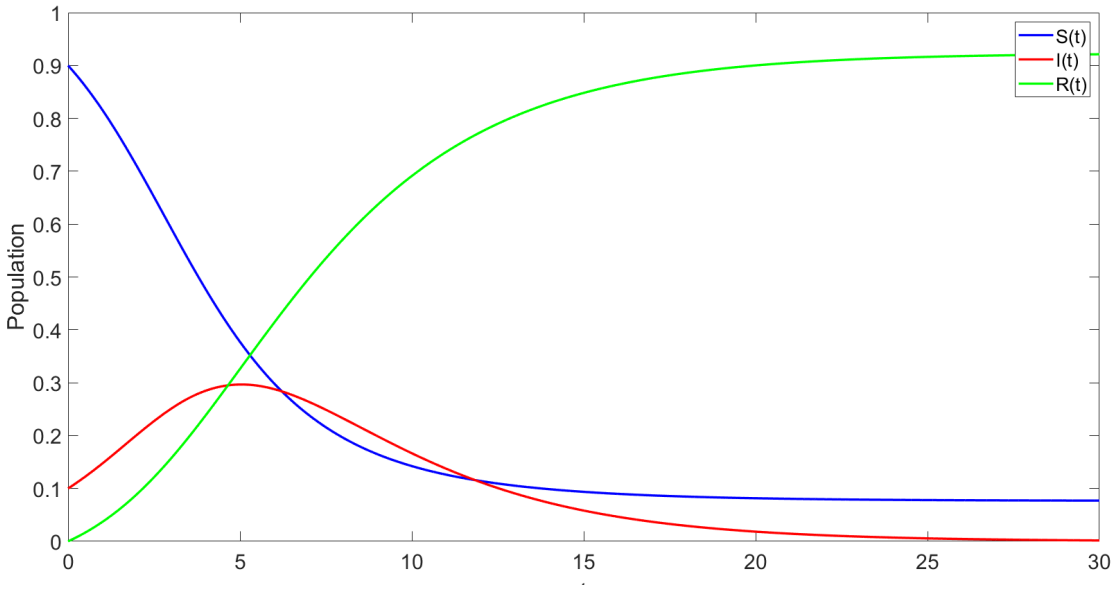


**Figure 1:** Evolution of the populations in the SIR model.

the infected group for the removed one with another probability. Let us define these probabilities: we call the per capita contact rate $0 \leq c \leq 1$, i.e. the probability a contact occurs between an infectious and a susceptible individual, per time unit. We then call $0 \leq p \leq 1$ the probability of infection given a contact. We can now define $\beta = pc$, the transmission rate constant. This means that the number of individual that leaves the $S$ class for the $I$ class per time unit is $\beta SIN$. Let us call $0 \leq \gamma \leq 1$ the probability of leaving $I$ for $R$, i.e. recovery rate, we can now easily derive the following ODEs system:

$$\begin{cases} S'(t) &= -\beta IS \\ I'(t) &= \beta IS - \gamma I \\ R'(t) &= \gamma I. \end{cases} \tag{1}$$

This system describes the evolution of the epidemic given some specific initial conditions $S(0)$, $I(0)$ and $R(0)$. Given the physical meaning of the variables we have of course: $S(t), I(t), R(t) \geq 0, \forall t$. Of particular interest is $I(t)$, called prevalence of the disease. It is easy to verify that the system yields $N'(t) = 0$, i.e. the total population is constant.

Some consideration on the SIR model are in order. First of all, we have that $S' < 0, \forall t$. $S$ is hence decreasing and positive, we can therefore state $lim_{t\to\infty} S(t) = S_\infty$. The same reasoning, overturned, can be applied to $R(t)$, obtaining $lim_{t\to\infty} R(t) =$

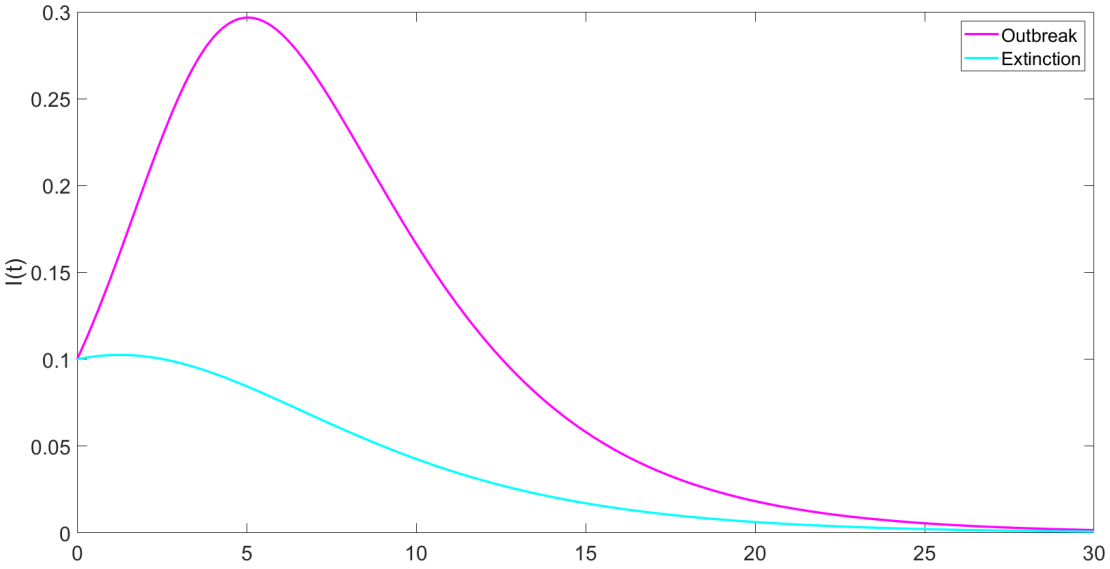


**Figure 2:** The two different cases of outbreak and extinction of the epidemic

$R_\infty$. More interestingly, the behavior of the incidence strictly depends on initial conditions. One of the two following scenarios will show. If $\beta S(0) - \gamma < 0$, then $I'(0) < 0$: the infected population decreases in time and the epidemic is avoided. On the other hand, if $\beta S(0) - \gamma > 0$, an outbreak occurs. The incidence first rises and then falls to zero: we have an epidemic. It is interesting to notice how the system yields

$\frac{dS}{dR} = -\frac{\beta}{\gamma} S$ .

Solving,

$S = S(0)e^{-\frac{\beta}{\gamma}R} \geq S(0)e^{-\frac{\beta}{\gamma}N} > 0$

and therefore $S_\infty > 0$. Moreover, it is possible to show that $I_\infty = 0$ for every initial condition (see [13]). This means that an epidemic always dies out and not all the susceptible individuals contract the illness. Given the simplicity of the model an analytical study can be easily carried out to find, for example, intensity and timing of the peak.

### 1.2.2 The SIS model

The SIR model is founded on the quite tight assumption that recovery gives a person total immunity from the disease. While this is true for some illnesses such as measles and chicken pox, it is false for others, such as influenza. Relaxing this hypothesis bring us to the SIS model. In the simplest version, we assume that people who leave the infected group become susceptible right away. The classes in this model are

therefore just two, susceptible $S$ and infected $I$. The same reasoning applied before gives the ODEs system:

$$\begin{cases} S'(t) &= -\beta IS + \gamma I \\ I'(t) &= \beta IS - \gamma I \end{cases} \tag{2}$$

Being the total population $N = S + I$, the system (2) can be reduced to the logistic equation:

$$I'(t) = rI(1 - \frac{I}{K}), \tag{3}$$

where $r = \beta N - \gamma$ and $K = \frac{r}{\beta}$. Let us call $r$ growth rate and distinguish two cases:

- If $r < 0$, the number of new infected per unit of time is lower than the number of recovered per unit of time. Analytically, we have $I'(t) \leq rI(t)$. This means that $I'(t) < 0 \ \forall t$ and $I(t)$ approaches 0 exponentially in time.
- If $r > 0$, we have to solve the logistic equation to find the evolution of the incidence. The solution is (see [13], chapter 2.3)

  $$I(t) = \frac{KBe^{rt}}{1 + Be^{rt}}\,, \tag{4}$$

  where $B = \frac{I(0)}{(K - I(0))}$. We have $lim_{t\to\infty} I(t) = K$, this means that the disease does not die out and becomes endemic.

Therefore, we can define the reproduction number $\mathscr{R}_0$, that characterize the trend of the epidemic, as $\mathscr{R}_0 = \frac{\beta N}{\gamma}$. It is easy to see that if $\mathscr{R}_0 > 1$ we are in the endemic case, if $\mathscr{R}_0 < 1$ the disease dies out. "Epidemiologically, the reproduction number gives the number of secondary cases one infectious individual will produce in a population consisting only of susceptible individuals" (Martcheva, 21).

We have briefly discussed two of the simplest models in mathematical epidemiology. These models can be improved to take into account many different characterizations, such as age [13], and possible interventions, such as lockdowns and hospitalizations [3].

## 1.3 The kinetic approach

In recent years, an agent-based approach to a wide variety of social and biological issues has been largely adopted. These methods are founded on the Boltzmann

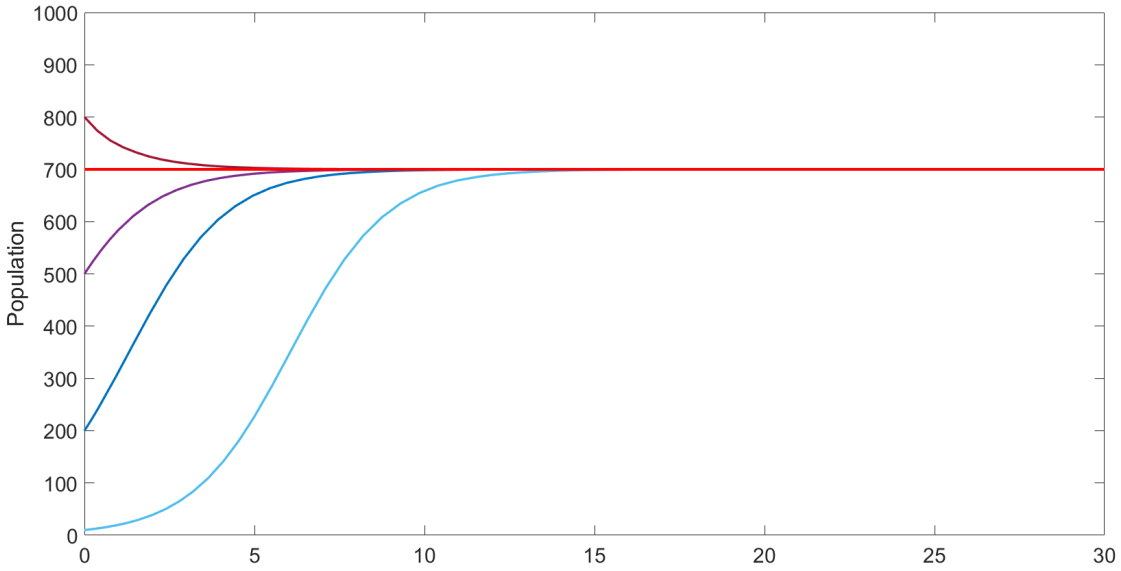


**Figure 3:** Some endemic solutions of the logistic equation, for different initial conditions.

kinetic gas theory and in particular on the Boltzmann equation. The framework offered by the kinetic theory is proven to be versatile and successful by the rich literature that has been flourishing in the most different areas of study, from biology [17, 18] to economics [15, 16], from sociology [19, 20, 21] to opinion formation [22, 23] and vehicular traffic [24, 25, 26]. The key idea shared by these works is to employ the mathematical formalism offered by physics of gasses to describe the behavior of interacting agents in the place of molecules that collide. While in gas dynamics molecules interact by exchanging kinetic energy and are characterized by properties as position and velocity, other type of agents may have microscopic state, or states, of different nature and may interact following different rules, depending on the single application. As in the classical application to gasses collective properties arise from simple microscopic interacting rules when a large number of particles is considered, so they do in social or biological systems. As a large number of agents is considered, they are described statistically. In particular, as the total number of agents is always assumed constant, a probability distribution function can be introduced for describing the statistical distribution of the states of the agents and it may be used in order to define macroscopic quantities through the moments of the probability distribution. Its evolution is described by the Boltzmann equation. For a complete overview on the methodologies and applications of kinetic theory we recommend [34].The kinetic theory developed by Boltzmann [27] provides us with sophisticated mathematical tools to study this type of systems. In particular, the integro-differential Boltzmann equation allows us to derive macroscopic equations for various moments of the state of the agents, at least in simple analytical settings.

In general this equation can be hard to solve analytically and numerical methods are required to find a solution. These numerical methods often are Monte Carlo direct simulations (DSMC) [28] in the form of Bird [29] or Nanbu-Babovsky [30] schemes. The physical phenomena described by epidemiology are well suited to be investigated by means of the kinetic approach. In a large and interconnected population, agents interact with each other and disease carriers - such as viruses or bacteria - are transferred from one person to the other. It is no surprise then the fact that this approach has been applied to the matter of epidemiology in different forms [31, 32]. Of particular interest for this dissertation is the innovative non-conservative kinetic equations introduced in [32]. The thesis aims at developing the findings of this work and proposes two epidemiological models based on these equations.

# 2 Mathematical tools

In this chapter we introduce some mathematical tools that will be used in the epidemiological models discussed later. Firstly, a simple derivation of the Boltzmann equation is carried out and some of its properties outlined. Then, we introduce the innovative Markov-type label switching process and we plug it into the kinetic model. A mass-varying interacting multi-agent system is obtained. The hydrodynamic limit is then discussed as it will be crucial to the analysis of the time-varying parameters cases. Lastly, we examine the Nanbu-Babovsky scheme for Monte Carlo simulations of multi-agents systems that will be massively employed as a numerical method to validate theoretical findings.

## 2.1 Boltzmann equation

The Boltzmann equation is the theoretical starting point of the study of multi-agent interacting systems from the kinetic point of view. First introduced by Ludwig Boltzmann in 1872 [37], it is a partial integro-differential equation that describes the evolution of the density of a rarefied gas. In one of its more general forms, it reads:

$$\frac{\partial f(t,x,\xi)}{\partial t} = -\xi \cdot \nabla_x f(t,x,\xi) + \alpha Q(f,f)(t,x,\xi) \tag{5}$$

where $f(t,x,\xi)$ is the particle density function. This means that $f(t,x,\xi)dxd\xi$ indicates the number of particles with position $x \in [x, x+dx]$ and velocity $\xi \in [\xi, \xi+d\xi]$ at time $t$. The terms in the right-hand side of the equation account, respectively, for the free particle transport and for the collisional interaction between particles. It is founded of the assumumption called Boltzmann ansatz, which states a statistical independence of positions and velocities of particles. An informal derivation of this equation is now proposed, based on [33]. We want to study the behavior of the particles that elastically collide in a gas. Mathematically, we consider $N$ identical hard spheres of diameter $\sigma$, whose position $x_i \in \Omega \in \mathbb{R}^3$ and velocity $\xi_i \in \mathbb{R}^3$, $i = 1, .., N$, is represented by a point in the phase space. We indicate with $z(x,\xi)$ the 6-dimensional point vector in this space. The probability density in the phase space is the non-negative function $f(t,z)$ and its domain is the set $\Omega^N \times \mathbb{R}^{3N}$, with $\Omega \subseteq \mathbb{R}^3$. It is possible to demonstrate [33] that, in absence of external forces, $f$ is constant along the trajectory of $z$ in the phase space. Let us define the set $\Lambda$ as $\Lambda = \Omega^N \times \mathbb{R}^{3N} \setminus \Upsilon$ , where $\Upsilon = \{z : \exists i,j \in \{1,2,...,N\}(i \neq j) : |x_i - x_j| < \sigma\}$. Saying that $f(t,z) > 0$ in $\Upsilon$ would mean that two spheres are coexisting in the same spatial coordinates and this is impossible, since they are hard. Therefore, we will

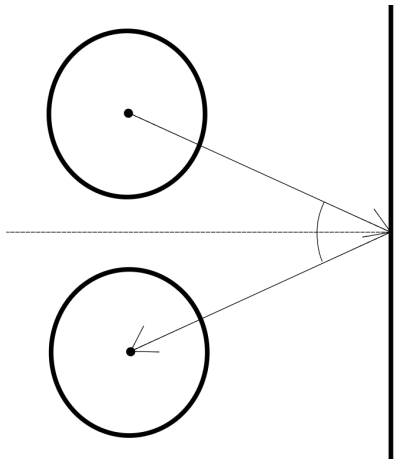

**Figure 4:** The symmetry of pre and post collision velocities. Here $\xi_2 = 0$, hence $V_{12} = \xi_1$.

have $f(t, z) = 0 \ \forall z \in \Upsilon$, we will also take $f(t, z)$ differentiable with respect to $z$ and $t$ on $\Lambda$. Under this hypothesis the so called Liouville equation states that [33]:

$$\frac{\partial f}{\partial t} + \sum_{i=1}^{N} \xi_i \cdot \frac{\partial f}{\partial x_i} = 0 \quad (z \in \Lambda). \tag{6}$$

Equation (6) needs to be completed with suitable initial and boundary conditions. The former will simply be the value $f(0, z)$, while the latter will have to account for the non-overlapping condition, even if the movement is boundless. To do so, it is necessary to assess the properties of the collision between two spheres. From the physics of elastic collisions we know that conservation of momentum and energy must hold. Being $(\xi_1, \xi_2)$ the pre-collision velocities and $(\xi_1', \xi_2')$ the post-collision ones, this yields:

$$\begin{aligned} \xi_1 + \xi_2 &= \xi_1' + \xi_2' \\ |\xi_1|^2 + |\xi_2|^2 &= |\xi_1'|^2 + |\xi_2'|^2. \end{aligned} \tag{7}$$

Moreover, we know that the directions of $\xi_i, i = 1, 2$ change instantly when a collision occurs. What happens is that the relative velocity $V_{12} = \xi_1 - \xi_2$ undergoes a specular reflection. This is schematized in Figure 4, where a sphere is represented before and after an elastic collision, with the respective velocities.

Since the collision creates a discontinuity in velocities, on the boundaries of $\Lambda$, i.e. where these collision happen, we must impose that:

$$f(t, z) = f(t, z') \quad (z \in \Lambda) \tag{8}$$

and explaining the variables, equation (8) reads [33]:

$$f(t, x_1, \xi_1, ..., x_i, \xi_i, ..., x_j, \xi_j, ..., x_N, \xi_N) = \\ f(t, x_1, \xi_1, ..., x_i, \xi_i - n_{ij}(n_{ij} \cdot V_{ij}), ..., x_j, \xi_j + n_{ij}(n_{ij} \cdot V_{ij}), ..., x_N, \xi_N) \tag{9}$$

if $|x_i - x_j| = \sigma \ \ (i \neq j)$, where $V_{ij} = \xi_i - \xi_j$ and $n_{ij}$ is the unit vector directed as $x_i - x_j$.

Obviously, other boundaries conditions will have to be added if one wants to consider a domain that is a subset of $\mathbb{R}^3$. In the study of actual gasses, equation (6) can not be applied. The order on magnitude of N, and therefore the number of variables, is $10^{23}$ and some sort of adjustment needs to be carried out. The Boltzmann equation serves us for this purpose. Let us consider the sphere labeled as 1 and the relative one-particle distribution function $f^{(1)}(t, x, \xi)$. This function depends only on the position and velocity of the sphere, other than the time. The challenge here is to obtain a closed equation for $f^{(1)}$, i.e. one that does not depend explicitly on $f^{(2)}$. Boltzmann did so by means of a heuristic argument.

Without any collision, the density $f^{(1)}$ would satisfy the Liouville equation (6) with $N = 1$ [33]. It seems reasonable to investigate the effects of the collisions on $f^{(1)}$ to obtain an evolution equation. For a particle, let us say particle 1, to collide it is necessary to have at least another particle, let us say particle 2. Hence, we have to consider two particles, $f^{(2)} = f^{(2)}(t, x_1, \xi_1, x_2, \xi_2)$. We introduce now a correction of the equation (6), that reads

$$\frac{\partial f^{(1)}}{\partial t} + \sum_{i=1}^{N} \xi_i \cdot \frac{\partial f^{(1)}}{\partial x_i} = G - L \tag{10}$$

where $G$ and $L$ are gain and loss terms with the following meaning:

- $G dx_1 d\xi_1$ is the expected number of particles gaining position in $[x_1, x_1 + dx_1]$ and velocity in $[\xi_1, \xi_1 + d\xi_1]$ due to a collision in $[t, t + dt]$. With abuse of terminology we can say that the particle enters the $[x_1, x_1 + dx_1] \times [\xi_1, \xi_1 + d\xi_1]$ box.
- $L dx_1 d\xi_1$is the expected number of molecules leaving that same box in the time interval $[t, t + dt]$ due to a collision.

For the sake of simplicity, let us imagine sphere 1 as at rest and with a double diameter, i.e. radius $\sigma$, and any other particle as a mass point of velocity with respect to particle 1 $V_i = \xi_i - \xi_1$. The number of collisions particle 1 will have is the number of expected collisions any particle will have with it. Let us call $g$ and $l$ the contributions of a single particle, say particle 2, to, respectively, gain and loss.

Being $(N-1)$ the other particles, we obtain:

$$\begin{aligned} G =&(N-1)g \\ L =&(N-1)l. \end{aligned}$$

Let us focus on the collision between particles 1 and 2. We take the point $x_2$ on sphere 1. Being $n$ the unit vector normal to the surface, we build the cylinder with height $dh = |\xi_2 \cdot n \cdot dt|$ and infinitesimal base $dS = \sigma^2 dn$, so that it contains the particles with velocity $\xi_2$ that reach the base $dS$ in the time interval $[t, t+dt]$. The volume of the cylinder is $dh \cdot dS = |\xi_2 \cdot n|\sigma^2 dndt$. We can now compose the probability of a collision between particles 1 and 2, respectively in the boxes $[x_1, x_1 + dx_1] \times [\xi_1, \xi_1 + d\xi_1]$ and $[x_2, x_2 + dx_2] \times [\xi_2, \xi_2 + d\xi_2]$, in $[t, t+dt]$ and that occurs in $dS$, as $f^{(2)}(t, x_1, \xi_1, x_2, \xi_2)dx_1 d\xi_1 d\xi_2 \times |\xi_2 \cdot n|\sigma^2 dndt$. Some of the collisions will contribute to the gain term, whereas others to the loss term. If $\xi_2 \cdot n < 0$, particle 2 is moving toward particle 1. This means that the collision is about to happen and will remove the particle from the considered range. If $\xi_2 \cdot n > 0$, particle 2 is moving away from particle 1. This means that the collision has already happened and has moved the particle into the considered range. The former case will add to the loss term and the latter to the gain one. To consider the whole sphere and all the possible velocities of particle 2 we integrate over $dn$ and $d\xi_2$. We denote with $S_-$ the hemisphere corresponding to the loss and with $S_+$ the hemisphere corresponding to the gain:

$$L = (N-1)\sigma^2 \int_{\mathbb{R}^3} \int_{S_-} f^{(2)}(t, x_1, \xi_1, x_1 + \sigma n, \xi_2)|(\xi_2 - \xi_1) \cdot n| d\xi_2 dn \tag{11}$$

$$G = (N-1)\sigma^2 \int_{\mathbb{R}^3} \int_{S_+} f^{(2)}(t, x_1, \xi_1, x_1 + \sigma n, \xi_2)|(\xi_2 - \xi_1) \cdot n| d\xi_2 dn. \tag{12}$$

To plug these results into the modified Liouville equation (10) we need to account for the probability density's property of continuity at collisions, equation (9), that for $i = 1$ and $j = 2$ and integrated with respect to the other $N-2$ particles reads [33]:

$$f^{(2)}(t, x_1, \xi_1, x_2, \xi_2) = f^{(2)}(t, x_1, \xi_1 - n(n \cdot V), x_2, \xi_2 + n(n \cdot V)) \tag{13}$$

if $|x_1 - x_2| = \sigma$, where $V = \xi_1 - \xi_2$ and $n = -n_{12}$.

We note that, from the physics of collisions explained in equation (7)

$$\begin{aligned}\xi_1' &= \xi_1 - n(n \cdot V)\\ \xi_2' &= \xi_2 + n(n \cdot V).\end{aligned} \tag{14}$$

Thus, we have:

$$G = (N-1)\sigma^2 \int_{\mathbb{R}^3} \int_{S_+} f^{(2)}(t, x_1, \xi_1', x_1 + \sigma n, \xi_2')|(\xi_2 - \xi_1) \cdot n| d\xi_2 dn. \tag{15}$$

Let us introduce the molecular chaos hypothesis. When a real gas is considered, the number of particles involved in the dynamics is enormous and their diameter is very small. To give some context, if we take a $1\,cm^3$ box of gas we have $N \approx 10^{20}$ and $\sigma \approx 10^{-10}\,m$. This means that the product $N \cdot \sigma^2$ is finite but we can neglect the quantity $\sigma n$. When $N \to \infty$ and $\sigma \to 0$ with $N \cdot \sigma^2$ finite we are in the so-called Boltzmann-Grad limit. In this limit the molecular chaos hypothesis, or Boltzmann ansatz, can be considered valid. It states that [35] collisions are so rare that only binary ones are considered and that two particles about to collide are randomly chosen and their one-particle distribution functions are statistically independent. This yields, for particles about to collide:

$$\begin{aligned}f^{(2)}(t, x_1, \xi_1, x_2, \xi_2) &= f^{(1)}(t, x_1, \xi_1) \cdot f^{(1)}(t, x_2, \xi_2)\\ &= f^{(1)}(t, x_1, \xi_1) \cdot f^{(1)}(t, x_1 + \sigma n, \xi_2).\end{aligned} \tag{16}$$

In the Boltzmann-Grad limit and by means of the Boltzmann ansatz we can write the equation for the loss term as

$$L = N\sigma^2 \int_{\mathbb{R}^3} \int_{S_+} f^{(1)}(t, x_1, \xi_1) \cdot f^{(1)}(t, x_1, \xi_2)|(\xi_2 - \xi_1)n| d\xi_2 dn \tag{17}$$

and for the gain term, with the post-collision velocities instead of the pre-collision ones and thanks to the transformation (14):

$$G = N\sigma^2 \int_{\mathbb{R}^3} \int_{S_+} f^{(1)}(t, x_1, \xi_1') \cdot f^{(1)}(t, x_1, \xi_2')|(\xi_2 - \xi_1)n| d\xi_2 dn. \tag{18}$$

We can now write the Boltzmann equation by plugging these definitions into equation (10):

$$\begin{aligned}\frac{\partial f^{(1)}}{\partial t} + \sum_{i=1}^{N} \xi_i \cdot \frac{\partial f^{(1)}}{\partial x_i} =& N\sigma^2 \int_{\mathbb{R}^3} \int_{S_+} \Big[ f^{(1)}(t, x_1, \xi_1') \cdot f^{(1)}(t, x_1, \xi_2') + \\ &- f^{(1)}(t, x_1, \xi_1) \cdot f^{(1)}(t, x_1, \xi_2) \Big] \cdot |(\xi_2 - \xi_1)n| d\xi_2 dn.\end{aligned} \tag{19}$$

If we drop the distribution superscript to lighten the notation, equation (19) is equivalent to equation (5) if $\int_{\mathbb{R}^3}\int_{S_-}\Big[f^{(1)}(t,x_1,\xi_1')\cdot f^{(1)}(t,x_1,\xi_2') - f^{(1)}(t,x_1,\xi_1)\cdot f^{(1)}(t,x_1,\xi_2)\Big]\cdot|(\xi_2-\xi_1)n|d\xi_2 dn = Q(f,f)(t,x,\xi)$ and $N\sigma^2=\alpha$.

By boiling down the notation for the derivative with respect to time, Boltzmann equation reads

$$D_t f(t,x,\xi) = \alpha Q(f,f)(t,x,\xi). \tag{20}$$

$Q(f,f)(t,x,\xi)$ is often referred to as the interaction kernel and $\alpha$ is connected to the collision frequency. When the Boltzmann equation is applied to problems different from the gas dynamics, the interaction kernel adapts to the specific situation considered, defining the physics of the agents' interactions. For the sake of simplicity, we now replace position and velocity in the phase space with the generic variable $v \in V \subseteq \mathbb{R}$, that represents the microscopic state of the agent. In the study of interacting multi-agent systems it is of pivotal importance the mass conservation property of the interaction kernel $Q$, i.e. the trivial fact that agents do not disappear in interactions. Mathematically, this translates in

$$\int_{\mathbb{R}} Q(f,f)(t,v)dv = 0 \quad \forall t. \tag{21}$$

This property allows us to give the density $f(v,t)$ a probabilistic sense. If we start with a density $f(v,0)$ such that $\int_{\mathbb{R}} f(0,v)dv = 1$, we will be sure that this will continue to be true for all subsequent times. Hence

$$\int_{\mathbb{R}} f(t,v)dv = 1 \ \forall t > 0. \tag{22}$$

The probabilistic interpretation of the one-particle distribution function naturally implies the possibility of computing averages. For a generic observable $\varphi(v), \varphi : V \to \mathbb{R}$, it is possible to calculate the average at time $t$ over a generic random variable $X$ with probability distribution $f(t,v)$ as

$$\langle\varphi(X,t)\rangle = \int_{\mathbb{R}} \varphi(v)f(t,v)dv. \tag{23}$$

Of particular interest in our dissertation will be the observable quantities $\varphi(v)=1$ and $\varphi(v)=v$, i.e. the moments of order 0 and 1 of the microscopic state. In other applications higher order moments are used. As an example, if we assume $\varphi(v)=1$, we multiply this quantity to both members of (20) and we perform the integral on

both members we obtain an expression for the evolution of the mass in time as

$$\frac{d}{dt}\int f(t,x,\xi)dxd\xi = 0.$$

Hence, we have formally shown that the mass is conserved in time.

### 2.1.1 Maxwellian distribution

If we write the Boltzmann equation as in (20), it is clear that if a function $f = f(t,x,\xi)$ exists such that $Q(f,f) = 0$ this function is a good candidate as equilibrium point for the system. It can be proven that, if $f$ is a non-negative function such that $log(f)Q(f,f)$ is integrable, such function exists and has the form [33]

$$f(t,x,\xi) = A \cdot exp(-b(\xi - v)^2). \tag{24}$$

Equation (24) is the so-called Maxwellian distribution. Non-drifting distributions, i.e. Maxwellians with $v = 0$, are often considered. Moreover, it can be proven that the Maxwellian distribution is in fact a statistical equilibrium point for the system if and only if the parameters $A, b, v$ depends on $t$ and $x$ [33]. In fact, by means of the acclaimed H theorem [37], Boltzmann proved that the distribution function $f(t,x,\xi)$ of a rarefied gas described by the Boltzmann equation converges toward a Maxwellian distribution.

## 2.2 Binary interaction models

The type of interaction kernel that we will be using in this thesis describes binary interactions between agents. In particular, we will be dealing with interactions that involve a non-negative microscopic state that changes following an interaction rule of the type

$$\begin{aligned} v' &= p_1 v + q_1 w \\ w' &= p_2 v + q_2 w \quad p_i, q_i > 0, i = 1,2. \end{aligned} \tag{25}$$

where $v$ and $w$ are the microscopic states of the interacting agents and $p_i, q_i$ are referred to as mixing parameters and can be either stochastic or deterministic. In this work we will be dealing with symmetric interactions with $p_1 = p_2$ and $q_1 = q_2$. Let us investigate what happens to an observable quantity $\varphi(v)$ due to interactions in the more general case of stochastic parameters. If we take the interactions as instantaneous, and the event of an interaction distributed as a Bernoulli probability

distribution $T \in \{0, 1\}$ of parameter $\Delta t$ we obtain

$$\langle \varphi(v') \rangle = \langle \varphi(p_1 v + q_1 w) \rangle \cdot \Delta t + \langle \varphi(v) \rangle (1 - \Delta t),$$

where the $\langle \cdot \rangle$ indicates the expected value after a time interval $\Delta t$. Hence,

$$\frac{\langle \varphi(v') \rangle - \langle \varphi(v) \rangle}{\Delta t} = \langle \varphi(p_1 v + q_1 w) \rangle - \langle \varphi(v) \rangle. \tag{26}$$

If we compute the limit for $\Delta t \to 0^+$ we obtain $\frac{d}{dt}\langle \varphi(v) \rangle = \langle \varphi(v') \rangle - \langle \varphi(v) \rangle$. Let us explicit the average through (23):

$$\frac{d}{dt} \int_V \varphi(v) f(t, v) dv = \langle \iint_{V \times V_*} \varphi(v') f^{(2)}(t, v, w) dv dw \rangle - \int_V \varphi(v) f(t, v) dv. \tag{27}$$

In equation (27) the $\langle \cdot \rangle$ indicates the expected value over the stochastic parameters $p_i, q_i, i = 1, 2$ and $V_*$ indicates the domain of the second agent involved in the interaction. Function $f^{(2)}(t, v, w)$ is the two particle density function. Without loss of generality we shall consider $V = V_*$. The Boltzmann ansatz allows us to factorize the density function $f^{(2)}(t, v, w) = f(t, v) f(t, w)$ and, remembering the mass conservation property's consequence (22), we obtain

$$\frac{d}{dt} \int_V \varphi(v) f(t, v) dv = \langle \iint_{V \times V} \Big( \varphi(v') - \varphi(v) \Big) f(t, v) f(t, w) dv dw \rangle. \tag{28}$$

Equation 28 is the weak form of the Boltzmann equation, whose meaning is that the variation in time of the average of an observable quantity is equal to the mean variation of that same observable quantity in all interactions.

Let us show some properties of physical systems that can be obtained through this formula.

- Mass conservation is immediately clear by taking $\varphi(v) = 1$:

  $$\frac{d}{dt} \int_V 1 \cdot f(t, v) dv = 0 \Longrightarrow \int_V f(t, v) dv = cost. \tag{29}$$

  Which means that the number of agents does not change.

- Setting $\varphi(v) = v$ in (28) allows us obtain the evolution of the microscopic state that depends on the interaction rule. If the mixing parameters are such that

  $$\langle p_1 + q_2 \rangle = \langle p_2 + q_1 \rangle = 1, \tag{30}$$

  we have a so-called conservative model and the average $\int_V v f(t, v) dv = m(t)$

is conserved. In the symmetric case we have

$$\frac{dm(t)}{dt} = \langle p + q - 1 \rangle m, \tag{31}$$

that is 0 if (30) is true. Otherwise, $m$ has an exponential trend either toward 0 or $\infty$.

- If we take $\varphi(v) = v^2$ we obtain the second moment of the microscopic state, namely the energy of the system. In fact, we know from physics that the second order moment of velocity is, disregarding the mass, the kinetic energy $K(t)$. The kinetic energy has two components, one due to molecular agitation, called internal energy, and the other due to the mean movement $m(t)$ of molecules. Mathematically, with unitary mass, this reads

$$K(t) = e(t) + m(t)^2 \,. \tag{32}$$

If we impose $\int_V v^2 f(v,t)dv = K(t)$ and we compute the variance of the probability distribution $f(v,t)$, we obtain

$$\begin{aligned} Var(f) &= \int_V (v-m)^2 f(t,v)dv = \\ &= \int_V v^2 f(t,v)dv - 2m \int_V v f(t,v)dv + m^2 \int_V f(t,v)dv = \\ &= K(t) - m(t)^2 = e(t) \,. \end{aligned} \tag{33}$$

Thus, the variance of the probability distribution is equal to the internal energy of the system. For symmetric interactions the evolution of the energies reads

$$\begin{aligned} \frac{dE}{dt} &= \langle p^2 + q^2 - 1 \rangle E + 2\langle pq \rangle m^2, \\ \frac{de}{dt} &= \langle p^2 + q^2 - 1 \rangle e + \langle (p + q - 1)^2 \rangle m^2 \end{aligned} \tag{34}$$

and both tend asymptotically to a finite non-vanishing value if $\langle p^2 + q^2 \rangle < 1$.

The Boltzmann equation with the appropriate binary interaction rule allows us to describe manifold physical systems in which the interaction between agents is determinant for the dynamics of the system. As we will see, often other mechanisms can affect the dynamics and the challenge is to include them into this theoretical framework.

## 2.3 Label switch process

One of the mechanisms above mentioned is a label switch process. This idea has been introduced in [32]. Let us imagine that agents in the system are equipped with a label that identifies the group whose the agent belongs to. The label is $x \in \mathcal{I} = \{1, ..., n\}$. Let us consider here a non-negative microscopic state. The agents' label changes following a discrete Markov-type stochastic jump process defined by a transition probability

$$T = T(t, v; x|y) \in [0, 1] \quad \forall v \in \mathbb{R}_+, x, y \in \mathcal{I}, t > 0. \tag{35}$$

Hence, an agent in the group $y$ has a probability $T$, that depends on his state $v$ and on time, to jump into group $x$ at time $t$, if a transition occurs. T is a probability density if satisfies the normalization condition:

$$\int_{\mathcal{I}} T(t, v; x|y)dx = \sum_{i=1}^{n} T(t, v; i|y) = 1 \quad \forall v \in \mathbb{R}_+, y \in \mathcal{I}, t > 0. \tag{36}$$

This also ensures the mass conservation property to hold. The agents are therefore divided into groups when they interact in the binary interaction model. The model accounts for possible differences in interaction rules for contacts within the same group or between different groups. In order to unify these mechanisms we have to give a kinetic description of the label switch process. Thus, we take a distribution function $f(t, x) \geq 0$ of agents with label $x$ at time $t$ and compute its evolution with a kinetic equation describing the jump process, of the same type as equation (28):

$$\frac{d}{dt} \int_{\mathcal{I}} \varphi(x) f(t, x)dx = \lambda \iint_{\mathcal{I}\times\mathcal{I}} \Big(\varphi(x) - \varphi(y)\Big) T(t; x|y) f(t, y)dxdy. \tag{37}$$

Where $\lambda > 0$ represents the constant switch frequency. We can exploit the fact that $\mathcal{I}$ is discrete to decompose $f(t, x)$ in separated components such that

$$f(t, x) = \sum_{i=1}^{n} f_i(t)\delta(x - i), \tag{38}$$

where $f_i(t)$ is the probability distribution restricted to the $i$-th group and $\delta(x - i)$ is the Dirac distribution centered in $x = i$. By plugging this definition into equation (37) and replacing the integral with a sum, we obtain

$$\sum_{i=1}^{n} \varphi(i) f_i'(t) = \lambda \sum_{i=1}^{n} \sum_{j=1}^{n} \Big(\varphi(i) - \varphi(j)\Big) T(t; i|j) f_j(t). \tag{39}$$

It is possible now to show the evolution of a single group's distribution. If we chose $\varphi(i) = 1$ for a certain $i \in \mathcal{I}$ and $\varphi(x) = 0\ \forall x \in \mathcal{I} \setminus \{i\}$ we are counting agents with label $i$. By plugging this observable into equation (39), we obtain the evolution of the density of one group as

$$f_i'(t) = \lambda \left( \sum_{j=1}^{n} T(t; i|j) f_j(t) - f_i(t) \right) \quad i = 1, ..., n. \tag{40}$$

We are now ready to merge the two descriptions, i.e. interacting agents that are characterized by a switching label. We present the calculations for the most simple case, in which agents are equipped with one microscopic state $v$ and one label $x$ and there is only one mechanism that influence each variable. More complicated cases can easily be derived from this description and will be covered in the next chapters, where we will discuss two labels and two state-involving mechanisms for the application to epidemiology. Thus, we want to write a weak Boltzmann equation for the joint distribution function $f(t, x, v) \geq 0$, namely the proportion of agents with label $x \in \mathcal{I}$ and microscopic state in $[v, v + dv]$ at time $t$. With the same reasoning adopted before we can discretize the distribution

$$f(t, x, v) = \sum_{i=1}^{n} f_i(t, v) \delta(x - i). \tag{41}$$

As we have shown above, both for the interaction process and the jump process the mass conservation property holds. Hence, we can assign a probabilistic sense to $f(t, x, v)$ by normalization:

$$\sum_{i=1}^{n} \int_{\mathbb{R}_+} f_i(0, v) dv = 1,$$

and hence,

$$\sum_{i=1}^{n} \int_{\mathbb{R}_+} f_i(t, v) dv = 1 \ \ \forall t > 0. \tag{42}$$

The addends of the sum are the masses of the agents with label $i$,

$$\rho_i(t) := \int_{\mathbb{R}_+} f_i(t, v) dv, \tag{43}$$

that satisfies

$$0 \leq \rho_i(t) \leq 1 \ \ \forall i,$$

$$\sum_{i=1}^{n} \rho_i(t) = 1 \ \ \forall t > 0.$$

Let us consider the random variable pair $(X_t, V_t) \in \mathcal{I} \times \mathbb{R}_+$ representing label and state of an agent at time $t$. During the small time interval $\Delta t > 0$ the agent may change their label or state, depending on if a label switch occurred or a binary interaction occurred instead. None of them and both of them are also possibilities. This situation is easily described with a discrete time random process involving the random variables $(X_t, V_t)$:

$$\begin{cases} X_{t+\Delta t} &= (1-\Theta)X_t + \Theta J_t \\ V_{t+\Delta t} &= (1-\Xi)V_t + \Xi V_t' \,. \end{cases} \tag{44}$$

Where $J_t$ is the new label, $V_t'$ the post interaction state and $\Theta, \Xi$ are Bernoulli random variables, independent from the other quantities, that represent the event of, respectively, a label switch or a binary interaction. Considering the time interval $\Delta t$ we take

$$\begin{cases} P(\Theta = 1) &= \lambda \Delta t \\ P(\Xi = 1) &= \mu \Delta t \,, \end{cases} \tag{45}$$

with $\Delta t \leq min\{\frac{1}{\lambda}; \frac{1}{\mu}\}$ for consistency, being $P$ a probability. Quantities $\frac{1}{\lambda}$ and $\frac{1}{\mu}$ are mean time intervals between two consecutive interactions or label switches, respectively. We are assuming as true the intuitive fact that the bigger the time interval, the bigger the probability of having an event and we are considering time intervals small enough to contain, with satisfactory approximation, a single event of the same type. We are characterizing the label switch process with the random variable $J_t \in \mathcal{I}$ and the interactions with the random variable $V_t' \in \mathbb{R}_+$ . If $P(t, j, v)$ is the joint probability distribution function of the post label switch pair $(J_t, V_t)$, we will have

$$P(t, j, v) = \int_{\mathcal{I}} T(t, v; j|y) f(t, y, v) dy = \sum_{i=1}^{n} T(t, v, j|i) f_i(t, v). \tag{46}$$

This means that the probability for an agent with microscopic state $v$ to be at time $t$ in the $j$-th group is the sum of the transition probabilities from all the groups toward group $j$, multiplied by the density of each group.

If a binary interaction happens instead, the post event pair will be $(X_t, V_t')$. To account for possible differences in the interaction rule depending on the groups, let

us define

$$V_t' \hat{=} \delta_{X_t,Y_t}\bar{V}_t' + (1-\delta_{X_t,Y_t})\tilde{V}_t' \,, \tag{47}$$

where $\delta_{X_t,Y_t}$ is the Kronecker delta and

$$\begin{aligned}\bar{V}_t' &= \bar{p}V_t + \bar{q}V_t^* \\ \tilde{V}_t' &= \tilde{p}V_t + \tilde{q}V_t^* \,,\end{aligned}$$

where $V_t^*$ is the state of the other agent in the interaction and $\bar{p}, \bar{q}, \tilde{p}, \tilde{q} \in \mathbb{R}$ are mixing parameters. Let us investigate the evolution of a observable quantity $\varphi = \varphi(x,v) : \mathcal{I} \times \mathbb{R}_+ \to \mathbb{R}$. If we consider a time interval $\Delta t$, the mean variation of $\varphi$ is

$$\frac{\langle \varphi(X_{t+\Delta t}, V_{t+\Delta t})\rangle - \langle \varphi(X_t, V_t)\rangle}{\Delta t}$$

and, plugging in the information from equations (44) and (45):

$$\begin{aligned}\frac{\langle \varphi(X_{t+\Delta t}, V_{t+\Delta t})\rangle - \langle \varphi(X_t, V_t)\rangle}{\Delta t} &= \left.\frac{(1-\lambda\Delta t)\cdot(1-\mu\Delta t)\langle\varphi(X_t,V_t)\rangle}{\Delta t}\right\} no\, event \\ &+ \left.\frac{(1-\lambda\Delta t)\cdot\mu\Delta t\langle\varphi(X_t,V_t')\rangle}{\Delta t}\right\} interaction \\ &+ \left.\frac{\lambda\Delta t\cdot(1-\mu\Delta t)\langle\varphi(J_t,V_t)\rangle}{\Delta t}\right\} label\, switch \\ &+ \left.\frac{\lambda\Delta t\cdot\mu\Delta t\langle\varphi(J_t,V_t')\rangle}{\Delta t}\right\} both \\ &- \frac{\langle\varphi(X_t,V_t)\rangle}{\Delta t}\,.\end{aligned} \tag{48}$$

If we let $\Delta t \to 0^+$ and perform the limit, we obtain, for the istantaneous time variation:

$$\frac{d}{dt}\langle\varphi(X_t,V_t)\rangle = \lambda\langle\varphi(J_t,V_t)\rangle + \mu\langle\varphi(X_t,V_t')\rangle - (\lambda+\mu)\langle\varphi(X_t,V_t)\rangle. \tag{49}$$

Let us stress how the case where both events occur, as it is quadratic with respect to time, has been neglected as $\Delta t \to 0^+$. We can further divide the interaction member in the left-hand side due to equation (47) and obtain

$$\begin{aligned}\frac{d}{dt}\langle\varphi(X_t,V_t)\rangle &= \lambda\langle\varphi(J_t,V_t)\rangle + \mu\langle\delta_{X_t,Y_t}\varphi(X_t,\bar{V}_t')\rangle + \\ &+ \mu\langle(1-\delta_{X_t,Y_t})\varphi(X_t,\tilde{V}_t')\rangle - (\lambda+\mu)\langle\varphi(X_t,V_t)\rangle.\end{aligned} \tag{50}$$

Considering (41), we have:

- $\langle \varphi(J_t, V_t) \rangle = \sum_{i=1}^{n} \sum_{j=1}^{n} \int_{\mathbb{R}_+} \varphi(i, v) \cdot T(t, v; i|j) f_j(t, v) dv \,,$
- $\langle \delta_{X_t, Y_t} \varphi(X_t, \bar{V}_t') \rangle = \sum_{i=1}^{n} \int_{\mathbb{R}_+} \int_{\mathbb{R}_+} \langle \varphi(i, \bar{v}') \rangle \cdot f_i(t, v) f_i(t, v_*) dv dv_* \,,$
- $\langle (1 - \delta_{X_t, Y_t}) \varphi(X_t, \tilde{V}_t') \rangle = \sum_{i=1}^{n} \sum_{j=1, j \neq i}^{n} \int_{\mathbb{R}_+} \int_{\mathbb{R}_+} \langle \varphi(i, \tilde{v}') \rangle \cdot f_i(t, v) f_j(t, v_*) dv dv_* \,,$

where, likewise we did before, the mean value inside the integral has to be intended with respect to possible stochastic mixing parameters and the hypothesis of molecular chaos holds. It is now possible to finally write a weak Boltzmann-type equation for the joint distribution function:

$$\begin{aligned} \frac{d}{dt} \sum_{i=1}^{n} \int_{\mathbb{R}_+} \varphi(i, v) f_i(t, v) dv = \lambda \sum_{i=1}^{n} \sum_{j=1}^{n} \int_{\mathbb{R}_+} \varphi(i, v) T(t, v; i|j) f_j(t, v) dv \\ + \mu \sum_{i=1}^{n} \int_{\mathbb{R}_+} \int_{\mathbb{R}_+} \langle \varphi(i, \bar{v}') \rangle f_i(t, v) f_i(t, v_*) dv dv_* \\ + \mu \sum_{i=1}^{n} \sum_{j=1, j \neq i}^{n} \int_{\mathbb{R}_+} \int_{\mathbb{R}_+} \langle \varphi(i, \tilde{v}') \rangle f_i(t, v) f_j(t, v_*) dv dv_* \\ - (\lambda + \mu) \sum_{i=1}^{n} \int_{\mathbb{R}_+} \varphi(i, v) f_i(t, v) dv \,. \end{aligned} \tag{51}$$

Equation (42) allows us to include the loss term (the last term in the left-hand side of equation (51)) into the gain terms. If we take $\varphi(x, v) = \psi(x)\phi(v)$, with $\psi(i) = 1$ for a certain $i$ and $\psi(j) = 0 \; \forall j \neq i$ we can write equation (51) for a single group $i$ as

$$\begin{aligned} \frac{d}{dt} \int_{\mathbb{R}_+} \phi(v) f_i(t, v) dv = \lambda \int_{\mathbb{R}_+} \phi(v) \Big( \sum_{j=1}^{n} T(t, v; i|j) f_j(t, v) - f_i(t, v) \Big) dv \\ + \mu \int_{\mathbb{R}_+} \int_{\mathbb{R}_+} \langle \phi(v') - \phi(v) \rangle f_i(t, v) f_i(t, v_*) dv dv_* \\ + \mu \sum_{j=1, j \neq i}^{n} \int_{\mathbb{R}_+} \int_{\mathbb{R}_+} \langle \phi(\tilde{v}') - \phi(v) \rangle f_i(t, v) f_j(t, v_*) dv dv_* \\ i = 1, ..., n \,. \end{aligned} \tag{52}$$

Equation (52) is a non-conservative weak Boltzmann equation for the density of each group $f_i$. Of course, the agents' mass within each group is not constant and the mass conservation property holds only for the whole system. If we take $\phi(v) = 1$

we can compute the mass for the i-th group as

$$\begin{aligned}\frac{d}{dt}\rho_i(t) &= \lambda \int_{\mathbb{R}_+} \sum_{j=1}^{n} T(t,v;i|j) f_j(t,v) - f_i(t,v) dv \\ &= \lambda \sum_{i=1}^{n} \int_{\mathbb{R}_+} T(t,v;i|j) f_j(t,v) dv - \lambda \rho_i(t)\,. \end{aligned} \tag{53}$$

Not surprisingly, it turns out to depend on the label switch process only, since the interactions only involve the microscopic state $v$ and not the label $x$.

The formalism just introduced is quite general and allows to describe a wide plethora of situations. We recommend [32] and [36] for a complete dissertation on the topic.

As for this thesis in concerned, two interaction cases will be adopted in the next chapters: same interaction rule for all agents and interaction among agents in the same group only. Let us discuss these two situations:

- To have the same interaction rule for all agents means, mathematically, that $\bar{v}' = \tilde{v}' = v'$ and equation (52) becomes

$$\begin{aligned}\frac{d}{dt}\int_{\mathbb{R}_+} \phi(v) f_i(t,v) dv = \lambda \int_{\mathbb{R}_+} \phi(v) \Big( \sum_{j=1}^{n} T(t,v;i|j) f_j(t,v) - f_i(t,v) \Big) dv \\ + \mu \sum_{j=1}^{n} \int_{\mathbb{R}_+} \int_{\mathbb{R}_+} \langle \phi(v') - \phi(v) \rangle f_i(t,v) f_j(t,v_*) dv dv_* \\ i = 1, ..., n\,. \end{aligned} \tag{54}$$

- To have interaction among same-labelled agents only could be modeled by letting the inter-group interactions be ineffective. Mathematically, this can be achieved by imposing $\tilde{v}' = v$. Thus, we obtain

$$\begin{aligned}\frac{d}{dt}\int_{\mathbb{R}_+} \phi(v) f_i(t,v) dv = \lambda \int_{\mathbb{R}_+} \phi(v) \Big( \sum_{j=1}^{n} T(t,v;i|j) f_j(t,v) - f_i(t,v) \Big) dv \\ + \mu \int_{\mathbb{R}_+} \int_{\mathbb{R}_+} \langle \phi(v_i') - \phi(v) \rangle f_i(t,v) f_i(t,v_*) dv dv_* \\ i = 1, ..., n\,. \end{aligned} \tag{55}$$

  Here, the post-interaction state $v_i'$ and therefore the interaction rule is taken potentially dependent on the label of the agents. It is of pivotal importance to remember that interactions among agents with different labels do not vanish, they happen without producing an effect. This seemingly subtle difference is fundamental when numeric simulations are implemented, since the algorithm

has to account for this. The expected number of interactions is $\mu\Delta t$ and not counting the effect-less interactions in this number leads to perform to many interactions.

## 2.4 Hydrodynamic limit

The description of a system by means of the Boltzmann equation is by its very essence microscopic. If we want to analyze a system composed by a large number of particles it is often more convenient to appeal to macroscopic equations. The same thing is true when we want to consider the effects of slower mechanisms influencing a system of agents interacting on a much faster scale. The hydrodynamic limit is the mathematical tool that allows to describe the system on larger scales, both spatial and temporal. To introduce this, let us take a step back and consider a physical system of particles in a gas. Remembering the notation used in sec. 2.1, we consider the density function $f = f(t, x, \xi)$ describing the probability to find a particle with position in $[x, x + \Delta x]$ and $[\xi, \xi + \Delta\xi]$ at time $t$. We consider a box $\Lambda^\delta$ of side $\delta^{-1}$, where $\delta$ will be sent to zero as the limit is performed. We assume that the number of particles in the box is proportional to its volume ([33]):

$$\int_{\Lambda^\delta \times \mathbb{R}^3} f(t, x, \xi) dx d\xi = \delta^{-3} \quad \forall t. \tag{56}$$

The Boltzmann equation describes the time evolution of the system. Hence, we have

$$D_t f(t, x, \xi) = \alpha Q(f, f)(t, x, \xi)\,, \tag{57}$$

where $D_t = \frac{\partial}{\partial t} + \xi \frac{\partial}{\partial x}$ indicates whole derivation with respect to time. If we look at the whole system, though, the microscopic variables $t$ and $x$ are inappropriate to well describe the behavior of the gas and we would prefer variables of the same order of magnitude of the box. Hence, let us define the new variables

$$\begin{aligned} r &= \delta x \quad r \in \Lambda \\ T &= \delta t \quad T \in \mathbb{R}_+ \end{aligned} \tag{58}$$

and the density function

$$\hat{f}(r, \xi, t) = f(x, \xi, t) \tag{59}$$

normalized to unity

$$\int_{\Lambda\times\mathbb{R}_+} \hat{f}(r,\xi,t)drd\xi = 1. \tag{60}$$

Owing to equation (59), macroscopic and microscopic description are equivalent and they differ only on the scale of the parameters. Since microscopic quantities such as mean free path and mean free time are of the same order as $\delta$, if we assume $\delta \to 0^+$, on the macroscopic scale they turn out to be infinitesimal. If we write the macroscopic Boltzmann equation

$$\frac{\partial \hat{f}}{\partial T} + \xi \cdot \frac{\partial \hat{f}}{\partial r} = \delta^{-1}\alpha Q(f,f)(T,r,\xi)\,, \tag{61}$$

we note that the right-hand side is scaled by a factor $\delta^{-1}$. This means that the interaction kernel has to be of the same order as $\delta$ to secure equation (61) to hold, i.e. each interaction account for a infinitesimal change of the variables [35]. Let us now consider a neighborhood of point $r \in \Lambda$. According to the kinetic theory, on the fast time scale $t$ the density function of the portion of gas in this neighborhood will assume, reaching equilibrium, the shape of a Maxwellian. This distribution will have parameters $A(\delta^{-1}r), b(\delta^{-1}r), v(\delta^{-1}r)$ related with fluid-dynamic macroscopic quantities such as density, energy and drift. This parameters will evolve on the macroscopic scale according to the classical fluid-dynamic laws. Thus, we have individuated two dimensional scales. The microscopic scale is the one where the kinetic interpretation holds and where Maxwellian equilibrium is quickly reached, the macroscopic scale is the one where fluid-dynamic laws hold and is where the Maxwellian parameters evolve. For a rigorous and complete description we recommend [35].

In this dissertation, we will be dealing with a scaling that involves only the time variable $t$. Let us introduce a kinetic system in the variables $(t,v) \in \mathbb{R}_+ \times \mathbb{R}$ with two different kernels $Q(f,f)(t,v)$ and $P(f,f)(t,v)$. We can write a Boltzmann-type equation for the evolution of this system as

$$D_t f(t,v) = \lambda Q(f,f)(t,v) + \mu P(f,f)(t,v)\,, \tag{62}$$

where $\lambda, \mu$ take the meaning of interaction rates. Let us assume that the two events take place on very different time scales. Mathematically, we let $\delta \to 0$ and we state $\lambda \approx 1$ and $\mu \approx \delta^{-1}$. Without loss of generality we can take $\lambda = 1$ and $\mu = \delta^{-1}$. By

means of this argument equation (62) can split in

$$\begin{aligned} D_t f(t,v) &= \delta^{-1} \cdot P(f,f)(t,v) \\ D_t f(t,v) &= Q(f,f)(t,v)\,, \end{aligned} \tag{63}$$

where the first equation operates on the fast time scale, while the second equation operates on the slow one. Let us note that for equation (63) to hold we have to assume that $P$ is of the same order as $\delta$. Let us define a new time scale

$$\tau \hat{=} \delta^{-1} t \tag{64}$$

and refer to it as the fast time, while the slow time is $t$, and a new density function

$$\tilde{f}(\tau, v) = f(t, v). \tag{65}$$

Hence, we can rewrite equation (63) as

$$\begin{aligned} D_\tau f(\tau,v) &= P(f,f)(\tau,v) \\ D_t f(t,v) &= Q(f,f)(t,v) \end{aligned} \tag{66}$$

and give the following interpretation. On the fast time $\tau$ the density $f$ quickly evolves by action of $P$ toward its (possible) equilibrium, e.g. a Maxwellian distribution. On the slow time the reached configuration evolves through the evolution of its characteristic parameters, e.g. density, mean microscopic state and energy, by action of $Q$.

## 2.5 Numerical Methods

In the previous sections, we have presented the main analytical tools that will be employed in this thesis. In particular, the Boltzmann equation (5) is the foundation of the models here depicted. Unfortunately, as an integro-differential equation, it is analytically solvable only in a few simplified cases and sophisticated numerical methods are required. Moreover, as it is common in this field, theoretical findings will be supported by numerical simulations. It is therefore clear that numerical methods are of pivotal importance in the study we are carrying out in this dissertation. We propose here a brief description of the algorithms and techniques adopted in the following sections, for a more complete picture we recommend [41]. The large number of agents in the population and the non-linear integral that describes the interaction among them makes the numerical solution of the Boltzmann equation

(5) computationally expensive [41]. A probabilistic Monte Carlo (MC) approach to the matter has proven to be preferable to deterministic methods for two main reasons. The computational cost is noticeably reduced and no discretization grid is required, since variables can assume any value.

Firstly, let us define Monte Carlo integration in general terms and investigate its approximating error. We want to evaluate the integral

$$I[g] = \int_{\Omega} g(x) \cdot f(x) dx, \ \Omega \subseteq \mathbb{R}^d, d \geq 1 \,, \tag{67}$$

where $0 \leq f(x) \leq 1$ is a probability density function. If we take the random vector $X$ distributed as $f(x)$, the equality

$$I[g] = \mathbb{E}\Big(g(X)\Big) \tag{68}$$

holds [34]. Moreover, if $X_n$ is a sequence of $N$ pseudo-random vectors distributed as $f(x)$, we can write [34]

$$\bar{I}_N[g] = \frac{1}{N} \sum_{i=1}^{N} g(X_i), \quad \mathbb{E}\Big(\bar{I}[g]\Big) = I[g]. \tag{69}$$

Remembering the law of large numbers

$$\lim_{N \to \infty} P(|\bar{I}_N[g] - I[g]| > \varepsilon) = 0 \ \ \forall \varepsilon > 0 \,, \tag{70}$$

where $\bar{I}_N[g]$ is the integration by means of Monte Carlo method of the integral $\int_{\Omega} g(x) \cdot f(x) dx$. Let us now define the independent identically distributed random sequence

$$Y_n = \frac{\Big(I[g] - g(X_n)\Big)}{\sigma_g} \tag{71}$$

where $\sigma_g^2 = \int_{\Omega} \Big(g(x) - I[g]\Big)^2 f(x) dx$ is the variance of $g(X_n)$. We have, given equation (68),

$$\begin{aligned} \mathbb{E}(Y_i) &= 0 \\ \mathbb{E}(Y_i^2) &= \int_{\Omega} \frac{\Big(I[g] - g(X_n)\Big)^2}{\sigma_g^2} dx = 1 \\ \mathbb{E}(Y_i \cdot Y_j) &= 0 \ \ i \neq j \,. \end{aligned} \tag{72}$$

Let us define the Monte Carlo integration error as

$$\epsilon_N[g] := I[g] - \bar{I}_N[g]. \tag{73}$$

If we consider the sum $S_N[g] = \frac{1}{N}\sum_{i=1}^{N} Y_i = \frac{\epsilon_N[g]}{\sigma_g}$ and we remember the independence of $Y_i$'s:

$$\begin{aligned}
\mathbb{E}(S_N^2[g]) &= \mathbb{E}\left(\frac{1}{N^2}\left(\sum_{i=1}^{N} Y_i\right)^2\right) \\
&= \frac{1}{N^2}\left[\mathbb{E}\left(\sum_{i=1}^{N} Y_i^2\right) + \mathbb{E}\left(\sum_{i=1}^{N}\sum_{j=1,j\neq i}^{N} Y_i \cdot Y_j\right)\right] \\
&= \frac{1}{N^2}(N+0) = \frac{1}{N}\,.
\end{aligned} \tag{74}$$

We thus obtain for the Monte Carlo error

$$\mathbb{E}(\epsilon_N[g]^2)^{\frac{1}{2}} = \mathbb{E}\Big((I[g] - \bar{I}_N[g])^2\Big)^{\frac{1}{2}} = \sigma_g N^{-\frac{1}{2}}. \tag{75}$$

Hence, the convergence rate of the Monte Carlo integration is $O(\sigma_g N^{-\frac{1}{2}})$. In addition to that, by means of the central limit theorem we can assert that $(\bar{I}_N[g] - I[g])/(\sigma_g N^{-\frac{1}{2}})$ is distributed as a standard normal distribution [34]. Let us remark that, for a deterministic grid-based method of order $r$, the convergence rate is $O(N^{-\frac{r}{d}})$ [34], this means that Monte Carlo integration should be better if $\frac{r}{d} \leq \frac{1}{2}$. As a general rule, Monte Carlo methods are less precise than deterministic algorithms, but they are preferable when the dimension of the problem $d$ is high. As we have seen, the error in MC integration is $\varepsilon_N = O(\sigma_g N^{-\frac{1}{2}})$, which means that a low variance $\sigma_g$ of the statistical samples is the key to a precise and computationally feasible integration. Thus, various variance reduction methods have been developed, we recommend [44]. This general argument can be restricted to the computation of integral of the type $\int_\Omega g(x)dx,\ \ d \geq 1$ by taking $X_n$ uniformly distributed. In fact, we will be mainly interested in evaluating moments of order zero and one of the density $f(x)$, i.e.

$$\begin{aligned}
M^k[f] &= I[x^k] = \int_\Omega f(x)\cdot x^k dx \ \ k = 0, 1 \\
\bar{M}_N^k[f] &= \frac{1}{N}\sum_{n=1}^{N}(X_n)^k \ \ k = 0, 1.
\end{aligned} \tag{76}$$

We will be focusing on algorithms known as direct simulation Monte Carlo (DSMC) and in particular on the so-called Nanbu-Babovsky scheme [39]. Another important DSMC scheme is the one owed to G.A. Bird [40]. These methods consist in evolving

a finite set of agents that randomly interact with one another. Hence, in some sense they simulate the physics of the process at a microscopic level rather than to solve the Boltzmann equation. Let us consider a gas system and the Boltzmann equation with initial condition that describes the distribution of its particles

$$\begin{aligned} \frac{\partial f(t,x,\xi)}{\partial t} + \xi \cdot \nabla_x f(t,x,\xi) &= \alpha Q(f,f)(t,x,\xi) \\ f(0,x,\xi) &= f_0(x,\xi)\,. \end{aligned} \tag{77}$$

Usually, a splitting operation is used to simplify the problem. The collision term and the convection term are solved separately, the latter using as initial condition the result of the former. Hence, the first step will be to integrate for all $x \in \Omega$

$$\begin{cases} \frac{\partial \mathring{f}}{\partial t} & = \alpha Q(\mathring{f},\mathring{f}) \\ \mathring{f}(0,x,\xi) & = f_0(x,\xi) \end{cases} \tag{78}$$

and the second will be to solve

$$\begin{cases} \frac{\partial f}{\partial t} + \xi \cdot \nabla_x f & = 0 \\ f(0,x,\xi) & = \mathring{f}(\Delta t,x,\xi)\,. \end{cases} \tag{79}$$

This process gives the solution after a time step $\Delta t$ and can be iterated at will to obtain the evolution of $f(t,x,\xi)$. The schemes from Bird and Nanbu apply to the first step, it being the non linear and hence the more complicated one. Let us assume that the operator is spatially homogeneous and that it can be divided into its gain and loss components as in system (80). This is true for Boltzmann equation for Maxwellian gas [41], i.e. gases where $Q(f,f)(\xi) = \int_{\mathbb{R}^3}\int_S \sigma(n)\cdot\Big[f(\xi_1')f(\xi_2') - f(\xi_1)f(\xi_2)\Big]dnd\xi_2$. Problem (78) now reads

$$\begin{cases} \frac{\partial \mathring{f}}{\partial t} & = \alpha\Big[Q^+(\mathring{f},\mathring{f}) - \mu f\Big] \\ \mathring{f}(0,x,\xi) & = f_0(x,\xi)\,, \end{cases} \tag{80}$$

where $\mu \neq 0$ is a constant. We divide the time interval $[0,t_{max}]$ into $n_{TOT}$ steps of size $\Delta t = \frac{t_{max}}{n_{TOT}}$. If we apply the forward Euler scheme to the problem we obtain

$$f^{n+1} = (1-\alpha\mu\Delta t)f^n + \alpha\mu\Delta t\cdot\frac{Q^+(f^n,f^n)}{\mu}, \tag{81}$$

where $f^n(\xi)$ is an approximation of $f(n\cdot\Delta t,\xi)$. Equation (81) can be interpreted as

follows. In each time step, a particle with velocity $\xi$ does not interact with probability $(1-\alpha\mu\Delta t)$ and does interact with inverse probability $\alpha\mu\Delta t$. If the interaction happens, the interaction law contained in the collision kernel applies. A version of Nanbu's scheme for velocity-independent kernels is reported in Algorithm 1.

**Algorithm 1** Nanbu scheme

**Data:**

- $N \in \mathbb{N}$ total number of particles.
- $\mathbb{V}^0 := \{\xi_1^0, ..., \xi_N^0\}$ initial velocities, sampled from initial density $f_0(\xi)$.
- $\Delta t$ time interval and $n_{TOT}$ number of time steps.

```
for n = 1 to n_TOT
    for i = 1 to N
        sample Ξ ~ Bernoulli(αμΔt)
        if Ξ == 0
            set ξ_i^{n+1} = ξ_i^n
        else
            select a random particle j
            set ξ^{n+1} according to the interaction rule
            between particle i and particle j
    end for
end for
```

The main problem rising from Algorithm 1 is that energy and impulse are not conserved in each collision, but only on average [42]. Babovsky [39] tackled this objection, introducing a conservative version of the Nanbu's scheme, reported in Algorithm 2.

In this version of the algorithm particles are selected in pairs and both particles, at the same time, evolve according to the microscopic rule that describes the binary collision, making it possible to conserve energy and impulse. The Nanbu-Babovsky scheme converges to the solution of the Boltzmann equation under suitable constraints [43]. As we have seen, DSMC methods are straightforward and easy to implement and their computational cost is fairly low, it being $O(N)$ while the cost for deterministic methods is $O(N^\alpha)$with $\alpha \geq 2$ [34].

**Algorithm 2** Nanbu-Babovsky scheme

**Data:**

- $N \in \mathbb{N}$ total number of particles.
- $\mathbb{V}^0 := \{\xi_1^0, ..., \xi_N^0\}$ initial velocities, sampled from initial density $f_0(\xi)$.
- $\Delta t$ time interval and $n_{TOT}$ number of time steps.

**for** $n = 1$ to $n_{TOT}$

set $N_c = \lfloor \frac{N}{2} \alpha \mu \Delta t \rfloor$
sample $Round \sim Bernoulli(\frac{N}{2} \alpha \mu \Delta t - N_c)$
set $N_c = N_c + Round$
select $N_c$ pairs $(i, j)$ uniformly
set $\xi_i^{n+1}$ and $\xi_j^{n+1}$ according to the
interaction rule
set $\xi_i^{n+1} =$
$\xi_i^n$ for the particles that have not been selected

**end for**

# 3 Kinetic models for epidemiology

This dissertation aims to describe a possible kinetic approach to the study of epidemiology. The mathematical tools presented in the above section can successfully be applied to model various aspects of the spread of an infectious disease in a population and the confinement methods adopted to stem it. In the following sections we will firstly show how the classical models described above, i.e. SIR and SIS models, can be obtained in a kinetic environment directly from the label switch process of sec. 2.3. Then, we will analyze in depth two confinement methods, namely the quarantine of diagnosed individuals and the vaccination of the population. In fact, these have been the confinement strategies adopted in 2020 and 2021 by the majority of the nations on the planet to face the SARS-CoV-2 pandemic, and that are in effect while the authors are writing.

## 3.1 Classical models

The ODE-based models such as SIR and SIS describe the evolution of the epidemic through the evolution of the size of certain compartments of population. Individuals switch from one compartment to another following rules specific to the model and to the level of complexity adopted. In the simple SIR and SIS models described in sec. 1.2.1 and sec. 1.2.2 the transition rates are either constant or directly proportional to the classes' size. The microscopic label switch process described in sec. 2.3 can be seen as a model of the underlying dynamics happening in the population that lead to the macroscopic description of SIR and SIS models. In this section, we will show how these two models are specific cases of a kinetic Markov-type label switch process. Let us begin with the SIR model. We take three possible labels $x \in \mathcal{I}_{SIR} = \{1, 2, 3\}$, indicating, respectively, the three population classes susceptible, infected and removed. We also take the transition probability $T = T(t, x|y)$ in order to match, in the macroscopic limit, the SIR model. If we remember the meaning of the function $f = f(t, x)$ as relative mass of the agents with label $x$ at time $t$ and the discretization owed to (38), we can define the transition probabilities as

$$\begin{array}{ccc} T(t;1|1) = 1 - \beta f_2(t) & T(t;2|1) = \beta f_2(t) & T(t;3|1) = 0 \\ T(t;1|2) = 0 & T(t;2|2) = 1 - \gamma & T(t;3|2) = \gamma \\ T(t;1|3) = 0 & T(t;2|3) = 0 & T(t;3|3) = 1 \end{array} , \tag{82}$$

where $\beta$ is the transmission rate constant and $\gamma$ is the recovery rate with the same meaning as in sec. 1.2.1. Note that transition probabilities (82) are consistent proba-

bilities and satisfy the normalization condition $\sum_i T(t;i|j) = 1 \ \forall j$, that also ensures the mass conservation property to hold. We can now write the weak Boltzmann-type equation (39) for the evolution of an observable quantity $\varphi(x)$ within a class $i$:

$$\sum_{i=1}^{3} \varphi(i) f_i'(t) = \sum_{i=1}^{3}\sum_{j=1}^{3} \Big(\varphi(i) - \varphi(j)\Big) T(t;i|j) f_j(t), \tag{83}$$

where the superscript indicates the derivative with respect to time and $\lambda$ has been assumed unitary. Hence, it is possible to compute the time evolution of the mass of each class in the population in the same way we did for equation (40). Plugging in the transition probabilities (82), we obtain

$$\begin{cases} f_1' = & -\beta f_1 f_2 \\ f_2' = & \beta f_1 f_2 - \gamma f_2 \\ f_3' = & \gamma f_2, \end{cases} \tag{84}$$

that is a SIR model.

The same type of reasoning can be extended to the SIS model. In this case, the label will have only two possible values $x \in \mathcal{I}_{SIS} = \{1, 2\}$ and the transition probabilities will be

$$\begin{aligned} T(t;1|1) = 1 - \beta f_2(t) \quad & T(t;2|1) = \beta f_2(t) \\ T(t;1|2) = \gamma \qquad\quad & T(t;2|2) = 1 - \gamma. \end{aligned} \tag{85}$$

Thus, we obtain the SIS model

$$\begin{cases} f_1' = & -\beta f_1 f_2 + \gamma f_2 \\ f_2' = & \beta f_1 f_2 - \gamma f_1. \end{cases} \tag{86}$$

We have shown how the classical ODE-based epidemiological models can be derived from microscopic dynamics in a kinetic theory framework. For this purpose, we have employed the kinetic label switch process alone, meaning that binary interactions were not involved in the description. In this case the labels have been chosen to mimic the classes of the classical models. In the following models, we will merge the two processes and this will allow us to use the labels to add features to the model rather than to describe the epidemic dynamics, task that will be taken on by the microscopic state and by the binary interaction process.

## 3.2 Quarantined - non quarantined model

From a kinetic point of view, the evolution of an ongoing epidemic can be fruitfully described by the microscopic state that characterizes every agent in the population. In fact, if we assume that the microscopic state $v \in V = \mathbb{R}_+$ represents a *viral load*, the kinetic framework of sec. 2.2 implies that agents in a large population exchange *viral load* when interacting with each other. This seems a reasonable formalization of the contagion dynamics that takes place when an epidemic of an infectious disease occurs. The agents are therefore no longer divided into compartments and there is not a clear division between healthy and ill individuals, but a continuous quantity that measures the infection on a spectrum. It is important to point out that the *viral load* is not a medical quantity and it has to be intended as a mathematical-physical quantity for the sake of the model. Freed from their descriptive role, the labels can now represent another important aspect of the modeling of an epidemic: the containment strategies. The first kinetic epidemiological model considered is a quarantine model, based on [32]. It describes the evolution of the epidemic if diagnosed individuals are subject to quarantine and removed from the interaction process. The label switch process is therefore used to model the transition of the agents from the non-quarantined state to the quarantined state. Hence, we will be referring to this model by Q-nQ model. Mathematically, we assign to every agent the label $x \in \mathcal{I} = \{1, 2\}$, where $x = 1$ means that the agent is free and $x = 2$ means that the agent has been diagnosed and it is therefore quarantined. Undiagnosed people interact with each other and may eventually contract the illness. When an agent is diagnosed, they are not allowed to interact and they receive medical care. Therefore they undergo a healing process rather than a binary interaction one. A quarantined agent can heal and return to the undiagnosed population when their *viral load* is low enough. With the tools described in sec. 2.3, this can be seen as the case where interaction happens only among same-labeled agents, with the interaction rule depending on the label. Hence, we will refer to equation (55) for the evolution of an observable quantity $\phi(v)$, that we re-write here for clarity with $n = 2$:

$$\begin{aligned}\frac{d}{dt}\int_{\mathbb{R}_+}\phi(v)f_i(t,v)dv = \lambda\int_{\mathbb{R}_+}\phi(v)\Big(\sum_{j=1}^{n}T(t,v;i|j)f_j(t,v) - f_i(t,v)\Big)dv \\ + \mu\int_{\mathbb{R}_+}\int_{\mathbb{R}_+}\langle\phi(v_i') - \phi(v)\rangle f_i(t,v)f_i(t,v_*)dvdv_* \\ i = 1, 2\,.\end{aligned}$$

Let us assume the transition probabilities to be

$$\begin{aligned} &T(v;1|1) = 1-\alpha(v), \quad T(v;2|1) = \alpha(v) \\ &T(v;1|2) = \beta(v), \qquad T(v;2|2) = 1-\beta(v), \end{aligned} \tag{87}$$

where $0 \leq \alpha(v), \beta(v) \leq 1$. Parameters $\alpha(v)$ and $\beta(v)$ are, respectively, the probability that an agent with *viral load* $v$ is diagnosed and quarantined and the probability that a quarantined agent with *viral load* $v$ is reintegrated in the interaction process. Hence, it is reasonable to assume $\alpha(v)$ non-decreasing and $\beta(v)$ non-increasing in $v$.

The interaction rule is different for the two classes. For undiagnosed people, it reflects the binary interaction process and reads

$$v_1' = (1-\nu_1+\eta)v + \nu_2 v_* \,, \tag{88}$$

where $\nu_1, \nu_2 \in [0,1]$ are exchange rates and $\eta \in (\nu_1 - 1, +\infty)$ is a zero-mean random variable accounting for random fluctuations of the *viral load* in an agent. Recalling the definitions of sec. 2.2 the mixing parameters are $p_1 = p_2 = p = (1-\nu_1+\eta)$ and $q_1 = q_2 = q = \nu_2$. Hence, the interaction is symmetric, with a stochastic parameter and a deterministic one. For quarantined people, the interaction rule reflects the healing process and reads

$$v_2' = (1-\gamma+\xi)v, \tag{89}$$

where $\gamma \in [0,1]$ is the recovery rate and $\xi \in (\gamma-1, +\infty)$ is another zero-mean random variable, independent from $\eta$. The mixing parameters here are $p_1 = p_2 = (1-\nu_1+\eta)$ and $q_1 = q_2 = 0$ and hence the interaction is symmetric. Thus, we can separate equation (55) into its two components and write, for the undiagnosed people ($x = 1$),

$$\begin{aligned} \frac{d}{dt}\int_{\mathbb{R}_+} \phi(v) f_1(t,v)dv &= \lambda \int_{\mathbb{R}_+} \phi(v)\Big(\beta(v) f_2(t,v) - \alpha(v) f_1(t,v)\Big)dv \\ &= \mu \iint_{\mathbb{R}_+\times\mathbb{R}_+} \langle \phi(v_1') - \phi(v)\rangle f_1(t,v) f_1(t,v_*) dv dv_* \end{aligned} \tag{90}$$

and, for the quarantined people ($x = 2$),

$$\begin{aligned} \frac{d}{dt}\int_{\mathbb{R}_+} \phi(v) f_2(t,v)dv &= \lambda \int_{\mathbb{R}_+} \phi(v)\Big(\alpha(v) f_1(t,v) - \beta(v) f_2(t,v)\Big)dv \\ &= \mu \int_{\mathbb{R}_+} \langle \phi(v_2') - \phi(v)\rangle f_2(t,v) f_2(t,v_*) dv \,. \end{aligned} \tag{91}$$

Let us point out that in equation (91) the interaction kernel is linear with respect to $f_2$. This reflects the fact that, owing to $q_1 = q_2 = 0$, the healing process is not a

proper binary interaction process but a linear evolution of the state of quarantined people. Rigorously, it follows from equation (42) by noticing that interaction rule (89) does not contain $v_*$.

### 3.2.1 Constant transition probabilities

From equations (90) and (91) we can compute the evolution of the zero and first order moments. These two quantities together depict a detailed picture of the ongoing epidemic. In fact, while the former represents the evolution of the relative masses of the two classes, diagnosed and undiagnosed, the latter represents the evolution of the mean *viral load*, divided per class. Let us firstly investigate the simple case where the probabilities $\alpha, \beta$ are assumed constant. We assume the two processes to take place on the same time scale and therefore, without loss in generality, we can write

$$\lambda = \mu = 1.$$

We take $\phi(v) = 1$ to compute the evolution of the masses and $\phi(v) = v$ to compute the evolution of the mean *viral load*, we obtain the ODE system

$$\begin{cases} \frac{d\rho_1}{dt} & = -\alpha\rho_1 + \beta\rho_2 \\ \frac{d\rho_2}{dt} & = \alpha\rho_1 - \beta\rho_2 \\ \frac{d}{dt}(\rho_1 m_1) & = -[\alpha + (\nu_1 - \nu_2)\rho_1]\rho_1 m_1 + \beta\rho_2 m_2 \\ \frac{d}{dt}(\rho_2 m_2) & = \alpha\rho_1 m_1 - (\beta + \gamma)\rho_2 m_2. \end{cases} \tag{92}$$

We have of course $\rho_1 + \rho_2 = 1$ and $\frac{d\rho_1}{dt} + \frac{d\rho_2}{dt} = 0$. The natural initial conditions $\rho_{1,0} = 1$ and $\rho_{2,0} = 0$ lead to

$$\begin{aligned} \rho_1(t) &= \frac{\beta}{\alpha+\beta}\left(1 + \frac{\alpha}{\beta}e^{-(\alpha+\beta)\cdot t}\right) \\ \rho_2(t) &= \frac{\alpha}{\alpha+\beta}\left(1 - e^{-(\alpha+\beta)\cdot t}\right), \end{aligned} \tag{93}$$

that, in the limit for $t \to \infty$, yield

$$\begin{aligned} \rho_1^\infty &= \frac{\beta}{\alpha+\beta} \\ \rho_2^\infty &= \frac{\alpha}{\alpha+\beta}. \end{aligned}$$

This means that the quarantine is a condition a portion of the population remains subject to at any time. This could suggest that the illness can not be eradicated and becomes endemic. We need to carry out a more detailed investigation and look at the mean *viral load* to gain a more exhaustive perspective on the matter - and prove this conclusion false. We can rewrite the last two equations in (92) in vector form as

$$\frac{d}{dt}\begin{pmatrix} m_1 \\ m_2 \end{pmatrix} = \begin{pmatrix} (\nu_2-\nu_1)\rho_1 - \beta\frac{\rho_2}{\rho_1} & \beta\frac{\rho_2}{\rho_1} \\ \alpha\frac{\rho_1}{\rho_2} & -\Big(\alpha\frac{\rho_1}{\rho_2}+\gamma\Big) \end{pmatrix}\begin{pmatrix} m_1 \\ m_2 \end{pmatrix}. \tag{94}$$

The system matrix is time-dependent and hence the system is non-autonomous due to the presence of $\rho_1$ and $\rho_2$. We can study the large time behavior of the mean *viral load* by noticing that for equations (93) the masses reach their asymptotic values exponentially in time. We can therefore approximate $\rho_1 \approx \rho_1^\infty$ and $\rho_2 \approx \rho_2^\infty$ and obtain

$$\frac{d}{dt}\begin{pmatrix} m_1 \\ m_2 \end{pmatrix} = \begin{pmatrix} (\nu_2-\nu_1)\frac{\beta}{\alpha+\beta} - \alpha & \alpha \\ \beta & -\Big(\beta+\gamma\Big) \end{pmatrix}\begin{pmatrix} m_1 \\ m_2 \end{pmatrix}. \tag{95}$$

The most desirable scenario is of course the one where, asymptotically, $m_1^\infty = m_2^\infty = 0$. This would mean that the illness has been completely eradicated. The statistical configuration that corresponds to this scenario is

$$\begin{aligned} f_1^\infty(v) &= \frac{\beta}{\alpha+\beta}\delta(v) = \rho_1^\infty\delta(v) \\ f_2^\infty(v) &= \frac{\alpha}{\alpha+\beta}\delta(v) = \rho_2^\infty\delta(v). \end{aligned} \tag{96}$$

We want to assess the stability and attractiveness of this configuration. Let us focus on two significant cases. Firstly, we consider the case $\nu_1 = \nu_2$. In this case, the binary interaction process among non-quarantined agents does not affects the mean *viral load* value. In fact, the mixing parameters of this process are such that $\langle p+q\rangle = 1$ and the dynamics is therefore conservative. Conversely, the healing process of the quarantined agents has parameters such that $\langle p+q\rangle = 1-\gamma < 1$. Hence, we expect the mean *viral load* to decrease in time. We can study the behavior of the linear system (95) by investigating the eigenvalues $\lambda_1$ and $\lambda_2$ of the system matrix

$$A = \begin{pmatrix} -\alpha & \alpha \\ \beta & -(\beta-\gamma) \end{pmatrix} \Longrightarrow \lambda_{1,2} = \frac{-(\alpha+\beta+\gamma) \pm \sqrt{(\alpha+\beta+\gamma)^2 - 4\alpha\gamma}}{2}.$$

Hence, if we disregard the trivial case $\gamma = 0$ that leads to an overall conservative system, we obtain a globally asymptotically stable system if $\alpha > 0$, i.e. if there is a non-null probability of being quarantined. The speed of convergence, anyway, is massively effected by $\alpha$. If we perform the limit for $\alpha \to 0^+$ the eigenvalues $\omega_1$ and $\omega_2$ of system (95) will read

$$\begin{aligned}\lambda_1 &= -\frac{\alpha\gamma}{\beta+\gamma} + o(\alpha)\\ \lambda_2 &= -(\beta+\gamma) + o(1)\,.\end{aligned}$$

From the theory of linear stability, $\lambda_1$ makes the convergence speed potentially very low.

As a second case let us consider $\nu_1 = 0$, $\nu_2 > 0$. This means that each interaction increases, on average, the *viral load* of the agents. In fact, the mixing parameters of the binary interaction process are here such that $\langle p + q\rangle = 1 + \nu_2 > 1$. Hence, the interactions alone would have the *viral load* $m_1$ to blow up in time. The healing process owed to the quarantine state forces $m_1$ to converge to zero if $\alpha$ satisfies

$$\alpha > \alpha_\dagger := max\left\{ max\left\{0, \frac{-(2\beta+\gamma)+\sqrt{\gamma^2+4\nu_2\beta}}{2}\right\}, \frac{-\beta+\sqrt{\left(1+\frac{4\nu_2}{\gamma}\right)+4\nu_2\beta}}{2}\right\}.$$

This constraint has been obtained by means of the same kind of investigation on the eigenvalues carried out for the previous case. The expression of $\alpha_\dagger$ indicates that the higher the contagion rate $\nu_2$ is, the higher the diagnosing probability needs to be to contain the contagions.

### 3.2.2 Variable transition probabilities

A more realistic description is obtained with variable parameters $\alpha$ and $\beta$. The analysis in this case is more complicated and we need to appeal to some assumptions. Let us assume that the binary interactions take place on a much faster scale than the label switch process. Mathematically, without loss of generality, we assume

$$\lambda = 1\,, \quad \mu = \frac{1}{\delta}\,,$$

with $0 < \delta \ll 1$ small parameter. As we did in sec. 2.4, we can split equation (90) as

$$\frac{d}{dt}\int_{\mathbb{R}_+}\phi(v)f_1(t,v)dv = \frac{1}{\delta}\iint_{\mathbb{R}_+\times\mathbb{R}_+}\langle\phi(v_1')-\phi(v)\rangle f_1(t,v)f_1(t,v_*)dvdv_*$$
$$\frac{d}{dt}\int_{\mathbb{R}_+}\phi(v)f_1(t,v)dv = \int_{\mathbb{R}_+}\phi(v)\Big(\beta(v)f_2(t,v)-\alpha(v)f_1(t,v)\Big)dv\,. \tag{97}$$

If we introduce the new time scale

$$\tau := \frac{t}{\delta}$$

and we define

$$\tilde{f}_1(\tau,v) := f_1(t,v)\,,$$

system (97) reads

$$\frac{d}{d\tau}\int_{\mathbb{R}_+}\phi(v)\tilde{f}_1(\tau,v)dv = \iint_{\mathbb{R}_+\times\mathbb{R}_+}\langle\phi(v_1')-\phi(v)\rangle\tilde{f}_1(\tau,v)\tilde{f}_1(\tau,v_*)dvdv_* \tag{98}$$
$$\frac{d}{dt}\int_{\mathbb{R}_+}\phi(v)f_1(t,v)dv = \int_{\mathbb{R}_+}\phi(v)\Big(\beta(v)f_2(t,v)-\alpha(v)f_1(t,v)\Big)dv\,. \tag{99}$$

Remembering the interpretation of the hydrodynamic limit, we say that the interaction dynamics on the fast time $\tau$ quickly reaches an equilibrium profile while the label switch process is bound to the slow time $t$. It is interesting to investigate in this limit the conservative case $\nu_1 = \nu_2$. With this configuration, the equilibrium profile reached on the fast time scale by the interaction dynamics turns out to be parameterized by the two macroscopic quantities $\rho_1(t)$ and $m_1(t)$, both constant on the quick time scale $\tau$. Let us indicate the equilibrium distribution on the $t$-scale as

$$f_1(t,v) = \frac{\rho_1(t)}{m_1(t)}g_1\Big(\frac{v}{m_1(t)}\Big)\,, \tag{100}$$

where $g_1 : \mathbb{R}_+ \to \mathbb{R}_+$ satisfies the normalization conditions

$$\int_{\mathbb{R}_+} g_1(v)dv = 1\,, \qquad \int_{\mathbb{R}_+} v g_1(v) = 1\,.$$

If we apply the same reasoning to (91), with $\tilde{f}_2(\tau, v) := f_2(t, v)$, we obtain

$$\frac{d}{d\tau}\int_{\mathbb{R}_+}\phi(v)\tilde{f}_2(\tau,v)dv = \int_{\mathbb{R}_+}\langle\phi(v_2')-\phi(v)\rangle\tilde{f}_2(\tau,v)dv \tag{101}$$

$$\frac{d}{dt}\int_{\mathbb{R}_+}\phi(v)f_2(t,v)dv = \int_{\mathbb{R}_+}\phi(v)\Big(\alpha(v)f_1(t,v)-\beta(v)f_2(t,v)\Big)dv\,. \tag{102}$$

Here, the quick dynamics does not conserve mean *viral load* of the distribution and the $\tau$-asymptotic distribution on the $t$ scale is therefore parameterized only by the mass $\rho_2(t)$. Hence,

$$f_2(t,v) = \rho_2(t)g_2(v)\,, \tag{103}$$

where $g_2 : \mathbb{R}_+ \to \mathbb{R}_+$ satisfies

$$\int_{\mathbb{R}_+} g_2(v)dv = 1\,.$$

We can now solve the slow scale equation (99) by using distributions (100) and (103). Remembering $\rho_1(t) + \rho_2(t) = 1$ and re-scaling the distributions, we obtain

$$\begin{cases} \frac{d\rho_1}{dt} & = \left(\int_{\mathbb{R}_+}\beta(v)g_2(v)dv\right)\rho_2 - \left(\int_{\mathbb{R}_+}\alpha(m_1v)g_1(v)dv\right)\rho_1 \\ \rho_2 & = 1-\rho_1 \\ \frac{d}{dt}(\rho_1 m_1) & = \left(\int_{\mathbb{R}_+}v\beta(v)g_2(v)dv\right)\rho_2 - \left(\int_{\mathbb{R}_+}v\alpha(m_1v)g_1(v)dv\right)\rho_1 m_1\,. \end{cases} \tag{104}$$

To solve system (104) it is necessary to know the distributions $g_1(v)$ and $g_2(v)$. For the healing process in the quarantined class, it is easy to see that, being $\langle p+q\rangle = 1-\gamma < 1$, $m_2 \to 0^+$ exponentially in time. Hence, we have $g_2(v) = \delta(v)$. Let us now focus on the binary interaction process. Distribution $g_1(v)$ is a normalized distribution with mean value $m_1(t)$ and variance $Var(g_1) = K(t) - m(t)^2$ (see equation (33)). Considering that we are interested in the mean *viral load* and that it is not affected by the zero-mean fluctuations $\eta$ in the interaction rule (88), let us assume $\eta = 0$. We compute the second-order momentum

$$\frac{d}{d\tau}(\tilde{\rho}_1\tilde{K}_1) = \iint_{\mathbb{R}_+\times\mathbb{R}_+}\left[\Big((1-\nu)v+\nu v_*\Big)^2 - v^2\right]\tilde{f}_1(\tau,v)\tilde{f}_1(\tau,v_*)dvdv_*\,, \tag{105}$$

where $\tilde{K_1}$ represents the energy and $\nu = \nu_1 = \nu_2$. Remembering that on the fast time scale $\tau$ the mass $\rho_1$ is constant, we obtain

$$\frac{d}{d\tau}\tilde{K_1} = 2\nu(\nu-1)\rho_1\Big[\tilde{K_1} - \tilde{m}_1^2\Big]. \tag{106}$$

Solving linear non-homogeneous equation (106) leads to

$$\tilde{K_1}(\tau) = C \cdot e^{2\nu(\nu-1)\tilde{\rho_1}\tau} + \tilde{m}_1^2\,,$$

Where $C$ is a constant that depends on the initial conditions. With $0 < \nu < 1$ this yields

$$\tilde{K_1}^{\infty} = \tilde{m}_1^2$$

and hence $Var(g_1) = 0$. We can therefore consider, in this approximation with $\eta = 0$, the distribution $g_1(v)$ as a Dirac delta peaked in $\tilde{m_1}$:

$$g_1(v) = \delta(v - \tilde{m_1}). \tag{107}$$

For the sake of completeness, let us point out that distribution $g_1$ can be explicitly determined in a suitable quasi-invariant regime without imposing $\eta = 0$ [32].

System (104) can therefore be re-written as

$$\begin{cases} \frac{d\rho_1}{dt} & = \beta(0)(1-\rho_1) - \alpha(m_1)\rho_1 \\ \frac{d}{dt}(\rho_1 m_1) & = -\alpha(m_1)\rho_1 m_1\,, \end{cases} \tag{108}$$

that yields

$$\begin{aligned} \beta(0) - \rho_1^{\infty}\Big(\beta(0) + \alpha(m_1^{\infty})\Big) &= 0 \\ \alpha(m_1^{\infty})\rho_1^{\infty} m_1^{\infty} &= 0. \end{aligned}$$

Hence, we obtain, for $\beta(0) > 0$, that the mass of non quarantined people is non-null, $\rho_1^{\infty} > 0$. If we also assume $\alpha(v) > 0\ \forall v \neq 0$ and $\alpha(0) = 0$, then for the second equation we obtain $m_1^{\infty} = 0$. Plugging this result in the first equation we obtain, in conclusion

$$\rho_1^{\infty} = 1, \quad \rho_2^{\infty} = 0, \quad m_1^{\infty} = 0.$$

Hence, we have

$$f_1^\infty(v) = \delta(v), \quad f_2^\infty(v) = 0.$$

This means that, in the long period, the population fully recover and there are no quarantined people

.

## 3.3 Q-nQ model on the network

The Q-nQ model of the previous section is based on the assumption that every agent has the same probability to interact with every other agent in the population. While this assumption is acceptable when considering dense interconnected clusters such as neighbourhoods or cities, it is not accurate if we want to consider epidemics on larger scales. In this section, we propose a version of the Q-nQ model laid on a spatial network. The network can model, e.g., a number of interconnected cities. We consider each city as an interconnected cluster with agents that can transfer from one city to another following a given probability matrix. The mathematical tool used to model the network is the kinetic label switch process. Agents in this model will be equipped with two labels each, one that indicates whether the agent is quarantined or not and the other one that indicates in which city the agent is at the moment. In addition to that, agents are characterized by the microscopic state *viral load*, as in the simple Q-nQ model. Hence, we consider label $x \in \mathcal{I} = \{1, 2\}$ for the quarantine process and label $a \in \mathcal{C} = \{1, 2, ..., n\}$ to indicate the city. The interactions occur only among non-quarantined agents that are in the same city. Hence, we will refer to the same same-labeled interaction equation we did for the Q-nQ model, equation (55). However, the presence of a second label requires some adjustments on the results and definitions of sec. 2.3. The density distribution function $f$ can now be discretized as

$$f(t, x, a, v) = \sum_{i=1}^{2} \sum_{j=1}^{n} f_i^j(t, v)\delta(x - i)\delta(a - j),$$

where the subscript $i$ refers to the label $x$ and the superscript $j$ refers to the label $a$. The normalization yields

$$\sum_{i=1}^{2} \sum_{j=1}^{n} \int_{\mathbb{R}_+} f_i^j(t, v)dv = 1, \ \forall t > 0.$$

We can define the mass of the agents with label $x = i$ and in city $a = j$ as

$$\rho_i^j(t) := \int_{\mathbb{R}_+} f_i^j(t, v)dv.$$

The travel between two cities is modeled by a second label switch process and regulated by a transition probability matrix

$$R = R(t, v, x; a|b) \in [0, 1],\ \forall t, v \in \mathbb{R}_+,\ x \in \mathcal{I},\ a, b \in \mathcal{C}, \tag{109}$$

that we interpret as the probability that an agent with *viral load* $v$ and label $x$ travels at time $t$ from city $b$ to city $a$. For it to be consistent and for the conservation of mass to hold, $R$ has to satisfy

$$\sum_{a\in\mathcal{C}} R(t, v, x; a|b) = 1,\ \forall t, v \in \mathbb{R}_+,\ x \in \mathcal{I}.$$

If we consider the random variable triplet $(X_t, A_t, V_t) \in \mathcal{I} \times \mathcal{C} \times \mathbb{R}_+$ and the small time interval $\Delta t > 0$, following the same reasoning that led us to (44), we have

$$\begin{cases} X_{t+\Delta t} &= (1 - \Theta)X_t + \Theta J_t \\ A_{t+\Delta t} &= (1 - \Omega)A_t + \Omega B_t \\ V_{t+\Delta t} &= (1 - \Xi)V_t + \Xi V_t' \,. \end{cases}$$

Where $J_t$, $B_t$ and $V_t'$ are the post-event attributes and $\Theta$, $\Omega$ and $\Xi$ are the Bernoulli random variables that represent each event. They hold

$$\begin{cases} P(\Theta = 1) &= \lambda\Delta t \\ P(\Omega = 1) &= \omega\Delta t \\ P(\Xi = 1) &= \mu\Delta t\,, \quad \Delta t \leq min\{\frac{1}{\lambda}, \frac{1}{\omega}, \frac{1}{\mu}\}. \end{cases} \tag{110}$$

When the mean variation of the observable quantity $\varphi = \varphi(x, a, v)$ is considered, this leads to a modified version of equation (48) that includes the third process. In the limit for $\Delta t \to 0^+$, it reads

$$\begin{aligned} \frac{d}{dt}\langle\varphi(X_t, A_t, V_t)\rangle = \lambda\langle\varphi(J_t, A_t, V_t)\rangle + \omega\langle\varphi(X_t, B_t, V_t)\rangle + \mu\langle\varphi(X_t, A_t, V_t')\rangle + \\ - (\lambda + \omega + \mu)\langle\varphi(X_t, A_t, V_t)\rangle. \end{aligned} \tag{111}$$

If we choose $\varphi(x, a, v) = \phi(v)\psi(x)\chi(a)$ with $\psi(i) = 1$ for a certain $i \in \mathcal{I}$ and $\psi(j) = 0$ for $j \neq i$ and $\chi(i) = 1$ for a certain $i \in \mathcal{C}$ and $\chi(j) = 0$ for $j \neq i$, we can write the

weak Boltzmann-type equation for this model as

$$\begin{aligned}\frac{d}{dt}\int_{\mathbb{R}_+}\phi(v)f_i^j(t,v)dv &= \lambda\int_{\mathbb{R}_+}\phi(v)\Big(\sum_{k=1}^{2}T(t,v;i|k)f_k^j(t,v)-f_i^j(t,v)\Big)dv\\ &+\omega\int_{\mathbb{R}_+}\phi(v)\Big(\sum_{j=1}^{n}R(t,i,v;j|k)f_i^k(t,v)-f_i^j(t,v)\Big)dv\\ &+\mu\int_{\mathbb{R}_+}\int_{\mathbb{R}_+}\langle\phi(v_i')-\phi(v)\rangle f_i^j(t,v)f_i^j(t,v_*)dvdv_* \qquad (112)\\ &\qquad\qquad i\in\mathcal{I},j\in\mathcal{C}.\end{aligned}$$

Equation (112) accounts for the fact that interactions among agents in different cities are forbidden as well as interactions with quarantined people. The transition probability matrix $T$ is the same of the Q-nQ model, as are unmodified the interaction rules (88) and (89). Let us define transition probabilities between cities. It is clear that quarantined agents are forbidden to travel, hence

$$R(v,2;a|b)=1\,if\,a=b,\;\;R(v,2;a|b)=0\;\;\;if\;\;\;a\neq b\,.$$

Conversely, non-quarantined people are free to move between cities. Let us define the probability matrix $D(v,t)\in[0,1]^{n\times n}$ such that the probability for an undiagnosed agent with *viral load* $v$ to go at time $t$ from city $i$ to city $j$ is $D_{i,j}\in[0,1]$, $i,j\in\mathcal{C}$. $D$ satisfies

$$\sum_{j=1}^{n}D_{i,j}=1\,\forall i.$$

Let us now write the weak Boltzmann-type equations for undiagnosed people ($x=1$):

$$\begin{aligned}\frac{d}{dt}\int_{\mathbb{R}_+}\phi(v)f_1^i(t,v)dv &= \lambda\int_{\mathbb{R}_+}\phi(v)(\beta(v)f_2^i(t,v)-\alpha(v)f_1^i(t,v))dv\\ &+\omega\int_{\mathbb{R}_+}\phi(v)(\sum_{j=i,j\neq i}^{3}D_{j,i}(t,v)f_1^j(t,v)+\\ &\qquad-\sum_{j=1,j\neq i}^{3}D_{i,j}(t,v)f_1^i(t,v))dv\\ &+\mu\iint_{\mathbb{R}_+\times\mathbb{R}_+}\langle\phi(v_1')-\phi(v)\rangle f_1^i(t,v)f_1^i(t,v_*)dvdv_* \qquad (113)\\ &\qquad\qquad for\,i=1,...,n.\end{aligned}$$

We can lighten the notation by observing that, in the travel process, we can include the case $i = j$ in both the sums so they elide. Equation (113) now reads

$$\begin{aligned}\frac{d}{dt}\int_{\mathbb{R}_+}\phi(v)f_1^i(t,v)dv &= \lambda\int_{\mathbb{R}_+}\phi(v)(\beta(v)f_2^i(t,v)-\alpha(v)f_1^i(t,v))dv\\ &+\omega\int_{\mathbb{R}_+}\phi(v)(\sum_{j=i}^{m}D_{j,i}(t,v)f_1^j(t,v)+\\ &\qquad -\sum_{j=1}^{m}D_{i,j}(t,v)f_1^i(t,v))dv\\ &+\mu\iint_{\mathbb{R}_+\times\mathbb{R}_+}\langle\phi(v_1')-\phi(v)\rangle f_1^i(t,v)f_1^i(t,v_*)dvdv_*v_* \qquad (114)\\ &\qquad\qquad for\, i=1,...,n.\end{aligned}$$

For quarantined people ($x = 2$) we have

$$\begin{aligned}\frac{d}{dt}\int_{\mathbb{R}_+}\phi(v)f_2^i(t,v)dv &= \lambda\int_{\mathbb{R}_+}\phi(v)(\alpha(v)f_1^i(t,v)-\beta(v)f_2^i(t,v))dv\\ &+\mu\int_{\mathbb{R}_+}\langle\phi(v_2')-\phi(v)\rangle f_2^i(t,v)dvv_* \qquad (115)\\ &\qquad for\, i=1,...,n.\end{aligned}$$

Let us note that the travel-related label switch appears only in the equation for non-quarantined people, i.e. the only ones that can travel.

### 3.3.1 Constant transition probabilities

The same kind of analysis carried out in the previous section for the simple Q-nQ model can be applied to this version. If the transition probabilities $\alpha$, $\beta$ and $D$ are constant and we assume

$$\lambda = \omega = \mu = 1,$$

we obtain, for the time evolution of the mass and the mean *viral load*:

$$\begin{cases}\frac{d}{dt}\rho_1^i &= \beta\rho_2^i-\alpha\rho_1^i+\sum_{j=1}^n D_{j,i}\rho_1^j-\sum_{j=1}^n D_{i,j}\rho_1^i\\ \frac{d}{dt}\rho_2^i &= \alpha\rho_1^i-\beta\rho_2^i\\ \frac{d}{dt}\rho_1^i m_1^i &= \beta\rho_2^i m_2^i-\alpha\rho_1^i m_1^i+\sum_{j=1}^n D_{j,i}\rho_1^j m_1^j-\sum_{j=1}^n D_{i,j}\rho_1^i m_1^i-(\nu_1-\nu_2)\rho_1^i\rho_1^i m_1^i\\ \frac{d}{dt}\rho_2^i m_2^i &= \alpha\rho_1^i m_1^i-\beta\rho_2^i m_2^i-\gamma\rho_2^i m_2^i\,.\end{cases} \qquad (116)$$

The dimension of system (116) quickly rises when more than one city is considered. Hence, it is not well suited for the qualitative analysis of the previous model. However, it is possible to compute the evolution of aggregated macroscopic quantities, both over cities and over quarantine condition. If we sum over the superscript $i$ we obtain the evolution of mass and mean *viral load* on the whole network as

$$\begin{cases} \frac{d}{dt}\rho_1 & = \beta\rho_2 - \alpha\rho_1 \\ \frac{d}{dt}\rho_2 & = \alpha\rho_1 - \beta\rho_2 \\ \frac{d}{dt}(\rho_1 m_1) & = \beta\rho_2 m_2 - \alpha\rho_1 m_1 - (\nu_1 - \nu_2)\sum_{i=1}^{n} \rho_1^i \rho_1^i m_1^i \\ \frac{d}{dt}(\rho_2 m_2) & = \alpha\rho_1 m_1 - (\beta+\gamma)\rho_2 m_2 \,. \end{cases} \tag{117}$$

Note that this system is similar to the one obtained for the Q-nQ model with the difference that the interactions are restricted to agents in the same city. Let us investigate the two cases $\nu_1 = \nu_2$ and $\nu_1 = 0$, $\nu_2 > 0$. In the first case, system (118) resembles system (92) and therefore leads to the same results. In the second case, we notice that while first two equations and the last one remain unchanged, in the third equation we have $\sum_{i=1}^{n} \rho_1^i \rho_1^i m_1^i \leq \sum_{i=1}^{n} \rho_1^i \cdot \sum_{i=1}^{n} \rho_1^i \cdot \sum_{i=1}^{n} m_1^i = \rho_1 \rho_1 m_1$. Thus, for the masses we obtain

$$\begin{aligned} \rho_1^\infty &= \frac{\beta}{\alpha+\beta} \\ \rho_2^\infty &= \frac{\alpha}{\alpha+\beta}\,, \end{aligned}$$

as in the Q-nQ model. We also have

$$\frac{d}{dt}(\rho_1 m_1)^{NETWORK\,Q-nQ} \leq \frac{d}{dt}(\rho_1 m_1)^{SIMPLE\,Q-nQ}, \;\; \forall t > 0\,.$$

If we assume the same initial conditions between the two models and we study the asymptotic behavior assuming $\rho_i = \rho_i^\infty$, $i = 1, 2$, we can state

$$0 \leq (m_1(t))^{NETWORK\,Q-nQ} \leq (m_1(t))^{SIMPLE\,Q-nQ}.$$

Thus, owing to the so-called squeezing theorem, we can assure that, in the Q-nQ model on the network, $m_1$ converges to zero *at least* for $\alpha > \alpha_\dagger$, where $\alpha_\dagger$ is the same as in sec. 3.2.1. The speed of convergence is *at least* the same as the speed of convergence of the simple Q-nQ model.

As a side note, let us point out that if we aggregate over the subscript we obtain the system divided per city, with the time evolution of the population and mean *viral*

*load* inside each city, disregarding the quarantine condition. This is

$$\begin{cases} \frac{d}{dt}\rho^i & = \sum_{j=1}^n D_{j,i}\rho_1^j - \sum_{j=1}^n D_{i,j}\rho_1^i \\ \frac{d}{dt}\rho^i m^i & = \sum_{j=i}^n D_{j,i}\rho_1^j m_1^j - \sum_{j=1}^n D_{i,j}\rho_1^i m_1^i - (\nu_1-\nu_2)\rho_1^i\rho_1^i m_1^i - \gamma\rho_2^i m_2^i \,. \end{cases} \tag{118}$$

### 3.3.2 Variable transition probabilities

The same hydrodynamic limit analysis with variable transition probabilities of sec. 3.2.2 can be applied to the network case. We assume the transition probability matrix $D = D(t, v)$ to depend on time $t$ and on the *viral load* $v$. It seems reasonable to assume it non-increasing in $v$, for the higher the *viral load* of an agent, the less likely they will travel. Transition probabilities $\alpha$ and $\beta$ are assumed also to be variable. Here, we assume that both the label switch processes operate on the slow time scale $t$, while the binary interaction process operates on the fast time scale $\tau$, where $\tau := \frac{t}{\delta}$ with $0 < \delta \ll 1$. Hence, we have

$$\lambda = \omega = 1, \quad \mu = \frac{1}{\delta}\,.$$

Defining $\tilde{f}_1^i(\tau, v) := f_1^i(t, v)$ and $\tilde{f}_1^i(\tau, v) := f_2^i(t, v)$, we can split the weak Boltzmann equations (114) and (115) in

$$\frac{d}{d\tau}\int_{\mathbb{R}_+} \phi(v)\tilde{f}_1^i(\tau, v)dv = \iint_{\mathbb{R}_+\times\mathbb{R}_+} \langle\phi(v_1') - \phi(v)\rangle \tilde{f}_1^i(t, v)\tilde{f}_1^i(t, v_*)dvdv_* \tag{119}$$

$$\begin{aligned} \frac{d}{dt}\int_{\mathbb{R}_+} \phi(v)f_1^i(t, v)dv = &\int_{\mathbb{R}_+} \phi(v)\Big(\beta(v)f_2^i(t, v) - \alpha(v)f_1^i(t, v)\Big)dv \\ &+ \int_{\mathbb{R}_+} \phi(v)\left(\sum_{j=1}^n D_{j,i}(t, v)f_1^j(t, v) - \sum_{j=1}^n D_{i,j}(t, v)f_1^i(t, v)\right)dv \end{aligned} \tag{120}$$

and

$$\frac{d}{d\tau}\int_{\mathbb{R}_+} \phi(v)\tilde{f}_2^i(\tau, v)dv = \int_{\mathbb{R}_+} \langle\phi(v_2') - \phi(v)\rangle \tilde{f}_2^i(t, v)dv \tag{121}$$

$$\frac{d}{dt}\int_{\mathbb{R}_+} \phi(v)f_2^i(t, v)dv\frac{d}{dt} = \int_{\mathbb{R}_+} \phi(v)\Big(\alpha(v)f_1^i(t, v) - \beta(v)f_2^i(t, v)\Big)dv\,, \tag{122}$$

respectively. The interpretation of these equations is that on the fast time scale

$\tau$, agents in each city are isolated from other cities and in every cluster a different equilibrium profile based on the initial conditions will be rapidly reached. Travel and diagnosis processes are frozen to the slow time scale $t$. If we assume again $\nu_1 = \nu_2 = \nu$, we obtain the same equilibrium distributions as in the simple Q-nQ case, parameterized with local macroscopic quantities. These are

$$\begin{aligned} f_1^i(t,v) &= \frac{\rho_1^i(t)}{m_1^i(t)} g_1^i\Big(\frac{v}{m_1^i(t)}\Big) \\ f_2^i(t,v) &= \rho_2^i(t) g_2(t)\,, \end{aligned} \tag{123}$$

with the usual normalization

$$\int_{\mathbb{R}_+} g_1(v)dv = 1\,, \qquad \int_{\mathbb{R}_+} v g_1(v) = 1\,.$$

$$\int_{\mathbb{R}_+} g_2(v)dv = 1\,.$$

The general system for the evolution of the macroscopic quantities is therefore

$$\begin{cases} \frac{d}{dt}\rho_1^i & = \Big(\int_{\mathbb{R}_+}\beta(v)g_2(v)dv\Big)\rho_2^i\Big(\int_{\mathbb{R}_+}\alpha(m_1^1 v)g_1(v)dv\Big)\rho_1^i \\ & + \sum_{j=i}^M\Big(\int_{\mathbb{R}_+} D_{j,i}(m_1^j v,t)g_1(v)dv\Big)\rho_1^j - \sum_{j=1}^M\Big(\int_{\mathbb{R}_+} D_{i,j}(m_1^i v,t)g_1(v)dv\Big)\rho_1^i \\ \frac{d}{dt}\rho_2^i & = \Big(\int_{\mathbb{R}_+}\alpha(m_1^i v)g_1(v)dv\Big)\rho_1^i - \Big(\int_{\mathbb{R}_+}\beta(v)g_2(v)dv\Big)\rho_2^i \\ \frac{d}{dt}(\rho_1^i m_1^i) & = \Big(\int_{\mathbb{R}_+} v\beta(v)g_2(v)dv\Big)\rho_2^i - \Big(\int_{\mathbb{R}_+} v\alpha(m_1^i v)g_1(v)dv\Big)\rho_1^i m_1^i \\ & + \sum_{j=i}^M\Big(\int_{\mathbb{R}_+} vD_{j,i}(m_1^j v,t)g_1(v)dv\Big)\rho_1^j m_1^j + \\ & - \sum_{j=1}^M\Big(\int_{\mathbb{R}_+} vD_{i,j}(m_1^i v,t)g_1(v)dv\Big)\rho_1^i m_1^i \\ \frac{d}{dt}(\rho_2^i m_2^i) & = \Big(\int_{\mathbb{R}_+} v\alpha(m_1^1 v)g_1(v)dv\Big)\rho_1^i m_1^i - \Big(\int_{\mathbb{R}_+} v\beta(v)g_2(v)dv\Big)\rho_2^i\,. \end{cases} \tag{124}$$

By means of the same arguments adopted in the Q-nQ case, if we assume $\eta = 0$, we can state

$$g_1^i(v) = \delta(v - \tilde{m_1^i}), \quad g_2(v) = \delta(v)$$

and hence write the system

$$\begin{cases} \frac{d}{dt}\rho_1^i & = \beta(0)\rho_2^i - \alpha(m_1^i)\rho_1^i + \sum_{j=1}^n D_{j,i}(m_1^j,t)\rho_1^j - \sum_{j=1}^n D_{i,j}(m_1^i,t)\rho_1^i \\ \frac{d}{dt}\rho_2^i & = \alpha(m_1^i)\rho_1^i - \beta(0)\rho_2^i \\ \frac{d}{dt}(\rho_1^i m_1^i) & = -\alpha(m_1^i)\rho_1^i m_1^i + \sum_{j=1}^n D_{j,i}(m_1^j,t)\rho_1^j m_1^j - \sum_{j=1}^n D_{i,j}(m_1^i,t)\rho_1^i m_1^i \,. \end{cases} \tag{125}$$

We can now aggregate cities and investigate the overall evolution of the epidemics. We obtain,

$$\begin{cases} \frac{d}{dt}\rho_1 & = \beta(0)(1-\rho_1) - \sum_{i=1}^n \alpha(m_1^i)\rho_1^i \\ \rho_2 & = 1-\rho_1 \\ \frac{d}{dt}(\rho_1 m_1) & = -\sum_{i=1}^n \alpha(m_1^i)\rho_1^i m_1^i \,, \end{cases} \tag{126}$$

where $\sum_{i=1}^n \alpha(m_1^i)\rho_1^i \geq 0$ and $\sum_{i=1}^n \alpha(m_1^i)\rho_1^i m_1^i \geq 0$. Since $\rho_1 = 0 \leftrightarrow \rho_1^i = 0, i = 1, ..., n$, the first equation yields $\rho_1^\infty > 0$ and hence $\exists i \in \{1, ..., n\} : (\rho_1^i)^\infty \neq 0$. If we assume again $\alpha(v) > 0 \forall v \neq 0$ and $\alpha(0) = 0$, second equation yields $(\rho_1^i)^\infty \neq 0 \Rightarrow (m_1^i)^\infty = 0$, i.e. null *viral load* if there is population in the city. Thus, we obtain the same asymptotic results of the simple Q-nQ model

$$\rho_1^\infty = 1, \quad \rho_2^\infty = 0, \quad m_1^\infty = 0 \implies f_1^\infty(v) = \delta(v), \quad f_2^\infty(v) = 0.$$

In this dissertation we chose the transition probability $D = D(v,t)$ to depend on the microscopic state $v$ and on time $t$. Another possibility would have been to make it dependent on the mean *viral load* of diagnosed people in the various city, namely $D = D(m_2^i)$. This choice would have made it possible to elaborate a confinement strategy based on selective restriction on travels to stem the epidemic.

## 3.4 Vaccine model

In the last sections, we have showed how the binary interaction label switch joint description can describe the effects of a quarantine confinement strategy on an epidemic. Another massively used method to fight epidemics is vaccination. In this section, we will introduce a kinetic based description of the evolution of an infectious disease epidemic on a population subject to vaccination. We will refer to this model as the Vax model. It is important to point out that for modeling vaccination, we need to make a choice on what vaccination means from the transmission point of view. It can mean either that vaccinated people can no longer be infected, and they are therefore removed from the population, or it can mean that they can no longer

develop symptoms, but they still can get infected and infect other people. In this dissertation, we will focus on the worse-case scenario of vaccines that prevents symptoms but not infection, scenario that some studies, e.g. [45], suggest could be the one the world is facing due to Covid-19. Vaccines equip patients with antibodies to fight the disease they are designed for. Hence, while they can still spread the illness when infected, agents that have been vaccinated will quickly recover. Let us restore the *viral load* $v \in V = \mathbb{R}_+$ as the microscopic state of the binary interaction process. We then assume the label of the Markov-type label switch process $x \in \mathcal{I} = \{1, 2, 3\}$ such that $x = 1$ means that the agent has not been diagnosed, $x = 2$ means that the agent has been diagnosed and they are being cured and $x = 3$ means that the agent has been vaccinated. When an agent is diagnosed or vaccinated, they will take part in a healing process that will lower their *viral load* $v$. Hence, in this model there are two processes involving the *viral load*: the binary interaction process and a linear healing process that will update the value of $v$. Diagnosed people can return to the undiagnosed group when their *viral load* is low enough, but they can not be vaccinated. Undiagnosed people can be diagnosed when their *viral load* is high enough and can be vaccinated. Vaccinated people can not be diagnosed and remain vaccinated forever. Let us define the transition probability

$$T = T(t, v; x|y) \in [0, 1], \ \forall v \in \mathbb{R}_+, \ t > 0, \ x, y \in \mathcal{I}$$

as the probability the label of an agent with viral load $v$ has to change from $y$ to $x$ at time $t$. It holds

$$\sum_{x \in \mathcal{I}} T(t, v; x|y) = 1, \ \forall v \in \mathbb{R}_+, \ t > 0, \ y \in \mathcal{I}.$$

Since agents belonging to each group interact in the same way, we are in the case of same interaction rule described at the end of sec. 2.3. However, also in this case the presence of a second process involving $v$ produces some differences with respect to equation (54). The definition of the distribution function $f$ (41) holds, since there are only one microscopic state and one label. If we describe the state of an agent with the random variable pair $(X_t, V_t) \in \mathcal{I} \times \mathbb{R}_+$, since the new healing process influences the same quantity as the interaction process, equation (44) becomes

$$\begin{cases} X_{t+\Delta t} & = (1 - \Theta)X_t + \Theta J_t \\ V_{t+\Delta t} & = (1 - \Xi)(1 - \Omega)V_t + \Xi(1 - \Omega)V_t' \\ & \quad +(1 - \Xi)\Omega V_t'' + \Xi\Omega V_t''' \,, \end{cases}$$

where $V_t'$, $V_t''$ and $V_t'''$ are the post-event *viral loads* in the case an interaction occurred, the healing process activated or both events happened, respectively. Let us point out that $V_t'''$ will not show in the Boltzmann type equation as it appears only in order two or three in time addends, neglected as $\Delta t \to 0^+$. As usual, $J_t$ is the post label switch label and $\Theta$, $\Omega$, $\Xi$ are Bernoulli random variables. If we call the healing process' frequency with the parameter $\omega$, we can write the weak Boltzmann type equation for the evolution of an observable $\phi = \phi(v)$ as

$$\begin{aligned}\frac{d}{dt}\int_{\mathbb{R}_+}\phi(v)f_i(t,v)dv = \lambda\int_{\mathbb{R}_+}\phi(v)\Big(\sum_{j=1}^{3}R(t,v;i|j)f_j(t,v) - f_i(t,v)\Big)dv \\ + \mu\sum_{j=1}^{3}\iint_{\mathbb{R}_+\times\mathbb{R}_+}\langle\phi(v') - \phi(v)\rangle f_i(t,v)f_j(t,v_*)dvdv_* \\ + \omega\int_{\mathbb{R}_+}\langle\phi(v_i'') - \phi(v)\rangle f_i(t,v)dv \qquad (127) \\ for\, i = 1,2,3.\end{aligned}$$

The second term in the right-hand side of equation (127) allows interaction with agents from every group to happen. The interaction rule of the binary interaction process is the same as in the Q-nQ model

$$v' = (1 - \nu_1 + \eta)v + \nu_2 v_*. \qquad (128)$$

The healing process updates the *viral load* following the rule

$$v_i'' = (1 - \gamma_i + \xi)v\,, \qquad (129)$$

where we assume $\gamma_1 = 0$ since undiagnosed people does not receive any medical care. Let us define the transition probabilities as $T(t,v;i|j) = T_{i,j}$, where $T_{i,j}$ is the $i$-th, $j$-th component of the matrix $T$

$$T = \begin{pmatrix} 1-\alpha(v)-\zeta(t) & \beta(v) & 0 \\ \alpha(v) & 1-\beta(v) & 0 \\ \zeta(t) & 0 & 1 \end{pmatrix}.$$

We notice how $\sum_{i=1}^{3} T_{i,j} = 1$, $\forall j$. Finally, we can write the weak Boltzmann type equation for the Vax model. For undiagnosed people ($x = 1$) it reads

$$\begin{aligned}\frac{d}{dt}\int_{\mathbb{R}_+}\phi(v)f_1(t,v)dv &= \lambda\int_{\mathbb{R}_+}\phi(v)\Big(\beta(v)f_2(t,v) - \Big(\alpha(v)+\zeta(v)\Big)f_1(t,v)\Big)dv \\ &+ \mu\sum_{j=1}^{3}\iint_{\mathbb{R}_+\times\mathbb{R}_+}\langle\phi(v')-\phi(v)\rangle f_1(t,v)f_j(t,v_*)dvdv_* \\ &+ \omega\int_{\mathbb{R}_+}\langle\phi(v_1'')-\phi(v)\rangle f_1(t,v)dv\,. \end{aligned} \tag{130}$$

For diagnosed people ($x = 2$) it reads

$$\begin{aligned}\frac{d}{dt}\int_{\mathbb{R}_+}\phi(v)f_2(t,v)dv &= \lambda\int_{\mathbb{R}_+}\phi(v)\Big(\alpha(v)f_1(t,v) - \beta(v)f_2(t,v)\Big)dv \\ &+ \mu\sum_{j=1}^{3}\iint_{\mathbb{R}_+\times\mathbb{R}_+}\langle\phi(v')-\phi(v)\rangle f_2(t,v)f_j(t,v_*)dvdv_* \\ &+ \omega\int_{\mathbb{R}_+}\langle\phi(v_2'')-\phi(v)\rangle f_2(t,v)dv\,. \end{aligned} \tag{131}$$

For vaccinated people ($x = 3$) it reads

$$\begin{aligned}\frac{d}{dt}\int_{\mathbb{R}_+}\phi(v)f_3(t,v)dv &= \lambda\int_{\mathbb{R}_+}\phi(v)\zeta(v)f_1(t,v)dv \\ &+ \mu\sum_{j=1}^{3}\iint_{\mathbb{R}_+\times\mathbb{R}_+}\langle\phi(v')-\phi(v)\rangle f_3(t,v)f_j(t,v_*)dvdv_* \\ &+ \omega\int_{\mathbb{R}_+}\langle\phi(v_3'')-\phi(v)\rangle f_3(t,v)dv\,. \end{aligned} \tag{132}$$

### 3.4.1 Constant transition probabilities

Let us analyze the case with constant transition probabilities. If we assume $\alpha$, $\beta$ and $\zeta$ constant with $\zeta > 0$ and $\lambda = \mu = \omega = 1$ we obtain the ODE system

$$\begin{cases} \frac{d}{dt}\rho_1 & = \beta\rho_2 - (\alpha+\zeta)\rho_1 \\ \frac{d}{dt}\rho_2 & = \alpha\rho_1 - \beta\rho_2 \\ \frac{d}{dt}\rho_3 & = \zeta\rho_1 \\ \\ \frac{d}{dt}(\rho_1 m_1) & = \beta\rho_2 m_2 - (\alpha+\zeta)\rho_1 m_1 \\ & \quad +\nu_2\rho_1(\rho_1 m_1 + \rho_2 m_2 + \rho_3 m_3) - \nu_1\rho_1 m_1 \\ \frac{d}{dt}(\rho_2 m_2) & = \alpha\rho_1 m_1 - \beta\rho_2 m_2 \\ & \quad +\nu_2\rho_2(\rho_1 m_1 + \rho_2 m_2 + \rho_3 m_3) - \nu_1\rho_2 m_2 \\ & \quad -\gamma_2\rho_2 m_2 \\ \frac{d}{dt}(\rho_3 m_3) & = \zeta\rho_1 m_1 \\ & \quad +\nu_2\rho_3(\rho_1 m_1 + \rho_2 m_2 + \rho_3 m_3) - \nu_1\rho_3 m_3 \\ & \quad -\gamma_3\rho_3 m_3\,. \end{cases} \tag{133}$$

Let us firstly focus on the first part of system (133), the one concerning the masses. The first two equations are a stable linear ODE system that yields $\rho_1^\infty = \rho_2^\infty = 0$. Hence, we have $\rho_3^\infty = 1$. This is reasonable since the vaccination process aims to immunize the whole population. This leads the second part of the system to reduce to $\frac{d}{dt}m_3 = (\nu_2 - \nu_1 - \gamma_3)m_3$, that blows to infinity if $\nu_2 - \nu_1 - \gamma_3 > 0$ and goes to zero if $\nu_2 - \nu_1 - \gamma_3 < 0$. Anyway, in this situation the whole population has received the vaccine and therefore one could argue that the analysis on the mean *viral load* is unnecessary, since nobody can virtually contract the disease.

Albeit desirable, it can be hard to reach the complete vaccination of the population. Let us investigate a constant parameters case in which the portion of vaccinated people is a constant $0 \leq c \leq 1$ and $\zeta = 0$. The first part of system (133) modifies as

$$\begin{cases} \frac{d}{dt}\rho_1 & = \beta\rho_2 - \alpha\rho_1 \\ \frac{d}{dt}\rho_2 & = \alpha\rho_1 - \beta\rho_2 \\ \rho_1 + \rho_2 & = 1 - c\,, \end{cases} \tag{134}$$

**Table 1:**

| | | | | | | |
|---|---|---|---|---|---|---|
| Ex. 1 | $\alpha = 0.8$ | $\beta = 0.4$ | $\nu_1 = 0$ | $\nu_2 = 0.2$ | $\gamma_2 = 0.3$ | $\gamma_3 = 0.3$ |
| Ex. 2 | $\alpha = 0.8$ | $\beta = 0.4$ | $\nu_1 = 0$ | $\nu_2 = 0.2$ | $\gamma_2 = 0.1$ | $\gamma_3 = 0.3$ |
| Ex. 3 | $\alpha = 0.2$ | $\beta = 0.4$ | $\nu_1 = 0$ | $\nu_2 = 0.2$ | $\gamma_2 = 0.1$ | $\gamma_3 = 0.3$ |

that yields

$$\begin{aligned}
\rho_1^\infty &= (1-c)\frac{\beta}{\alpha+\beta} = a \\
\rho_2^\infty &= (1-c)\frac{\alpha}{\alpha+\beta} = b \\
\rho_3^\infty &= c\,.
\end{aligned}$$

If we plug in these values, the second part of system (133) reads

$$\begin{cases}
\frac{d}{dt}m_1 &= (-\alpha + \nu_2 a - \nu_1)m_1 + (\alpha + \nu_2 b)m_2 + (\nu_2 c)m_3 \\
\frac{d}{dt}m_2 &= (\beta + \nu_2 a)m_1 + (-\beta + \nu_2 b - \nu_1 - \gamma_2)m_2 + (\nu_2 c)m_3 \\
\frac{d}{dt}m_3 &= (\nu_2 a)m_1 + (\nu_2 b)m_2 + (\nu_2 c - \nu_1 - \gamma_3)m_3\,.
\end{cases} \tag{135}$$

The system matrix in this case is quite complicated and an analytical study of the stability through the computation of the eigenvalues is out of reach. In order to evaluate the stability properties of this case, a numerical computation of the eigenvalues has been carried out. In particular, we are interested in the evolution of the maximum eigenvalue when the parameter $c$ goes from 0 to 1. In fact, when the portion of population that has received the vaccine rises, it reaches a point where it is high enough to stem the epidemic. If we call that point $c_\dagger$ we have that the system blows if $c < c_\dagger$ and it is globally asymptotically stable if $c > c_\dagger$. The value of $c_\dagger$ depends on the values of $\alpha$, $\beta$, $\nu_1$, $\nu_2$, $\gamma_2$ and $\gamma_3$. Figure 5 shows the variation of the value of the maximum eigenvalue with $c$ when the other parameters have the value indicated in Table 1. In example 2, for instance, we have $c_\dagger \simeq 0.86$. Hence, in a situation with those parameters, the epidemic can be eradicated if at least 86% of the population gets the vaccine. This situation is often referred to as herd immunity.

### 3.4.2 Variable transition probabilities

Let us investigate the variable transition probabilities case for the Vax model. We assume variable probabilities $\alpha$ and $\beta$ with the same trend as previous models and a constant $\zeta$, since it is hard to imagine a probability of being vaccinated that varies on a (unknown) *viral load*. The binary interaction process and the healing process

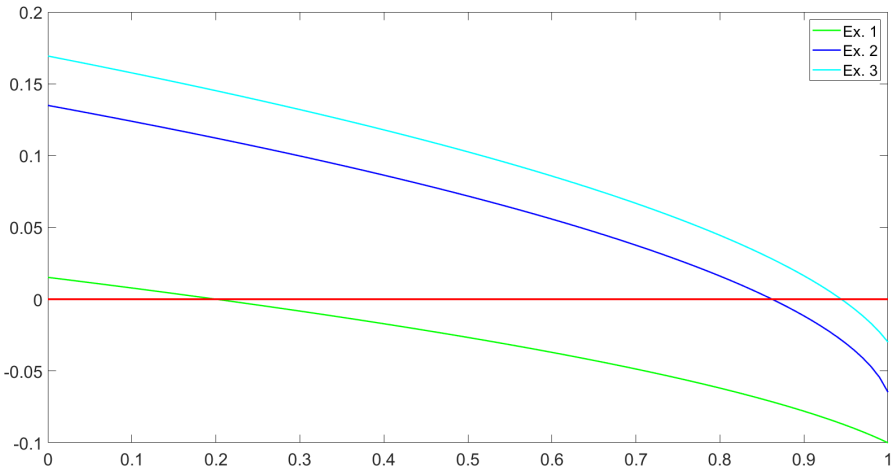


**Figure 5:** The evolution of the max eigenvalue of the system matrix of system (135) when $c$ goes from 0 to 1.

operate on the fast time scale $\tau$ and the label switch process operates on the slow time scale $t$. As usual, if we define a small parameter $0 < \delta \ll 1$ we can write

$$\lambda = 1\,, \quad \mu = \omega = \frac{1}{\delta}\,, \quad \tau := \frac{t}{\delta}$$

and separate equations (130), (131) and (132). On the fast time scale $\tau$ the equation reads the same for every group:

$$\begin{aligned} \frac{d}{d\tau}\int_{\mathbb{R}_+}\phi(v)\tilde{f}_i(\tau,v)dv = \sum_{j=1}^{3}\iint_{\mathbb{R}_+\times\mathbb{R}_+}\langle\phi(v')-\phi(v)\rangle\tilde{f}_i(\tau,v)\tilde{f}_j(\tau,v_*)dvdv_* \\ + \int_{\mathbb{R}_+}\langle\phi(v_i'')-\phi(v)\rangle\tilde{f}_i(\tau,v)dv \qquad (136) \\ for\, i = 1,2,3. \end{aligned}$$

On the slow time scale we need to diversify the equations, they read

$$\frac{d}{dt}\int_{\mathbb{R}_+}\phi(v)f_1(t,v)dv = \int_{\mathbb{R}_+}\phi(v)\Big(\beta(v)f_2(t,v) - \Big(\alpha(v)+\zeta\Big)f_1(t,v)\Big)dv \qquad (137)$$

$$\frac{d}{dt}\int_{\mathbb{R}_+}\phi(v)f_2(t,v)dv = \int_{\mathbb{R}_+}\phi(v)\Big(\alpha(v)f_1(t,v) - \beta(v)f_2(t,v)\Big)dv \qquad (138)$$

$$\frac{d}{dt}\int_{\mathbb{R}_+}\phi(v)f_3(t,v)dv = \int_{\mathbb{R}_+}\phi(v)\zeta f_1(t,v)dv\,. \qquad (139)$$

Considering a conservative binary interaction process $\nu_1 = \nu_2$ as in the previous analysis, owing to $\gamma_1 = 0$ and $\gamma_2, \gamma_3 > 0$ in interaction rule (129), we obtain an overall trend towards zero on the fast time scale $\tau$ that yields

$$f_i(t, v) = \rho_i(t)\delta(v)\,. \tag{140}$$

Hence, in this case, the fact that interactions occur among all groups in the same way leads to the complete eradication of the illness on the fast time scale $t$. This makes the hydrodynamic limit for the vaccine model quite uninteresting.

## 3.5 Age-structured vaccine model

One of the most important attributes an individual in an epidemiological model can be equipped with is the chronological age. From the medical point of view, age can affect the response of an agent both to the virus and to the cure, while from the perspective of population dynamics it can affect the rate at which an agent interacts with others. Both these aspects heavily influence the spread of an epidemic in a population. In addition to that, the vaccination campaigns often rely on age to choose who needs to be vaccinated first. For all these reasons, we propose an age-structured version of the Vax model. As we did for the quarantine model on the network, we base this additional characteristic of the agents on a second label $a \in \mathcal{A} = \{1, 2, ..., n\}$. Thus, we assume $n$ age classes the agents can belong to. Considering that an epidemic has usually a time horizon of a few years at most, if the number of age classes $n$ is sufficiently low, the aging of agents can be neglected. Hence, while the model contains two labels, only the label switch process regarding label $x \in \mathcal{I} = \{1, 2, 3\}$ is at work. The interactions happen among agent in every group and in every age class. Agents of different ages, however, can interact with different rates. In this dissertation we chose three age classes ($n = 3$), where $a = 1$ correspond to young agents, $a = 2$ to adult agents and $a = 3$ to elderly agents. Let us define a frequency adjustment coefficient $r_i$. An agent will interact with a probability $P = r_i\mu\Delta t$, that depends on their age as well as on the (small) time interval $\Delta t$. For probability $P$ to be consistent, it needs to be

$$\Delta t \leq \frac{1}{r_i\mu}, \forall i \in \{1, ..., n\}.$$

Moreover, if we want to maintain from the Vax model the expected number of interactions $\mathbb{E}(\mu\Delta t N)$, where $N$ is the total number of agents in the population, and we denote with $N^k$ the number of agents in the $k$-th age class, the adjustment

coefficient needs to satisfy

$$\mu N = \mu \sum_{k=1}^{n} r_k \cdot N^k \;\Rightarrow \sum_{k=1}^{n} \rho^k r_i = 1\,. \tag{141}$$

The introduction of the frequency adjustment coefficient just slightly modifies the derivation of the weak form of the Boltzmann equation in sec. 2.3. In fact, it only affects the computation of the mean of the post interaction observable quantity $\phi = \phi(X_t, A_t, V_t')$, that reads

$$\mu\langle\phi(X_t, A_t, V_t')\rangle = \mu \sum_{i,j,k,l} r_i \iint_{\mathbb{R}_+\times\mathbb{R}_+} \langle\phi(i,k,v')\rangle f_i^k(t,v) f_j^l(t,v_*) dv dv_*\,.$$

As mentioned before, age can affect the way a person respond to the same level of infection as well as the vaccination priority a person is subject to. Therefore, we let the transition probability matrix to depend on age, $T = T(t,a,v;x|y)$. In particular, we choose an age-dependent version of the simple Vax model transition probability

$$T = \begin{pmatrix} 1-\alpha(v,a)-\zeta(t,a) & \beta(v,a) & 0 \\ \alpha(v,a) & 1-\beta(v,a) & 0 \\ \zeta(t,a) & 0 & 1 \end{pmatrix}.$$

We can now write the weak Boltzmann-type equation for the age-structured Vax model. For undiagnosed people ($x = 1$) it reads

$$\begin{aligned} \frac{d}{dt}\int_{\mathbb{R}_+} \phi(v) f_1^k(t,v) dv = \lambda \int_{\mathbb{R}_+} \phi(v) \Big( \beta(v) f_2^k(t,v) - \big(\alpha(v)+\zeta(v)\big) f_1^k(t,v) \Big) dv \\ + \mu \sum_{j=1}^{3}\sum_{l=1}^{n} r_k \iint_{\mathbb{R}_+\times\mathbb{R}_+} \langle\phi(v') - \phi(v)\rangle f_1^k(t,v) f_j^l(t,v_*) dv dv_* \\ + \omega \int_{\mathbb{R}_+} \langle\phi(v_{1k}'') - \phi(v)\rangle f_1^k(t,v) dv\,. \end{aligned} \tag{142}$$

For diagnosed people ($x = 2$) it reads

$$\begin{aligned} \frac{d}{dt}\int_{\mathbb{R}_+} \phi(v) f_2^k(t,v) dv = \lambda \int_{\mathbb{R}_+} \phi(v) \Big( \alpha(v) f_1^k(t,v) - \beta(v) f_2^k(t,v) \Big) dv \\ + \mu \sum_{j=1}^{3}\sum_{l=1}^{n} r_k \iint_{\mathbb{R}_+\times\mathbb{R}_+} \langle\phi(v') - \phi(v)\rangle f_2^k(t,v) f_j^l(t,v_*) dv dv_* \\ + \omega \int_{\mathbb{R}_+} \langle\phi(v_{2k}'') - \phi(v)\rangle f_2^k(t,v) dv\,. \end{aligned} \tag{143}$$

For vaccinated people ($x = 3$) it reads

$$\frac{d}{dt}\int_{\mathbb{R}_+}\phi(v)f_3^k(t,v)dv = \lambda\int_{\mathbb{R}_+}\phi(v)\zeta(v)f_1^k(t,v)dv + \mu\sum_{j=1}^{3}\sum_{l=1}^{n}r_k\iint_{\mathbb{R}_+\times\mathbb{R}_+}\langle\phi(v')-\phi(v)\rangle f_3^k(t,v)f_j^l(t,v_*)dvdv_* + \omega\int_{\mathbb{R}_+}\langle\phi(v''_{3k})-\phi(v)\rangle f_3^k(t,v)dv\,. \tag{144}$$

Let us notice that the healing process produces an updated *viral load* $v''_{ik}$ that depends on both the labels $x$ and $a$. This is due to the fact that people with different ages can responsse

differently to the same medical treatment, and hence they can heal differently.

### 3.5.1 Constant transition probabilities

Let us discuss the constant transition probability case for the age-structured Vax model. It is interesting to study the case where $\alpha$ and $\beta$ are constant with respect to the *viral load* $v$ and $\zeta = 0$, with a fixed portion of population that has been vaccinated. Being $n = 3$, let us define $0 \leq c_i \leq 1$, $i = 1, 2, 3$ the portion of, respectively, young people, adults and elderly people that has received the vaccine. Let us express the dependency of the transition probabilities from the age as

$$\alpha(a) = \alpha_i \, for \, a = i$$
$$\beta(a) = \beta_i \, for \, a = i, \quad i = 1, 2, 3.$$

The ODE system for the macroscopic quantities obtained is

$$
\begin{cases}
\frac{d}{dt}\rho_1^k & = \beta_k\rho_2^k - \alpha_k\rho_1^k \\
\frac{d}{dt}\rho_2^k & = \alpha_k\rho_1^k - \beta_k\rho_2^k \\
\frac{d}{dt}\rho_3^k & = 0 \\
 & \\
\frac{d}{dt}(\rho_1^k m_1^k) & = \beta_k\rho_2^k m_2^k - \alpha_k\rho_1^k m_1^k \\
 & +r_k\Big(\nu_2\rho_1^k(\sum_{j=1}^3\sum_{l=1}^3\rho_j^l m_j^l) - \nu_1\rho_1^k m_1^k\Big) \\
\frac{d}{dt}(\rho_2^k m_2^k) & = \alpha_k\rho_1^k m_1^k - \beta_k\rho_2^k m_2^k \\
 & +r_k\Big(\nu_2\rho_2^k(\sum_{j=1}^3\sum_{l=1}^3\rho_j^l m_j^l) - \nu_1\rho_2^k m_2^k\Big) \\
 & -\gamma_{2k}\rho_2^k m_2^k \\
\frac{d}{dt}(\rho_3^k m_3^k) & = r_k\Big(\nu_2\rho_3^k(\sum_{j=1}^3\sum_{l=1}^3\rho_j^l m_j^l) - \nu_1\rho_3^k m_3^k\Big) \\
 & -\gamma_{3k}\rho_3^k m_3^k\,.
\end{cases}
\tag{145}
$$

The first part regarding the masses is composed by three uncoupled systems, whose asymptotic solutions are

$$\rho_1^{k,\infty} = (1-c_k)\frac{\beta_k}{\alpha_k+\beta_k} = a_k$$

$$\rho_2^{k,\infty} = (1-c_k)\frac{\alpha_k}{\alpha_k+\beta_k} = b_k$$

$$\rho_3^{k,\infty} = c_k\,.$$

If we plug these distributions in the second part of system (145) we can write

$$
\begin{cases}
a_k\frac{d}{dt}m_1^k & = \beta_k b_k m_2^k - \alpha_k a_k m_1^k \\
 & +r_k a_k\Big(\nu_2(\sum_{l=1}^3 a_l m_1^l + b_l m_2^l + c_l m_3^l) - \nu_1 m_1^k\Big) \\
b_k\frac{d}{dt}m_2^k & = \alpha_k a_k m_1^k - \beta_k b_k m_2^k \\
 & +r_k b_k\Big(\nu_2(\sum_{l=1}^3 a_l m_1^l + b_l m_2^l + c_l m_3^l) - \nu_1 m_2^k\Big) \\
 & -\gamma_{2k} b_k m_2^k \\
c_k\frac{d}{dt}m_3^k & = r_k c_k\Big(\nu_2(\sum_{l=1}^3 a_l m_1^l + b_l m_2^l + c_l m_3^l) - \nu_1 m_3^k\Big) \\
 & -\gamma_{3k} c_k m_3^k\,.
\end{cases}
$$

If $\rho_i^{k,\infty} \neq 0,\ for\, i,k = 1,2,3$, we can simplify the masses to obtain

$$\begin{cases} \frac{d}{dt}m_1^k &= \alpha_k m_2^k - \alpha_k m_1^k \\ &+r_k\Big(\nu_2(\sum_{l=1}^3 a_l m_1^l + b_l m_2^l + c_l m_3^l) - \nu_1 m_1^k\Big) \\ \frac{d}{dt}m_2^k &= \beta_k m_1^k - \beta_k m_2^k \\ &+r_k\Big(\nu_2(\sum_{l=1}^3 a_l m_1^l + b_l m_2^l + c_l m_3^l) - \nu_1 m_2^k\Big) \\ &-\gamma_{2k} m_2^k \\ \frac{d}{dt}m_3^k &= r_k\Big(\nu_2(\sum_{l=1}^3 a_l m_1^l + b_l m_2^l + c_l m_3^l) - \nu_1 m_3^k\Big) \\ &-\gamma_{3k} m_3^k\,. \end{cases} \tag{146}$$

We can numerically evaluate the eigenvalues of the $9\times 9$ system matrix to investigate the behavior of the mean *viral load*. In particular, it is interesting to see how the threshold $c_{i\dagger}$ changes according to the value of the parameters. Let us see a few examples. If we assume the value of $\alpha_k$, $\beta_k$, $\nu_1$, $\nu_2$, $\rho^k$, $r_k$ as listed in Table 2 and we let $\gamma_{i,k}$ change, we notice how the threshold for the vaccination of adult people $c_{2\dagger}$ changes if we assume that the most of the young population has been vaccinated, or the most of the elderly population has instead. Figure 6 shows the trend of the maximum real part of the eigenvalues of the matrix associated with system (146). The parameter $\gamma$ is assumed as listed in Table 3. The chart on the top correspond to the table on the left while the chart on the bottom to the table on the right. The two lines on each chart correspond to the two vaccination strategies adopted: the line in blue corresponds to the vaccination of the elderly people first, assumed completed at 95%, while only 5% of young population is vaccinated. The line in cyan corresponds to the opposite situation, where only 5% of elderly people and 95% of young people are vaccinated. As it is clear from the charts, the best strategy depends on the specific situation. In this example we have highlighted the dependency on the characteristics of the cure: if the medical care received by diagnosed people is much more effective on young people, it is best to vaccinate the elderly first; if the difference is less pronounced, it is best to vaccinate the young people first. This is due to the fact that young people have more interactions than elderly people and hence they allow the illness to proliferates. In fact, we can see from Figure 7 that if we assume $r_k = 1$ for $k = 1,2,3$, the best strategy is to vaccinate elderly people first, even in the case of a small difference in the effectiveness of the cure.

We do not investigate the hydrodynamic limit for this case as it proved uninteresting since the epidemic is eradicated on the fast time scale $t$.

**Table 2:**

| $\alpha_k$ | $\beta_k$ | $\nu_1$ | $\nu_2$ | $\rho^k$ | $r_k$ |
|---|---|---|---|---|---|
| $[0.5, 0.7, 0.8]$ | $[0.4, 0.4, 0.4]$ | 0 | 0.2 | $[0.33, 0.34, 0.33]$ | $[1.5, 1, 0.5]$ |

**Table 3:**

The values of $\gamma_{i,k}$ in the example

| | | |
|---|---|---|
| 0 | 0 | 0 |
| 0.5 | 0.3 | 0.07 |
| 0.5 | 0.5 | 0.4 |

| | | |
|---|---|---|
| 0 | 0 | 0 |
| 0.3 | 0.2 | 0.1 |
| 0.5 | 0.5 | 0.4 |

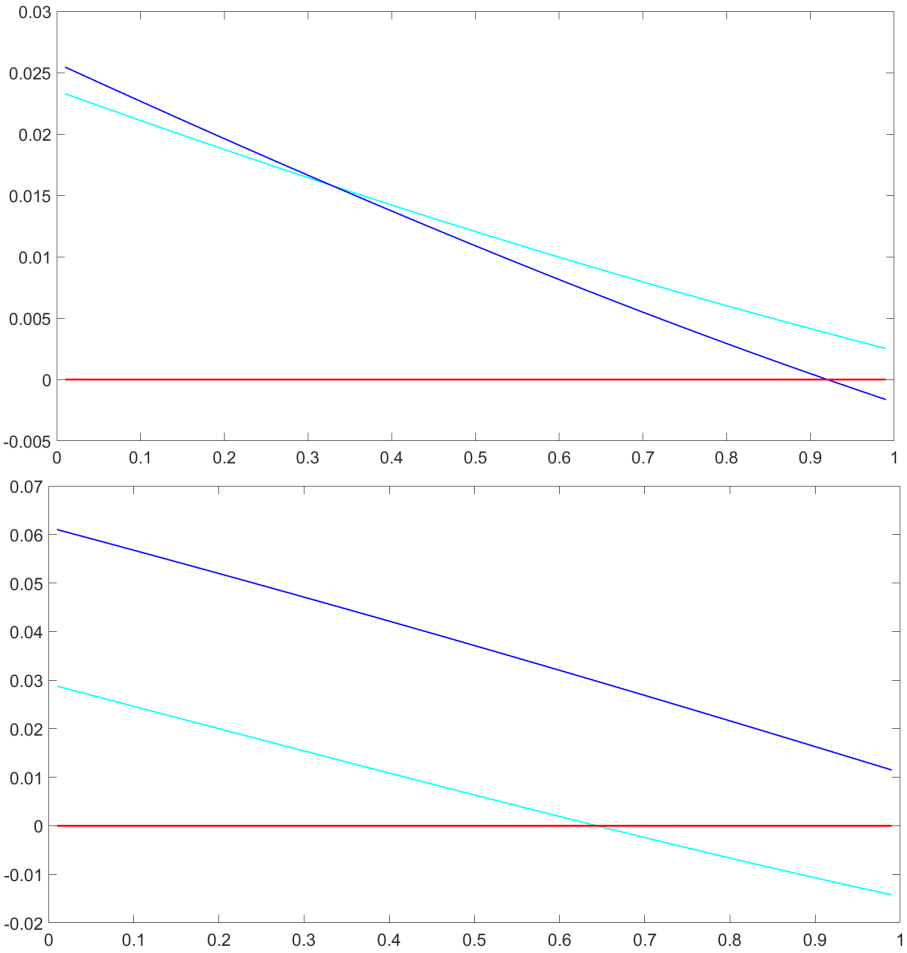


**Figure 6:** The maximum real part of eigenvalues of the matrix of the system (146). On the top $\gamma_{i,k}$ is assumed as listed in the left part of Table 3. On the bottom $\gamma_{i,k}$ is assumed as listed in the right part of Table 3.

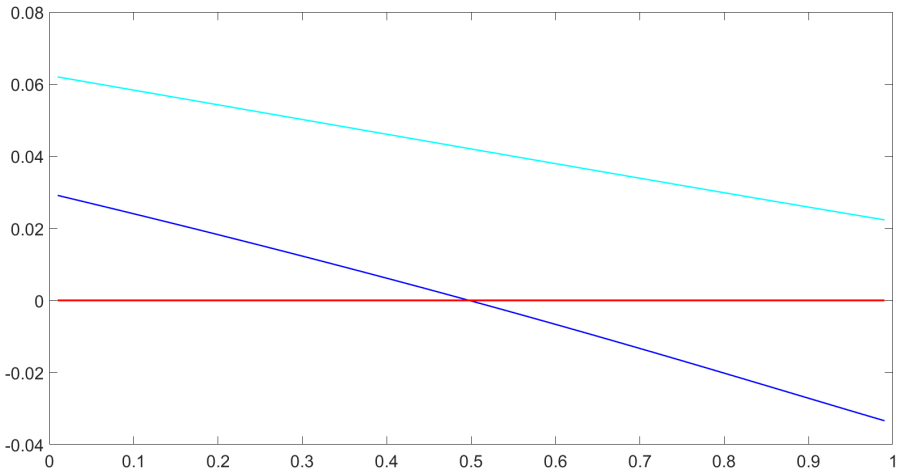


**Figure 7:** The case with $\gamma_{i,k}$ as in the right part of Table 3 with $r_k = 1$ for $k = 1, 2, 3$.

# 4 Numerical tests

All the kinetic models described in the previous section have been numerically simulated. The simulations have been carried out following a modified version of the Nanbu-Babovsky scheme described in sec. 2.5. This version includes, according to the circumstances, one or more mechanisms to transfer agents from one label to the other and a microscopic state updating mechanism for the healing process, in addition to the binary interaction process of the original version. General versions of the algorithms used for the simulations of the Q-nQ and Vax models are shown in Appendix. A large number ($N = 10^6$) of agents is considered in each one of the four algorithms implemented, one for each model. The algorithms aim to reproduce the time discrete microscopic processes of sec. 2.3 that led to the kinetic equations in the limit for $\Delta t \to 0^+$. Random variables $\Theta$, $\Xi$ and, if needed, $\Omega$ are sampled from the Bernoulli distribution (110). They define the agents that are involved in an event of interaction, label switch or healing, as appropriate. In the age-structured vaccination model, $\Xi$ needs to be differentiated according to the frequency adjustment coefficient $r_i$, $i = 1, 2, 3$. $J_t$ and $B_t$ are conditionally distributed as (87) and (109), respectively. $V_t'$ is defined according to the appropriate interaction rule ((88) or (89) for the Q-nQ models and (128) for the Vax models). If present, $V_t''$ is defined according to (129). Once the algorithm has established through $\Theta$, $\Xi$ and $\Omega$ which agent is involved in which event (or combination of events), the *viral load* and/or the label of those agents are updated. This happens according to the limitations of each case: a quarantined agent will not change their city label nor will interact, even if they were supposed to. Another important thing is that every process happens simultaneously. Hence, agents who are supposed to be subject to more than one

**Table 4:** Constant parameters for the simple Q-nQ model

| Parameter | $N$ | $\lambda$ | $\Delta t$ | $\nu_2$ | $\gamma$ |
|---|---|---|---|---|---|
| Value | $10^6$ | 1 | $10^{-2}$ | 0.2 | 0.3 |

**Table 5:** Parameters that change from test to test

| Parameter | Figure 8 | Figure 9 | Figure 10 | Figure 11 | Figure 12 | Figure 13 |
|---|---|---|---|---|---|---|
| $\mu$ | 1 | 1 | 10 | 1 | 10 | 1 |
| $\alpha$ | 0.8 | 0.2 | $0.8(1-e^{-v})$ | $0.8(1-e^{-v})$ | $0.8(1-e^{-v})$ | $0.8(1-e^{-v})$ |
| $\beta$ | 0.4 | 0.4 | $0.4e^{-v}$ | $0.4e^{-v}$ | $0.4e^{-v}$ | $0.4e^{-v}$ |
| $\nu_1$ | 0 | 0 | 0.2 | 0.2 | 0 | 0 |
| $\alpha_\dagger$ | 0.28 | 0.28 | / | / | / | / |

process do so at the same time. Let us refer to an example for more clarity: if an agent in the Q-nQ model on the network undergoes both the label switch processes, i.e. both label $x \in \mathcal{I}$ and $a \in \mathcal{C}$ change, in the same time interval $\Delta t$, all happens accordingly to the pre-event attributes. This means that if they were not quarantined and they are diagnosed in this $\Delta t$, they can still travel in the same time interval.

Let us now show the results of the simulations carried out following this scheme. For each model, some of the simulations are intended to confirm the theoretical findings. Hence, a comparison with the numerical solution of the ODE system obtained for the model from the kinetic equations is shown. In other cases the simulations are intended to investigate cases that are not covered by the developed theory, e.g. variable transition probabilities without scale separation or hydrodynamic limit with non-conservative interactions.

## 4.1 Q-nQ model

Let us begin with the simple Q-nQ model. The initial conditions in every test are such that none of the agents is quarantined at $t = 0$ and the *viral load* is sampled from a uniform distribution in $[0, 1]$:

$$f_{1,0}(v) = U_{[0,1]}(v), \quad f_{2,0}(v) = 0\,.$$

In Table 4 we list the parameters constant to all simulations while in Table 5 we list the parameters that change in the various tests.

Figure 8 and Figure 9 show the evolution of mass and mean *viral load* in the case of constant transition probabilities of sec. 3.2.1. In particular we show how if the diagnosis probability $\alpha$ is higher than the threshold $\alpha_\dagger$ the system converges to zero

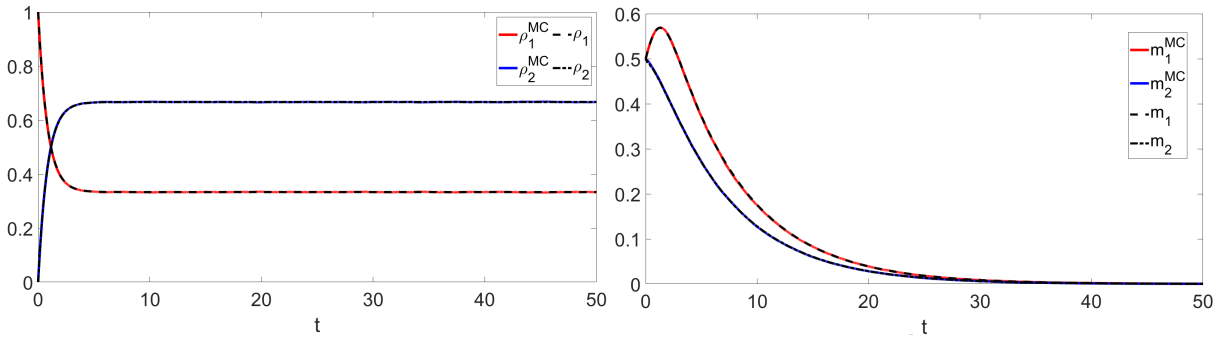


**Figure 8:** Evolution of mass and mean *viral load* in time with constant transition probabilities and $\alpha > \alpha_\dagger$.

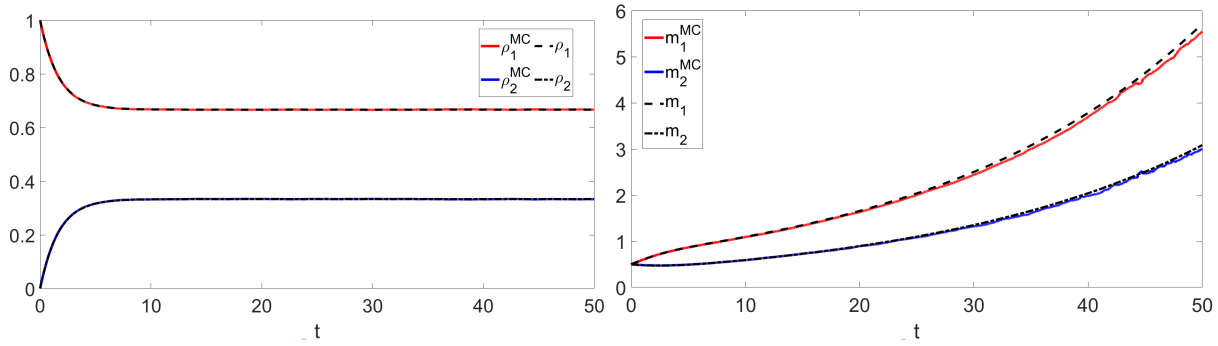


**Figure 9:** Evolution of mass and mean *viral load* in time with constant transition probabilities and $\alpha < \alpha_\dagger$.

(Figure 8), while if $\alpha < \alpha_\dagger$ it blows to infinity (Figure 9). We notice how the mass of quarantine people and non-quarantined people quickly reaches level predicted in (93), in both cases (Figure 8 and Figure 9). For both tests the solutions of the corresponding ODE systems (92) are shown. Numerical simulations and theoretical findings almost totally coincide.

Figure 10 refers to the case with variable transition probabilities and separated time scales. In particular, we chose $\alpha = 0.8(1 - e^{-v})$ non decreasing in $v$ and $\beta = 0.4e^{-v}$

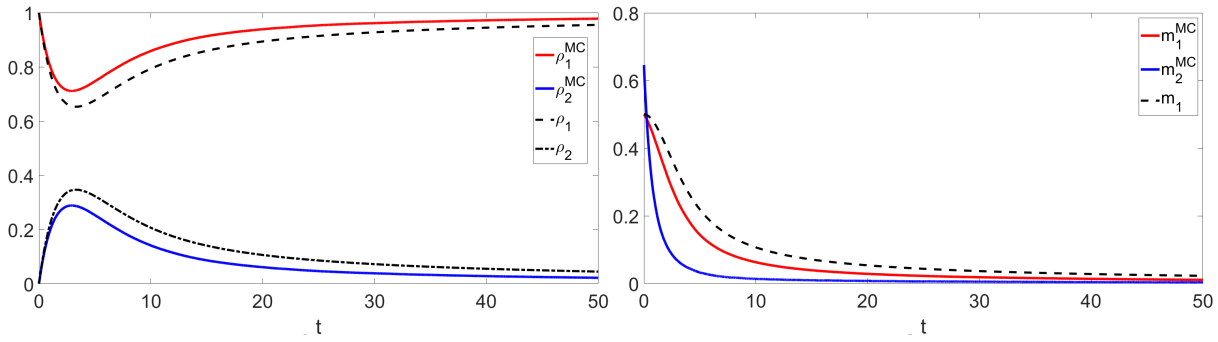


**Figure 10:** Evolution of mass and mean *viral load* in time with variable transition probabilities in the hydrodynamic limit $\mu \gg \lambda$.

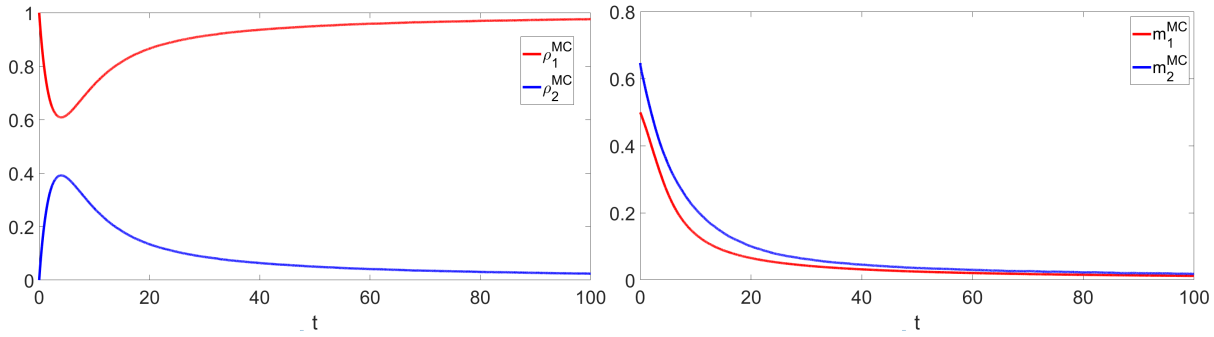


**Figure 11:** Evolution of mass and mean *viral load* in time with variable transition probabilities with $\mu = \lambda$ and $\nu_1 = \nu_2$.

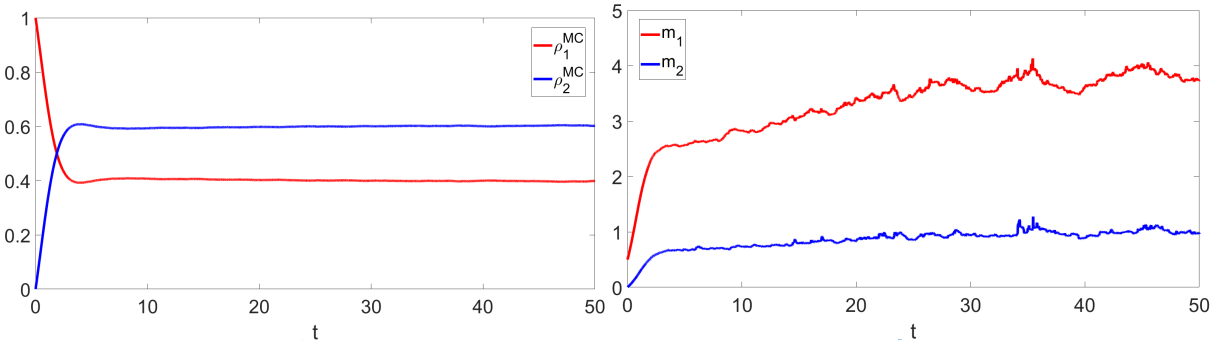


**Figure 12:** Evolution of mass and mean *viral load* in time with variable transition probabilities with $\mu \gg \lambda$ and $\nu_1 = 0$.

non increasing in $v$, as in sec. 3.2.2. In this case the numerical solution of the ODE system (104) follows less closely the trend of the numerical simulation. This is due to the finiteness of the simulation environment as well as the various approximations adopted to obtain the ODE system. Anyway, the numerical simulation shows that, as predicted by the qualitative analysis, the epidemic expires and no person is quarantined in the long run.

The last three simulations explore cases not investigated theoretically. First, let us

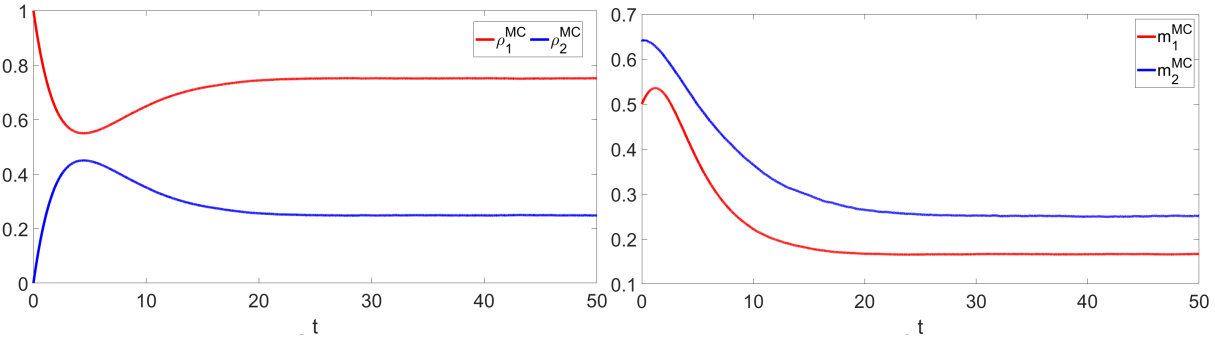


**Figure 13:** Evolution of mass and mean *viral load* in time with variable transition probabilities with $\mu = \lambda$ and $\nu_1 = 0$.

**Table 6:** Constant parameters

| Parameter | $N$ | $\lambda$ | $\omega$ | $\Delta t$ | $\nu_2$ | $\gamma$ |
|---|---|---|---|---|---|---|
| Value | $10^6$ | 1 | 1 | $10^{-3}$ | 0.2 | 0.3 |

**Table 7:** Parameters that change from test to test

| Parameter | Figure 14 | Figure 16 | Figure 17 | Figure 18 | Figure 19 |
|---|---|---|---|---|---|
| $\mu$ | 1 | 1 | 10 | 1 | 10 |
| $\alpha$ | 0.8 | 0.8 | $0.8(1-e^{-v})$ | $0.8(1-e^{-v})$ | $0.8(1-e^{-v})$ |
| $\beta$ | 0.4 | 0.4 | $0.4e^{-v}$ | $0.4e^{-v}$ | $0.4e^{-v}$ |
| $\nu_1$ | 0 | 0 | 0.2 | 0.2 | 0 |
| i.c. | as in (147) | as in (148) | as in (147) | as in (148) | as in (148) |

focus on the case with conservative binary interactions ($\nu_1 = \nu_2$) happening on the same time scale as label switches. This situation does not allow for the hydrodynamic limit. From the results in Figure 11 we see anyway that both the trends of mass and mean *viral load* are similar to the case $\mu \gg \lambda$. In fact, with a slightly slower convergence rate, in the long run the epidemic expires with no quarantined people. Figure 12 and Figure 13 refer to the case with variable transition probabilities and $\nu_1 = 0$. In the first case we assume $\mu \gg \lambda$ while in the second case $\mu = \lambda$. The comparison of the two cases well highlight the importance of the quarantine: Figure 12 shows that, if the diagnosis' process is too slow, the quarantine fails to stem the epidemic and the mean *viral load* is high despite a consistent portion of population is quarantined. Conversely, if the infected agents are promptly diagnosed, the mean *viral load* does not rise and the portion of quarantined people is reduced. This is shown in Figure 13.

## 4.2 Q-nQ on the network model

The simulations of the Q-nQ model on the network confirms the findings of the qualitative analysis of sec. 3.3. The initial condition in this case changes from test to test as it is a crucial factor in the realization of the simulation. Table 6 lists the constant parameters while Table 7 lists the parameters in the various tests.

Figure 14 and Figure 16 show the evolution of mass and mean *viral load* in the three cities when transition probabilities are assumed constant. In the former the initial condition is the same in every city, with *viral load* uniformly distributed in $[0, 1]$, hence

$$f^i_{1,0}(v) = U_{[0,1]}(v), \quad f^i_{2,0}(v) = 0\,,\ i = 1, 2, 3. \tag{147}$$

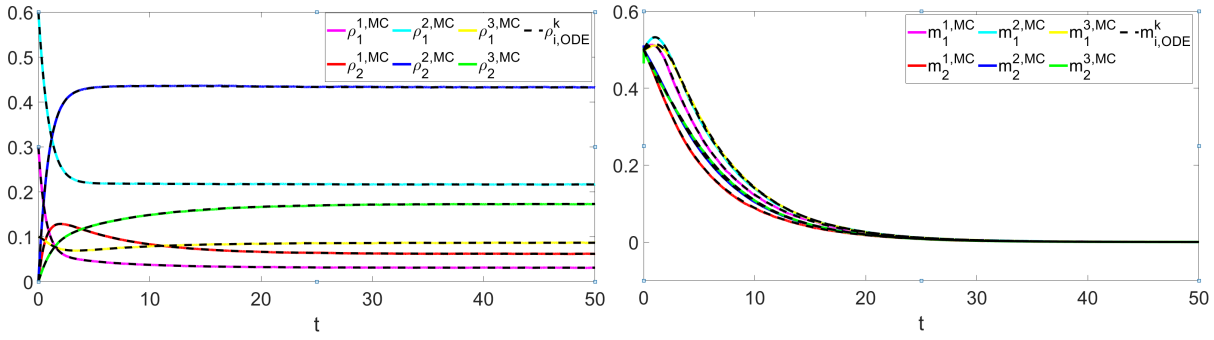


**Figure 14:** Evolution of mass and mean *viral load* in time with constant transition probabilities and epidemic that starts from every city in the same way.

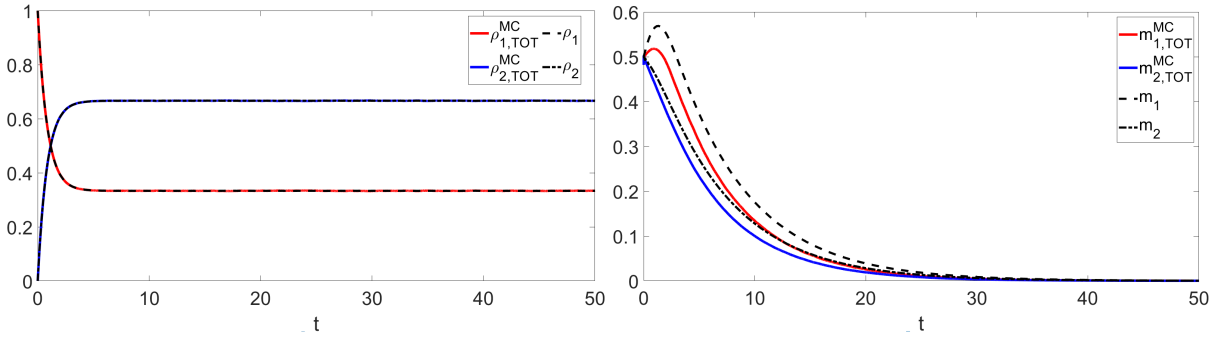


**Figure 15:** Evolution of aggregated mass and mean *viral load* in time with constant transition probabilities and equal initial conditions compared with the evolution of the same quantities in the simple Q-nQ model.

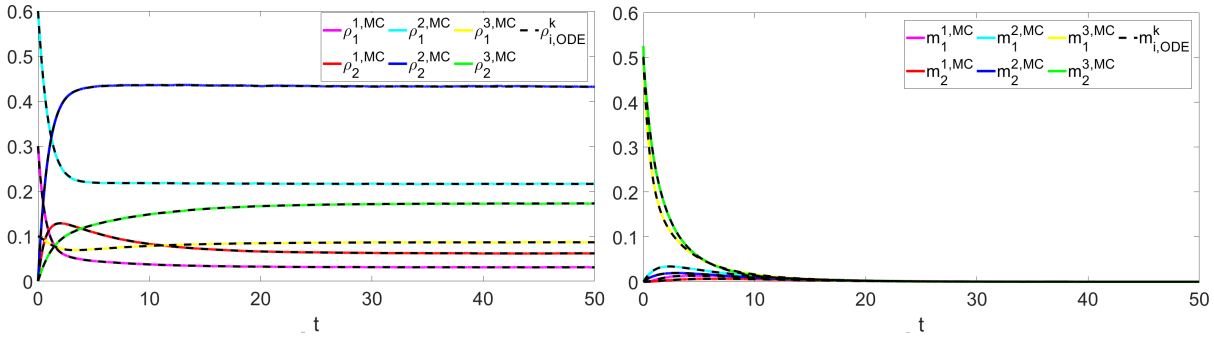


**Figure 16:** Evolution of mass and mean *viral load* in time with constant transition probabilities and the epidemic that starts from the smaller city.

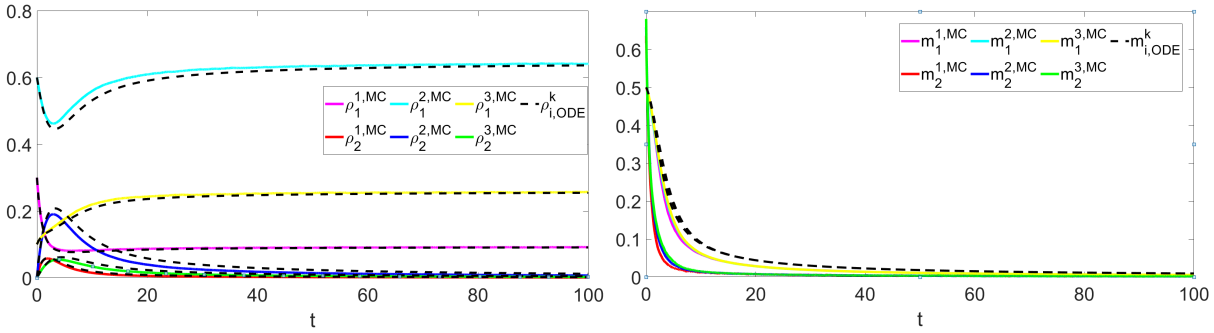


**Figure 17:** Evolution of mass and mean *viral load* in time with variable transition probabilities and the epidemic that starts in each city at the same way, with $\mu \gg \lambda, \omega$.

In the latter the epidemic is assumed to begin to spread from the smaller city, we have

$$f_{1,0}^3(v) = U_{[0,1]}(v), \quad f_{1,0}^i(v) = \delta(v)\,, \quad f_{2,0}^i(v) = 0\,,\ i = 1, 2. \tag{148}$$

This leads to two completely different trends in the epidemic. In the first case (Figure 14) the profile resembles the trends of the simple Q-nQ case with same parameters (Figure 8). We notice how the mean *viral load* reaches its highest point in the bigger city, where people make more interactions. In the second case (Figure 16) the epidemic quickly expires and mean *viral load* has really low peaks. The reduced possibility to interact in the small city makes it impossible for the illness to proliferate. In both cases, mean *viral load* converges to zero since $\alpha > \alpha_\dagger$ as predicted from the qualitative analysis. In particular Figure 15 shows how the speed of convergence is higher in the network case than in the simple Q-nQ case. In both cases, the mass and mean *viral load* obtained from the numerical solution of the ODE system (117) perfectly matches the outcome of the simulation.

Figure 17 refers to the hydrodynamic limit case: the transition probabilities are variable and the interactions happen on a much faster time scale than the label switches. As expected, the mean *viral load* converges to zero as well as the mass of quarantined people. The solution of the ODE system does not follow strictly the simulation due to approximation, as in the simple Q-nQ case; the trend is yet conserved. Figure 18 and Figure 19 shows the outcome of the simulations of two cases with variable transition probabilities not theoretically investigated. For both of the tests the initial condition was the one in (148) and the trend is similar to the one obtained with the same parameters in the simple Q-nQ model (Figure 11 and Figure 12).

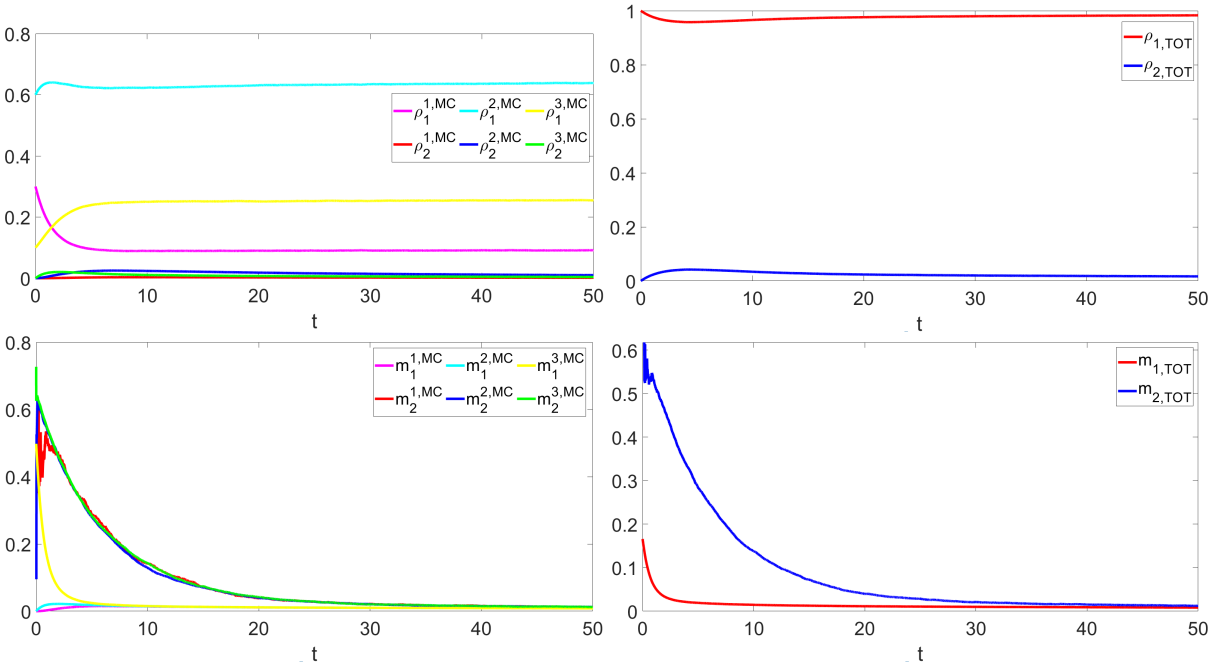


**Figure 18:** Evolution of mass and mean *viral load* in time with variable transition probabilities and the epidemic that starts in the small city, with $\mu = \lambda = \omega$. Both divided and aggregated by city.

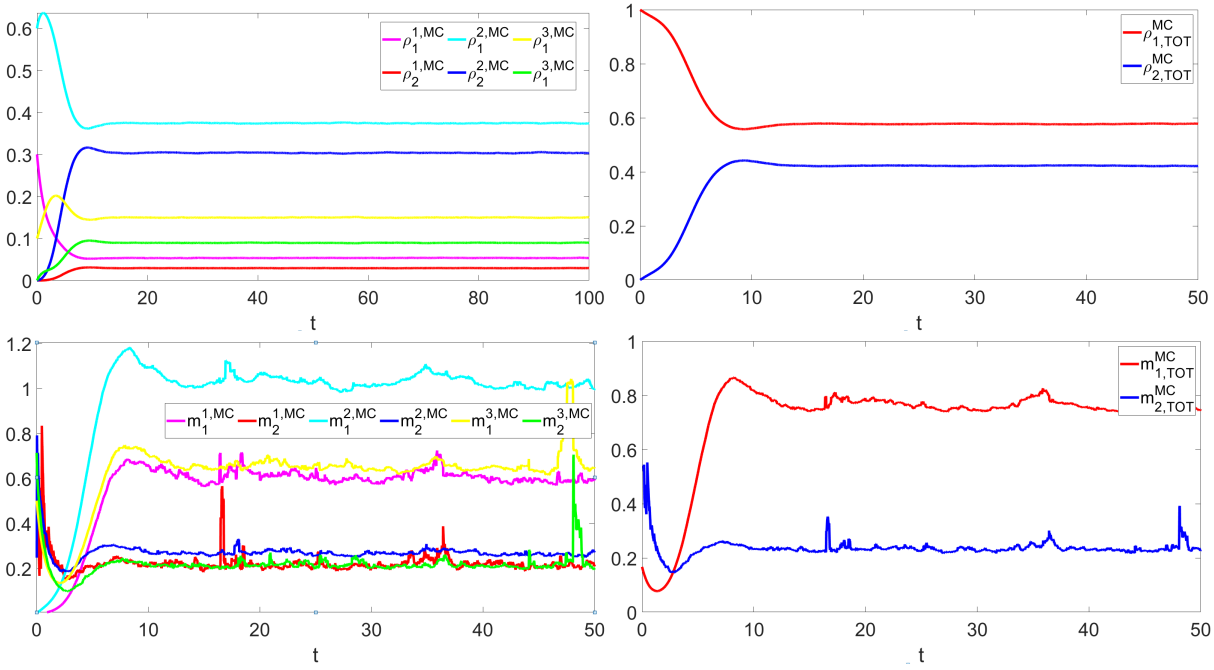


**Figure 19:** Evolution of mass and mean *viral load* in time with variable transition probabilities and the epidemic that starts in the small city, with $\mu \gg \lambda, \omega$ and $\nu_1 = 0$. Both divided and aggregated by city.

**Table 8:** Constant parameters

| Parameter | $N$ | $\lambda$ | $\Delta t$ | $\nu_2$ |
|---|---|---|---|---|
| Value | $10^6$ | 1 | $10^{-2}$ | 0.2 |

**Table 9:** Variable parameters

| Parameter | Figure 20 | Figure 21 | Figure 22 | Figure 23 |
|---|---|---|---|---|
| $\mu, \omega$ | 1 | 1 | 1 | 1 |
| $\alpha$ | 0.8 | 0.8 | 0.8 | 0.8 |
| $\beta$ | 0.4 | 0.4 | 0.4 | 0.4 |
| $\zeta$ | 0.1 | 0.1 | 0 | 0 |
| $\nu_1$ | 0 | 0 | 0 | 0 |
| $\gamma$ | $[0, 0.1, 0.1]$ | $[0, 0.1, 0.3]$ | $[0, 0.1, 0.3]$ | $[0, 0.1, 0.3]$ |
| $c$ | / | / | 0.8 | 0.9 |

| Parameter | Figure 24 | Figure 25 | Figure 26 | Figure 27 |
|---|---|---|---|---|
| $\mu, \omega$ | 10 | 10 | 10 | 10 |
| $\alpha$ | $0.8(1 - e^{-v})$ | $0.8(1 - e^{-v})$ | $0.8(1 - e^{-v})$ | $0.8(1 - e^{-v})$ |
| $\beta$ | $0.4e^{-v}$ | $0.4e^{-v}$ | $0.4e^{-v}$ | $0.4e^{-v}$ |
| $\zeta$ | 0.1 | 0.1 | 0 | 0 |
| $\nu_1$ | 0.2 | 0 | 0 | 0 |
| $\gamma$ | $[0, 0.1, 0.1]$ | $[0, 0.1, 0.1]$ | $[0, 0.1, 0.3]$ | $[0, 0.1, 0.3]$ |
| $c$ | / | / | 0.8 | 0.9 |

## 4.3 Vaccine model

We show now the simulations of the Vax model described in sec. 3.4. For all these tests the initial conditions are of two types, depending on the value of the vaccination rate $\zeta$. If $\zeta > 0$ we set the entire population in the non diagnosed group $x = 1$. The initial *viral load* is sampled from a uniform distribution, as usual. We have

$$f_{1,0}(v) = U_{[0,1]}(v), \quad f_{2,0}(v), f_{3,0}(v) = 0\,.$$

Otherwise, if $\zeta = 0$, the simulation aims to show the trend of the epidemic in a given vaccination scenario. Hence, we set

$$f_{1,0}(v) = f_{3,0}(v) = U_{[0,1]}(v)\,,$$

$$\rho_{1,0} = (1 - c)\,,\ \rho_{2,0} = 0\,,\ \rho_{3,0} = c\,.$$

Table 8 e Table 9 list the values of the constant and variable parameters, respectively.

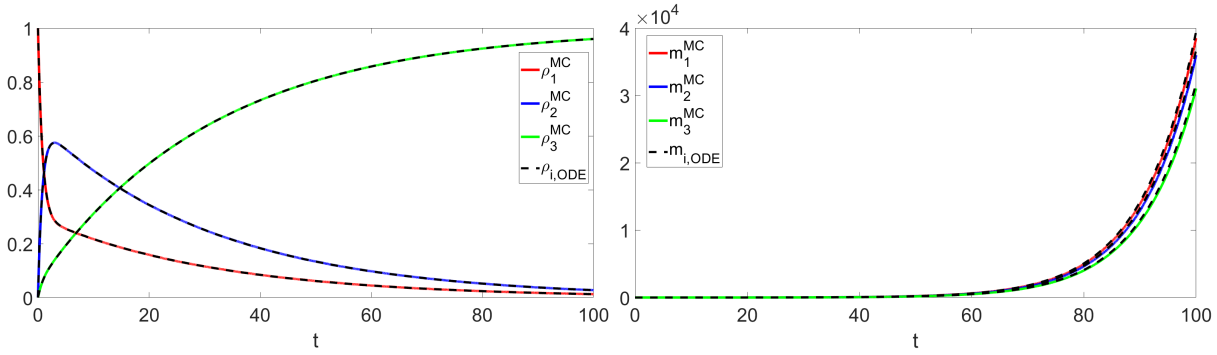


**Figure 20:** Evolution of mass and mean *viral load* in time with constant transition probabilities, increasing vaccination and $\gamma_3 < \nu_2 - \nu_1$.

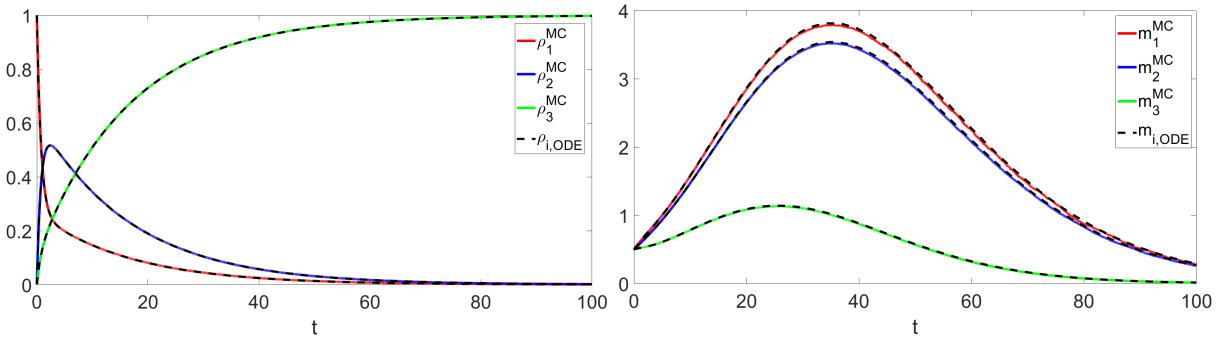


**Figure 21:** Evolution of mass and mean *viral load* in time with constant transition probabilities, increasing vaccination and $\gamma_3 < \nu_2 - \nu_1$.

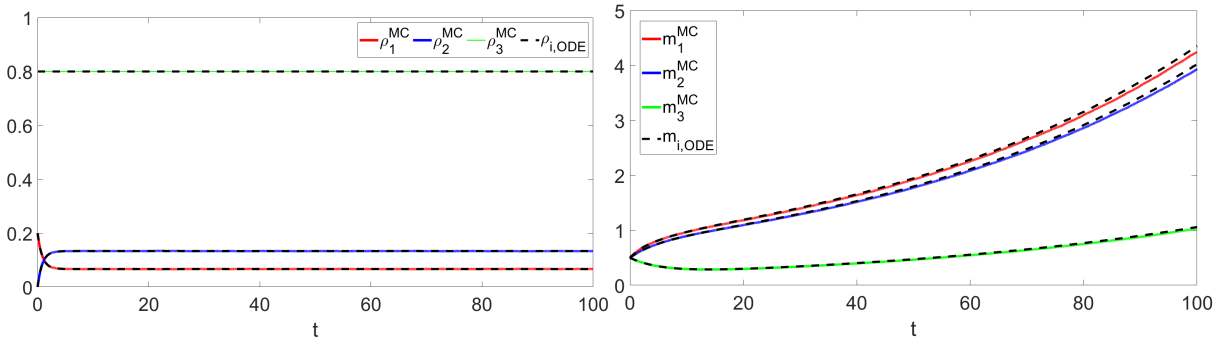


**Figure 22:** Evolution of mass and mean *viral load* in time with constant transition probabilities, fixed vaccination and $c < c_\dagger$.

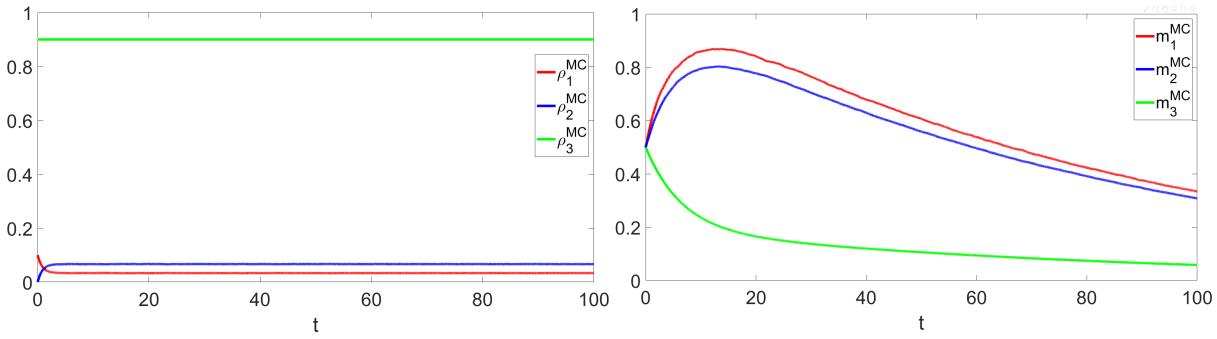


**Figure 23:** Evolution of mass and mean *viral load* in time with constant transition probabilities, fixed vaccination and $c > c_\dagger$.

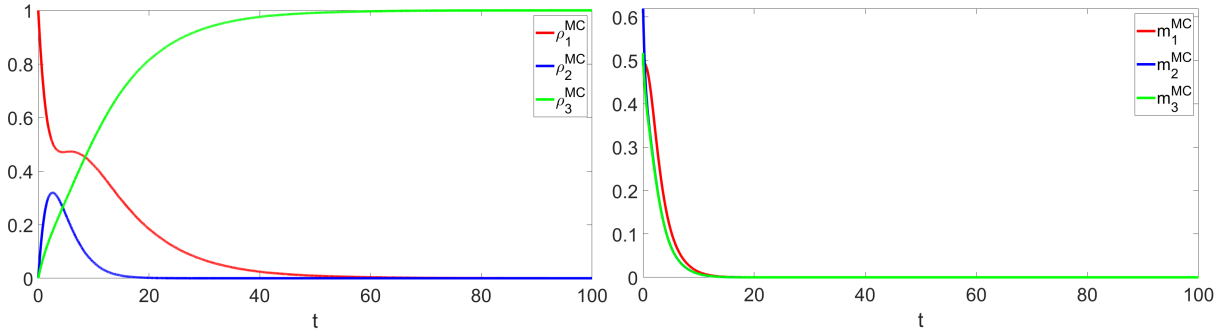


**Figure 24:** Evolution of mass and mean *viral load* in time with variable transition probabilities in the hydrodynamic limit $\mu, \omega \gg \lambda$, increasing vaccination and $\gamma_3 > \nu_2 - \nu_1$ ($\nu_1 = 0.2$).

The first four figures refer to the constant transition probability case. The behavior of each test has been predicted by the qualitative analysis in sec. 3.4.1. Figure 20 and Figure 21 show how with an increasing portion of population being vaccinated in time, the mean *viral load* may either blow to infinity or converge to zero depending on the value of $\gamma_3$. Figure 22 and Figure 23 show how the achievement of herd immunity makes the epidemic expire, and *vice versa*. In every case, the numerical solution of ODE systems (133) and (135) closely follows the trend of the simulations.

The last four figures refer to the variable transition probability case. Figure 24 shows that, accordingly to the qualitative analysis of sec. 3.4.2, the mean *viral load* converges to zero in the conservative binary interaction case $\nu_1 = \nu_2$. The other figures investigate situation that we did not cover with theoretical analysis. In the case of $\nu_1 = 0$ with $\mu, \omega \gg \lambda$ the epidemic does not expire since the healing power of the vaccine is not high enough to contrast the contagion process. Rather, the mean *viral load* blows to infinity as shown in Figure 25. Figure 26 and Figure 27 refer to the case with a single time scale and variable coefficients. Likewise the constant transition probability case, mean *viral load* blows if $c < c_\dagger$ and converges if $c > c_\dagger$.

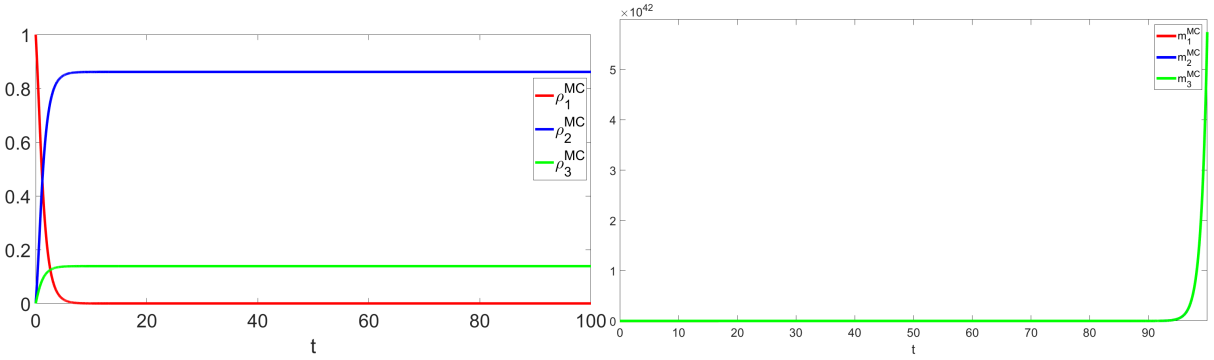


**Figure 25:** Evolution of mass and mean *viral load* in time with variable transition probabilities in the hydrodynamic limit $\mu, \omega \gg \lambda$, increasing vaccination and $\gamma_3 < \nu_2 - \nu_1$ ($\nu_1 = 0$).

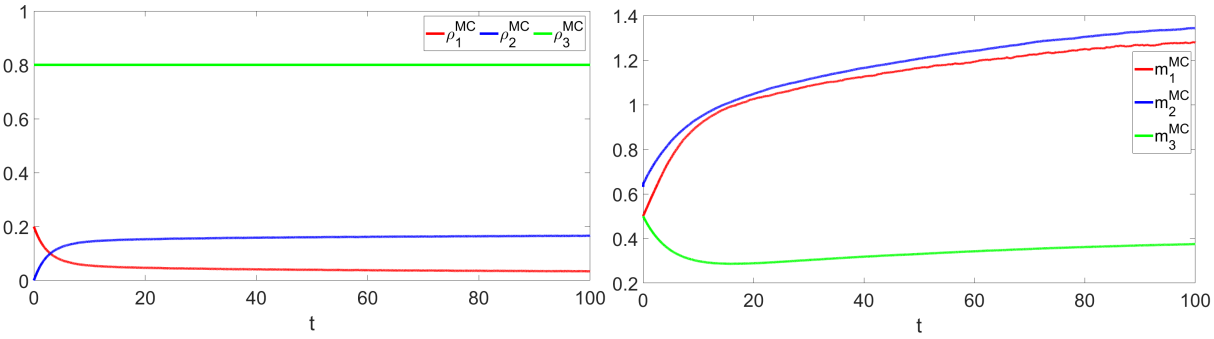


**Figure 26:** Evolution of mass and mean *viral load* in time with variable transition probabilities, fixed vaccination, $c < c_\dagger$ and $\mu = \omega = \lambda$.

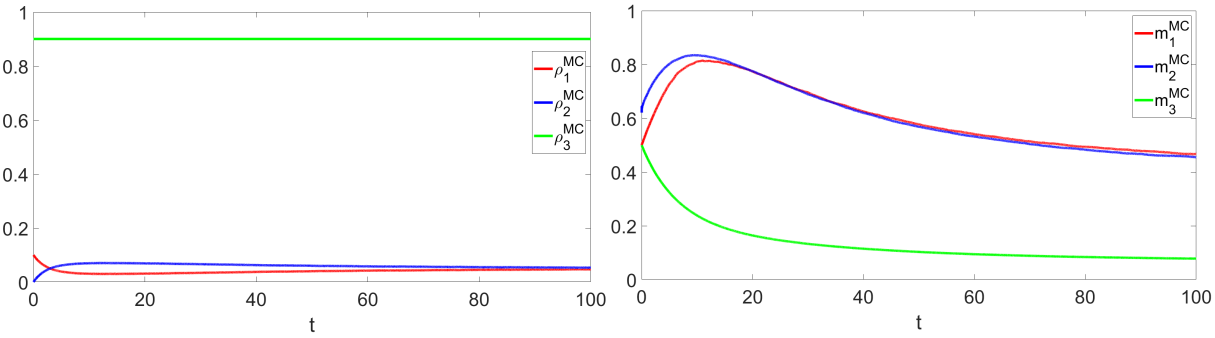


**Figure 27:** Evolution of mass and mean *viral load* in time with variable transition probabilities, fixed vaccination, $c > c_\dagger$ and $\mu = \omega = \lambda$.

**Table 10:** Constant parameters

| Parameter | $N$ | $\lambda$ | $\omega$ | $\mu$ | $\Delta t$ | $\nu_1$ | $\nu_2$ | $\alpha$ | $\beta$ | $\zeta$ |
|---|---|---|---|---|---|---|---|---|---|---|
| Value | $10^6$ | 1 | 1 | 1 | $10^{-3}$ | 0 | 0.2 | $[0.5, 0.7, 0.8]$ | $[0.4, 0.4, 0.4]$ | $[0, 0, 0]$ |

**Table 11:** Variable parameters

| Parameter | Figure 20 | Figure 21 | Figure 22 | Figure 23 |
|---|---|---|---|---|
| $r$ | $[1.5, 1, 0.5]$ | $[1.5, 1, 0.5]$ | $[1, 1, 1]$ | $[1.5, 1, 0.5]$ |
| $c$ | $[0.95, 0.15, 0.05]$ | $[0.95, 0.75, 0.05]$ | $[0.05, 0.75, 0.95]$ | $[0.05, 0.75, 0.95]$ |

## 4.4 Age-structured vaccine model

Finally, we present the simulation outcomes for the age-structured vaccine model. These simulations aim to confirm the results of the theoretical analysis of sec. 3.5.1. Hence, the initial conditions are such that:

$$f^k_{1,0}(v) = f^k_{3,0}(v) = U_{[0,1]}(v)\,,\ k = 1, 2, 3\,,$$

$$\rho^k_{1,0} = (1 - c_k)\,,\ \rho^k_{2,0} = 0\,,\ \rho^k_{3,0} = c_k\,,\ k = 1, 2, 3.$$

Table 10 lists the parameters constant in every test, while Table 11 lists those that change from test to test. For every simulations the healing rate is fixed as

$$\gamma = \begin{pmatrix} 0 & 0 & 0 \\ 0.3 & 0.2 & 0.1 \\ 0.5 & 0.5 & 0.4 \end{pmatrix},$$

i.e. as in example 2 of sec. 3.5.1. With the chosen parameters, we can evaluate the value of threshold $c_{2,\dagger}$ from Figure 6 (bottom) as $c_{2,\dagger} \approxeq 0.65$.

Figure 28 and Figure 29 refer to the strategy of vaccinating young people first. Hence, the 95% of the young population and the 5% of the elderly population have been vaccinated. With this value of the healing rate $\gamma$ this strategy allows to stem the epidemic if enough adults get the vaccine. In Figure 28 this threshold is not reached while in Figure 29 it is. Figure 30 and Figure 31 refer to the strategy of vaccinating elderly people first instead. This means that the percentages are inverted. In both cases the 75% of adult people is vaccinated but, as it is clear from the charts, in the first case this is enough to stem the epidemic while in the second it is not. This is due to the fact that in the first case every age group interact with the same frequency while in the second case the young people interact way more than the elderly people.

As predicted by the qualitative analysis, this affects the threshold $c_{2,\dagger}$ and produces the two behaviors shown here, even with the same value of $c_2$.

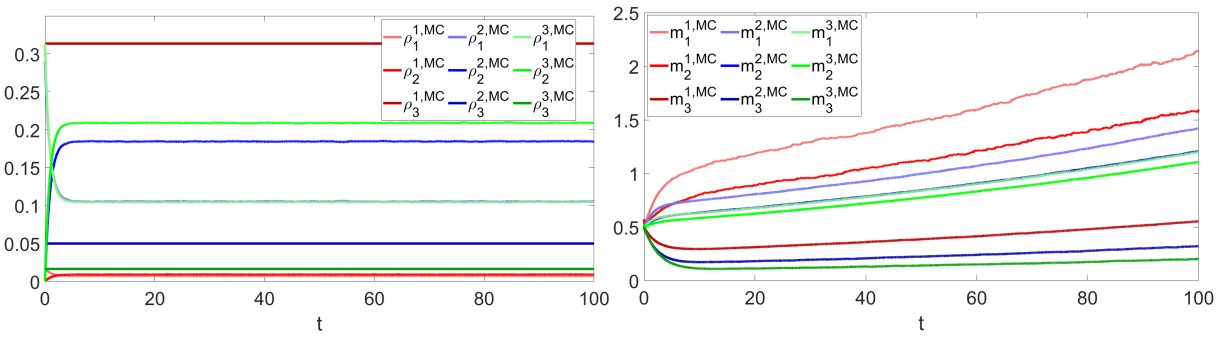


**Figure 28:** Evolution of mass and mean *viral load* in time with the majority of young people vaccinated,, diversified interaction rate and $c_2 < c_{2,\dagger}$.

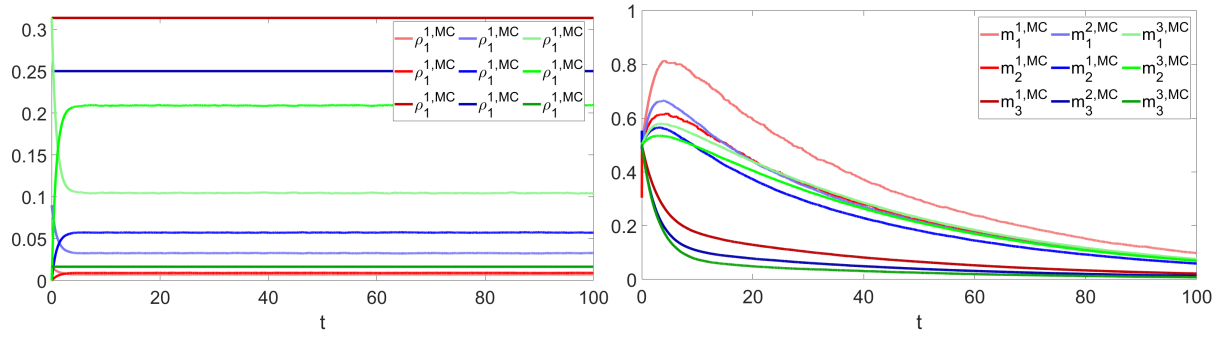


**Figure 29:** Evolution of mass and mean *viral load* in time with the majority of young people vaccinated, diversified interaction rate and $c_2 > c_{2,\dagger}$.

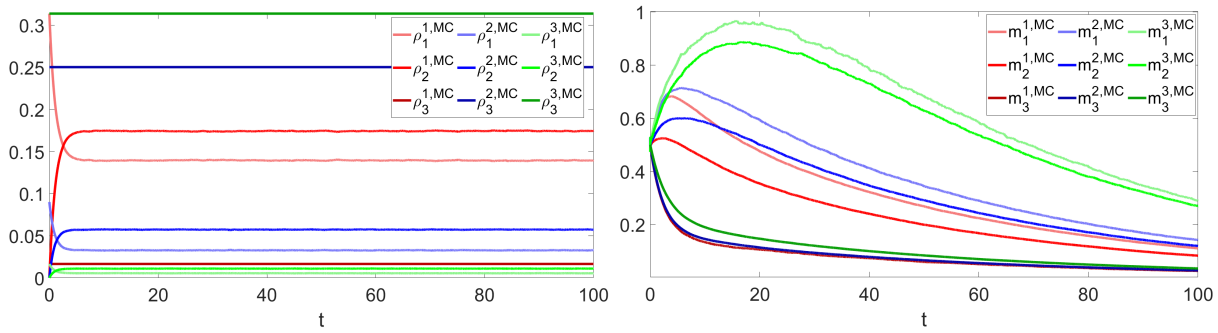


**Figure 30:** Evolution of mass and mean *viral load* in time with the majority of elderly people vaccinated, un-diversified interaction rate and $c_2 = 0.75 > c_{2,\dagger}$.

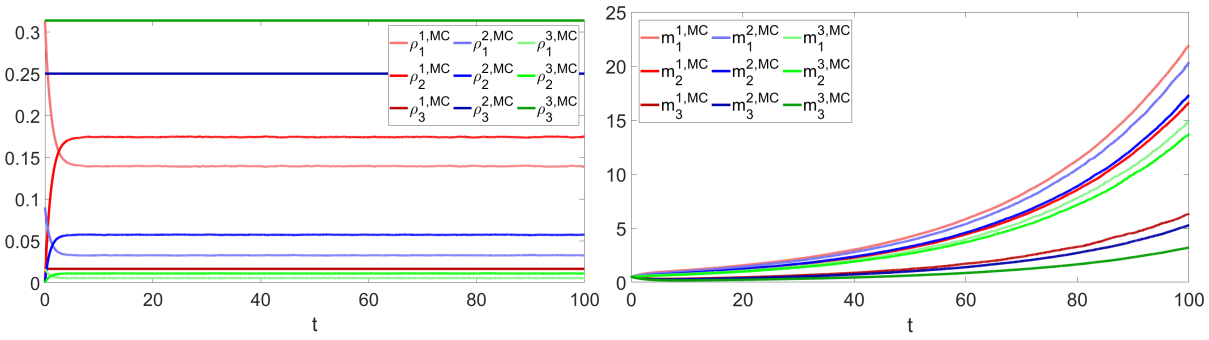


**Figure 31:** Evolution of mass and mean *viral load* in time with the majority of elderly people vaccinated, diversified interaction rate and $c_2 = 0.75$.

# 5 Conclusions

In this dissertation, we have applied tools and methodologies from the kinetic theory of gasses to epidemiology. In particular, Boltzmann-type non-conservative equations have been adopted to describe the time evolution of an epidemic in a large and interconnected population. The microscopic state the agents are equipped with has been intended as a *viral load*, whose first and zero order moments are able to describe the ongoing epidemic. In addition, the agents are characterized by one or more labels that model important epidemiological aspects, namely quarantine, vaccination, age and geographic distribution of agents. These labels change following a Markov-type *viral load*-dependent probabilistic jump process for which a microscopic kinetic description has been provided. The kinetic framework proved to be useful in the modeling of epidemics. The innovative models introduced in the thesis show a rich variety of behaviors while depending on few epidemiological parameters. They are a simple quarantine model, a quarantine model laid on a city network, a vaccine model and a age-structured vaccine model. Kinetic equations are derived for each model to describe the evolution of the epidemic. Through various analytical tools, among which the hydrodynamic limit provided by the kinetic theory, we have been able to gain some insights on the role and importance of various parameters of the models. In detail:

1. Quarantine can be an effective confinement strategy if the diagnose process is punctual. If diagnoses are too slow they fail to lower the *viral load* level and the epidemic explodes.

2. The higher the number of interacting people, the higher the mean *viral load*. When considering an epidemic on a cities network where interactions happen only within the same city, the max mean *viral load* reaches lower values than in the case where all agents can interact with each other.

3. We have been able to numerically evaluate a herd immunity threshold if the population is subject to a vaccination campaign. It depends on parameters such as diagnosis power, healing rate, infectivity.

4. The kinetic approach allow to account for different interaction rates based on the age of the agents. The fact that young agents usually have more interactions than older agents can affect the vaccination strategy: it may be best to vaccinate young people first, as they spread the virus more, even if older people heal less quickly. This depends on the parameters of the epidemic and of course holds within the model, reality is much more complicated.

Incidentally, the classical SIR and SIS models can be obtain as specific cases of

this kinetic description. Numerical algorithms based on a modified version of the Nanbu-Babovsky scheme have been developed to simulate all the four models. The numerical simulations confirm all the results of the theoretical analysis and provide us with a precious tool to investigate complicated situations that are hard to study analytically. In fact, explicit solutions are possible only in few simple cases and numerical simulations are needed to investigate more realistic scenarios. These simulations are quite efficient in simple models but computational time increases when the age or the spatial network are considered.

The label based kinetic description adopted in this dissertation allows the models to be merged or integrated to include additional features, e.g. different kind of therapies or a more detailed age-based characterization. Finally, we have carried out a theoretical analysis where parameters have been freely chosen to explore a wide range of scenarios. It would be interesting to focus on a real world epidemic for which large scale statistics are available and to extract the parameters of the model to test it in a "real life situation".

# References


[1] Graunt, John. Natural and political observations made upon the bills of mortality. No. 2. Johns Hopkins Press, 1939.

[2] Bernoulli, Daniel, and Sally Blower. "An attempt at a new analysis of the mortality caused by smallpox and of the advantages of inoculation to prevent it." Reviews in medical virology 14.5 (2004): 275.

[3] Dietz, Klaus, and J. A. P. Heesterbeek. "Daniel Bernoulli's epidemiological model revisited." Mathematical biosciences 180.1-2 (2002): 1-21.

[4] Hamer, W. "Epidemiology Old and New." Epidemiology Old and New. (1928).

[5] Soper, Herbert E. "The interpretation of periodicity in disease prevalence." Journal of the Royal Statistical Society 92.1 (1929): 34-73.

[6] Ross, Ronald. "Studies on malaria." Studies on Malaria. (1928).

[7] Kermack, William Ogilvy, and Anderson G. McKendrick. "A contribution to the mathematical theory of epidemics." Proceedings of the royal society of london. Series A, Containing papers of a mathematical and physical character 115.772 (1927): 700-721.

[8] Kermack, William Ogilvy, and Anderson G. McKendrick. "Contributions to the mathematical theory of epidemics. II.—The problem of endemicity." Proceed-

ings of the Royal Society of London. Series A, containing papers of a mathematical and physical character 138.834 (1932): 55-83.

[9] Kermack, William Ogilvy, and Anderson G. McKendrick. "Contributions to the mathematical theory of epidemics. III.—Further studies of the problem of endemicity." Proceedings of the Royal Society of London. Series A, Containing Papers of a Mathematical and Physical Character 141.843 (1933): 94-122.

[10] Hethcote, Herbert W. "The mathematics of infectious diseases." SIAM review 42.4 (2000): 599-653.

[11] Hethcote, Herbert W. "A thousand and one epidemic models." Frontiers in mathematical biology. Springer, Berlin, Heidelberg, 1994. 504-515.

[12] Vynnycky, Emilia, and Richard White. An introduction to infectious disease modelling. OUP oxford, 2010.

[13] Martcheva, Maia. An introduction to mathematical epidemiology. Vol. 61. New York: Springer, 2015.

[14] Acemoglu, Daron, et al. Optimal targeted lockdowns in a multi-group SIR model. Vol. 27102. National Bureau of Economic Research, 2020.

[15] Cordier, Stephane, Lorenzo Pareschi, and Giuseppe Toscani. "On a kinetic model for a simple market economy." Journal of Statistical Physics 120.1 (2005): 253-277.

[16] Slanina, František. "Inelastically scattering particles and wealth distribution in an open economy." Physical Review E 69.4 (2004): 046102.

[17] Loy, Nadia, and Luigi Preziosi. "Kinetic models with non-local sensing determining cell polarization and speed according to independent cues." Journal of mathematical biology 80.1 (2020): 373-421.

[18] Preziosi, Luigi, Giuseppe Toscani, and Mattia Zanella. "Control of tumor growth distributions through kinetic methods." Journal of Theoretical Biology 514 (2021): 110579.

[19] Dimarco, Giacomo, and Giuseppe Toscani. "Kinetic modeling of alcohol consumption." Journal of Statistical Physics 177.5 (2019): 1022-1042.

[20] Dimarco, Giacomo, and Giuseppe Toscani. "Social climbing and Amoroso distribution." arXiv preprint arXiv:2006.02942 (2020).

[21] Toscani, Giuseppe, Andrea Tosin, and Mattia Zanella. "Multiple-interaction kinetic modeling of a virtual-item gambling economy." Physical Review E 100.1 (2019): 012308.

[22] Pareschi, Lorenzo, et al. "Hydrodynamic models of preference formation in multi-agent societies." Journal of Nonlinear Science 29.6 (2019): 2761-2796.

[23] Fraia, Martina, and Andrea Tosin. "The Boltzmann legacy revisited: kinetic models of social interactions." arXiv preprint arXiv:2003.14225 (2020).

[24] Toscani, Giuseppe, Andrea Tosin, and Mattia Zanella. "Multiple-interaction kinetic modeling of a virtual-item gambling economy." Physical Review E 100.1 (2019): 012308.

[25] Tosin, Andrea, and Mattia Zanella. "Kinetic-controlled hydrodynamics for traffic models with driver-assist vehicles." Multiscale Modeling & Simulation 17.2 (2019): 716-749.

[26] Tosin, Andrea, and Mattia Zanella. "Uncertainty damping in kinetic traffic models by driver-assist controls." arXiv preprint arXiv:1904.00257 (2019).

[27] Boltzmann, Ludwig. Lectures on gas theory. Courier Corporation, 2012.

[28] Pareschi, Lorenzo, and Giovanni Russo. "An introduction to Monte Carlo method for the Boltzmann equation." ESAIM: Proceedings. Vol. 10. EDP Sciences, 2001.

[29] Bird, G. A. "Direct simulation and the Boltzmann equation." The Physics of Fluids 13.11 (1970): 2676-2681.

[30] Nanbu, Kenichi. "Direct simulation scheme derived from the Boltzmann equation. I. Monocomponent gases." Journal of the Physical Society of Japan 49.5 (1980): 2042-2049.

[31] De Lillo, Silvana, Marcello Delitala, and M. C. Salvatori. "Modelling epidemics and virus mutations by methods of the mathematical kinetic theory for active particles." Mathematical Models and Methods in Applied Sciences 19.supp01 (2009): 1405-1425.

[32] Loy, Nadia, and Andrea Tosin. "Non-conservative Boltzmann-type kinetic equations for multi-agent systems with label switching." arXiv e-prints (2020): arXiv-2006.

[33] Cercignani, Carlo, Reinhard Illner, and Mario Pulvirenti. The mathematical theory of dilute gases. Vol. 106. Springer Science & Business Media, 2013.

[34] Pareschi, Lorenzo, and Giuseppe Toscani. Interacting multiagent systems: kinetic equations and Monte Carlo methods. OUP Oxford, 2013.

[35] Cercignani, Carlo. "The boltzmann equation." The Boltzmann equation and its applications. Springer, New York, NY, 1988. 40-103.

[36] Loy, Nadia, and Andrea Tosin. "Markov jump processes and collision-like models in the kinetic description of multi-agent systems." arXiv preprint arXiv:1905.11343 (2019).

[37] Boltzmann, Ludwig. "Weitere studien über das wärmegleichgewicht unter gasmolekülen." Kinetische Theorie II. Vieweg+ Teubner Verlag, Wiesbaden, 1970. 115-225.

[38] Nanbu, Kenichi. "Direct simulation scheme derived from the Boltzmann equation. I. Monocomponent gases." Journal of the Physical Society of Japan 49.5 (1980): 2042-2049.

[39] Babovsky, Hans, and H. Neunzert. "On a simulation scheme for the Boltzmann equation." Mathematical methods in the applied sciences 8.1 (1986): 223-233.

[40] Bird, G. A. "Direct simulation and the Boltzmann equation." The Physics of Fluids 13.11 (1970): 2676-2681.

[41] Pareschi, Lorenzo, and Giovanni Russo. "An introduction to Monte Carlo method for the Boltzmann equation." ESAIM: Proceedings. Vol. 10. EDP Sciences, 2001.

[42] Koura, Katsuhisa. "Comment on “Direct Simulation Scheme Derived from the Boltzmann Equation. I. Monocomponent Gases”." Journal of the Physical Society of Japan 50.11 (1981): 3829-3830.

[43] Babovsky, Hans, and Reinhard Illner. "A convergence proof for Nanbu's simulation method for the full Boltzmann equation." SIAM journal on numerical analysis 26.1 (1989): 45-65.

[44] Caflisch, Russel E. "Monte carlo and quasi-monte carlo methods." Acta numerica 1998 (1998): 1-49.

[45] Bleier, Benjamin S., Murugappan Ramanathan Jr, and Andrew P. Lane. "COVID-19 vaccines may not prevent nasal SARS-CoV-2 infection and asymptomatic transmission." Otolaryngology–Head and Neck Surgery 164.2 (2021): 305-307.

# Appendix

**Algorithm 3** General simulation scheme for the Q-nQ model on the network. First part.

**Data:**

- $N \in \mathbb{N}$ total number of particles.
- $\mathbb{V}^0 := \{\xi_1^0, ..., \xi_N^0\}$ initial velocities, sampled from initial density $f_0(\xi)$.
- $\Delta t$ time interval and $n_{TOT}$ number of time steps.

```
for t = 1 to n_TOT
compute ρ_x^a(t) = N_x^a(t)/N , m_x^{a,n} = 1/N_x^a Σ_{agents in (x,a)} v^n ;
repeat
    pick randomly two agents i and j with i ≠ j .
    for h = i, j do
        sample Θ ~ Bernoulli(λΔt);
        if Θ = 1 then
            if x_h^n = 1 then
              sample J ∈ {1, 2}
              with prob {1 − α(v_h^n), α(v_h^n)};
            if x_h^n = 2 then
              sample J ∈ {1, 2}
              with prob {β(v_h^n), 1 − β(v_h^n)};
            set x_h^{n+1} = J;
        else
            set x_h^{n+1} = x_h^n;
        sample Ω ~ Bernoulli(ωΔt);
        if Ω = 1 then
            sample Q ∈ {1, .., #cities}
            with prob D_{h,k}(v_h^n);
            set a_h^{n+1} = Q;
        else
            set a_h^{n+1} = a_h^n;
    sample Ξ ~ Bernoulli(μΔt);
    Continues...
```

**Algorithm 4** General simulation scheme for the Q-nQ model on the network. Second part.

...

**if** $\Xi = 1$ **then**

  **if** $x_i^n = x_j^n = 1,\ a_i^n = a_j^n$ **then**

    update $v_i^n,\ v_j^n$ to $v_i^{n+1},\ v_j^{n+1}$ according to (88);

  **if** $x_i^n = 1, x_j^n = 2$ or *vice versa* **then**

    set $v_i^{n+1} = v_i^n$

    update $v_j^n$ to $v_j^{n+1}$ according to (89)

    or *vice versa*;

  **if** $x_i^n = x_j^n = 2$ **then**

    update $v_i^n,\ v_j^n$ to $v_i^{n+1},\ v_j^{n+1}$ acccording to (89);

  **if** $x_i^n = x_j^n = 1,\ a_i^n \neq a_j^n$ **then**

    set $v_i^{n+1} = v_i^n,\ v_j^{n+1} = v_j^n$;

**else**

  set $v_i^{n+1} = v_i^n,\ v_j^{n+1} = v_j^n$;

**until** no unused pairs are left

**Algorithm 5** General simulation scheme for the age-structured Vax model

**Data:**

- $N \in \mathbb{N}$ total number of particles.
- $\mathbb{V}^0 := \{\xi_1^0, ..., \xi_N^0\}$ initial velocities, sampled from initial density $f_0(\xi)$.
- $\Delta t$ time interval and $n_{TOT}$ number of time steps.

**for** $t = 1$ **to** $n_{TOT}$
compute $\rho_x^a(t) = \frac{N_x^a(t)}{N}$, $m_x^{a,n} = \frac{1}{N_x^a} \sum_{agents\, in\, (x,a)} v^n$;
**repeat**

pick randomly two agents $i$ and j with $i \neq j$.
**for** $h = i, j$ **do**

sample $\Theta \sim Bernoulli(\lambda \Delta t)$;
**if** $\Theta = 1$ **then**

**if** $x_h^n = 1$ **then**

sample $P \in \{1, 2, 3\}$
with prob $[1 - \alpha(v_h^n) -$
$\zeta(x_h^n), \alpha(v_h^n), \zeta(x_h^n)]$;

**if** $x_h^n = 2$ **then**

sample $P \in \{1, 2\}$
with prob $[\beta(v_h^n), 1 - \beta(v_h^n)]$;

**if** $x_h^n = 3$ **then**

set $P = 3$;

set $x_h^{n+1} = P$;

**else**

set $x_h^{n+1} = x_h^n$;

sample $\Omega \sim Bernoulli(\omega \Delta t)$;
**if** $\Omega = 1$ **then**

update $v_h^n$ to $v_h^{n+1}$ according to (129);

**else**

set $a_h^{n+1} = a_h^n$;

sample $\Xi \sim Bernoulli(\mu \Delta t \cdot r_{a_i} \cdot r_{a_j})$ ;
**if** $\Xi = 1$ **then**

update $v_i^n$, $v_j^n$ to $v_i^{n+1}$, $v_j^{n+1}$ according to (128);

**else**

set $v_i^{n+1} = v_i^n$, $v_j^{n+1} = v_j^n$;

**until** no unused pairs are left